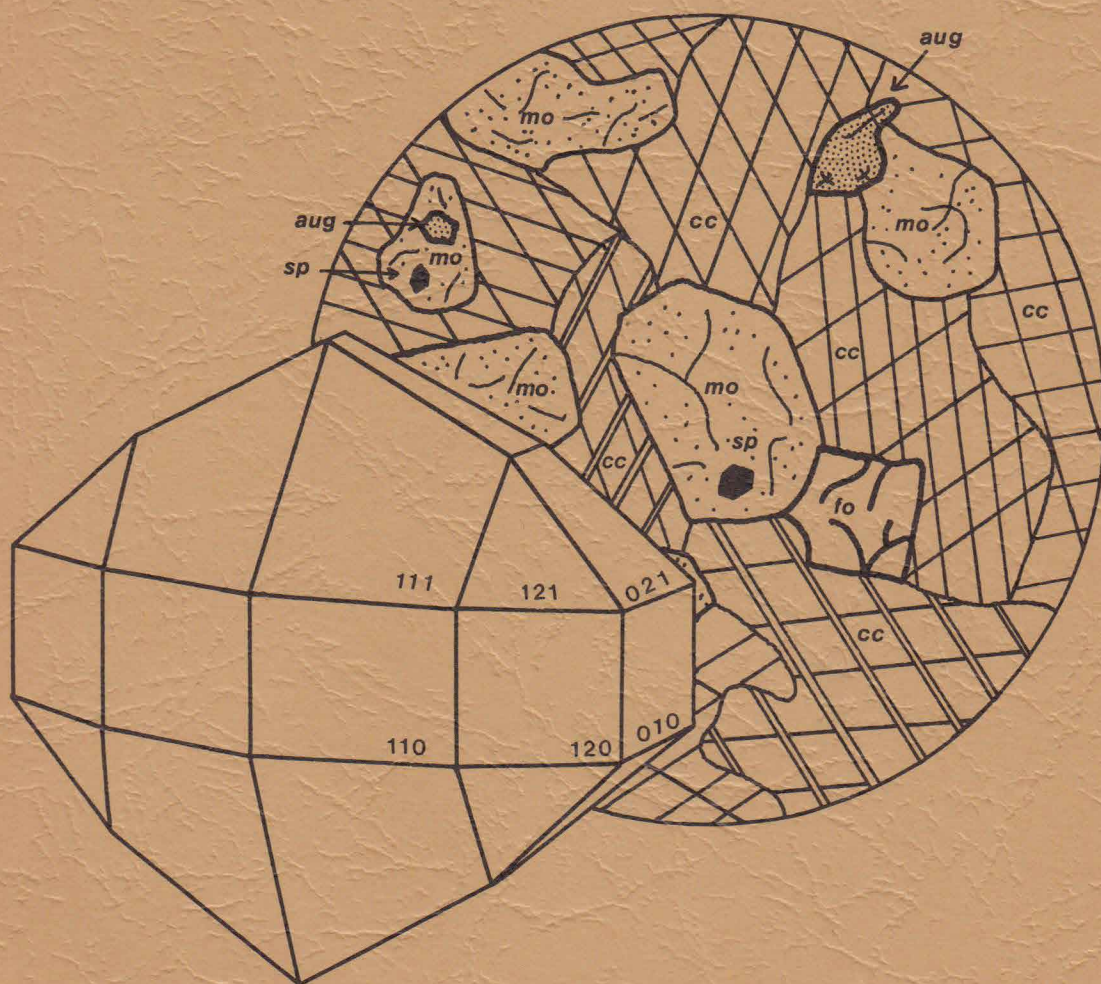


THE CASCADE SLIDE :
A MINERALOGICAL INVESTIGATION
OF A CALC-SILICATE BODY ON
CASCADE MOUNTAIN, TOWN OF
KEENE, ESSEX COUNTY, NEW YORK

BY THOMAS A. BAILLIEUL



CONTRIBUTION NO. 27
GEOLOGY DEPARTMENT
UNIVERSITY OF MASSACHUSETTS
AMHERST, MASSACHUSETTS

THE CASCADE SLIDE: A MINERALOGICAL INVESTIGATION OF A
CALC-SILICATE BODY ON CASCADE MOUNTAIN, TOWN OF KEENE,
ESSEX COUNTY, NEW YORK

by
Thomas A. Baillieul

Contribution No. 27
Department of Geology
University of Massachusetts
Amherst, Massachusetts
May, 1976

TABLE OF CONTENTS

ABSTRACT	1
INTRODUCTION	2
Location.....	2
Previous Work	2
Field Work	4
Methods	5
Acknowledgements	8
GENERAL GEOLOGY	9
PETROGRAPHY	14
Augite and monticellite marble	14
Scapolite gneiss and granulite	16
Wollastonite - garnet granulite	19
Augite granulite	21
Augite-garnet gneiss	23
Pyroxene-microperthite gneiss and anorthosite	24
MINERALOGY	29
Calcite	29
Augite	38
Scapolite	57
Garnet	66
Wollastonite	73
Monticellite	79
Olivine	85
Vesuvianite	88

Apatite	94
Titanite (sphene)	101
Graphite	102
Magnetite	104
Spinel	106
Harkerite	109
Phlogopite	112
Ilmenite	114
Perovskite	115
CRYSTAL SURFACE TEXTURES	117
COMPARISONS AND CONCLUSIONS	122
REFERENCES	126

LIST OF ILLUSTRATIONS

Figure

1. Index map	3
2. Flow chart detailing sample analysis scheme	6
3. Folded rock patterns in the 4th pool wall	12
4. Diagrammatic sketch of Cascade Slide structure	13
5. Thin section of Ca-22, montice-lite marble	17
6. SAM diagrams for metamorphosed argillaceous and siliceous dolomites	18
7. Sketch of scapolite megacrystal	20
8. Metasomatic reaction zone in augite granulite	22
9. ACF and AKF diagrams for gabbroic anorthosite and pyroxene-microperthite gneiss	26

10.	Stereographic projection for calcite I	31
11.	Stereographic projection for calcite II	32
12.	Infra-red absorption spectra of calcite	37
13.	Perspective drawings of augite	39
14.	Stereographic projection for augite	40
15.	Pyroxene quadrilateral with Cascade Slide augite compositions	45
16.	Stereographic projection for scapolite	58
17.	Perspective drawing of scapolite	59
18.	Plot of ratio $\text{CaO}/\text{Na}_2\text{O}$ against Cl concentration in Cascade Slide scapolite	63
19.	Plot of Ca concentration against Fe^{+3}/Al for Cascade Slide garnet	71
20.	Perspective drawing of monticellite	80
21.	Perspective drawing of vesuvianite	89
22.	Stereographic projection of vesuvianite	90
23.	Perspective drawings of apatite	95
24.	Photomicrograph of apatite crystals	96
25.	Stereographic projection of apatite	97
26.	Etch markings on augite megacrystal	118
27.	Crenulations on augite megacrystal I	119
28.	Crenulations on augite megacrystal II	120

PLATE

1.	Geologic Map of the Cascade Slide	in pocket
----	---	-----------

LIST OF TABLES

Table

1.	Estimated and measured modes of calc-silicate	15
2.	Measured modes of anorthosite and pyroxene- microperthite gneiss	25
3.	X-ray powder diffraction data for calcite	33
4.	Results of microprobe penetration of fluorine filled inclusion	35
5.	X-ray powder diffraction data for augite	42
6.	Electron microprobe analyses of augite	46
7.	Recalculations of augite compositions	52
8.	Results of dispersion analysis on augite	54
9.	Electron microprobe traverse across an augite megacrystal	56
10.	X-ray powder diffraction data for scapolite	61
11.	Electron microprobe analyses of scapolite	65
12.	X-ray powder diffraction data for garnet	67
13.	Electron microprobe analyses of garnet	70
14.	X-ray powder diffraction data for wollastonite	75
15.	X-ray powder diffraction data for wollastonite and parawollastonite	77
16.	Electron microprobe analyses of wollastonite	78
17.	X-ray powder diffraction data for monticellite	82
18.	Chemical analyses of monticellite	84
19.	X-ray powder diffraction data for forsterite	86

20.	Electron microprobe analyses of forsterite	87
21.	X-ray powder diffraction data for vesuvianite	91
22.	Electron microprobe analyses of vesuvianite	92
23.	X-ray powder diffraction data for apatite	98
24.	X-ray powder diffraction data for titanite	103
25.	X-ray powder diffraction data for magnetite	105
26.	X-ray powder diffraction data for graphite	105
27.	X-ray powder diffraction data for spinel	107
28.	Electron microprobe analyses of spinel	108
29.	X-ray powder diffraction data for harkerite	110
30.	X-ray powder diffraction data for phlogopite	113
31.	X-ray powder diffraction data for ilmenite	114
32.	X-ray powder diffraction data for perovskite	116

ABSTRACT

A mineralogical investigation has been made of a suite of calc-silicate minerals which occurs in a block of metamorphosed, siliceous and argillaceous dolomite and associated volcanics enfolded in the Adirondack anorthosite massif. Studies show that the calc-silicate body, locally called the Cascade Slide, has undergone high-grade regional rather than contact metamorphism, and that the original sedimentary layering is still preserved by the variable mineralogy of the assemblages present. Two phases of folding are visible.

Calc-silicate and associated assemblages present in the Cascade Slide include: coarse augite marble often accompanied by monticellite, spinel, magnetite, and vesuvianite; augite-garnet gneiss; augite granulite; grossular-diopside-wollastonite granulite; and scapolite-bearing rock related directly to a surrounding layer of pyroxene-microperthite gneiss. Limited metasomatism has occurred in the presence of an undetermined fluid phase.

All mineral species were examined by optical, X-ray powder diffraction, and morphological crystallographic methods. Chemical analyses by electron microprobe were carried out on many of these. Unusual crystal forms and surface textures were studied in an attempt to unravel the complex geologic history of the site.

INTRODUCTION

Location

The Cascade Slide is a narrow, rock-strewn stream valley located on the northern slope of Cascade Mountain, Keene, New York (see index map, figure 1). It is centered in the heart of the Adirondack Anorthosite Massif. Numerous falls of loose boulders, and a major avalanche before 1836 have given this valley its name. This avalanche also separated a narrow lake (once known as Long Pond) at the base of the mountain into two smaller bodies, Upper and Lower Cascade Lakes, respectively. The stream which flows through the Cascade Slide, and drains into the lower lake, has differentially cut into a body of less resistant calc-silicate rocks which are the subject of this study. High walls offer frequent good exposures of the various mineral assemblages present, but are very hazardous to climb. Omnipresent rubble, fallen trees, wet and moss covered rocks limit the amount of practical geology that can be done.

The section of the Slide examined in this study is approximately 150 m in length, and 10-20 m in width (see geologic map, plate 1). Elevations vary from 2220 ft. above sea level at the abandoned reservoir below the main gorge, to 2590 ft. at the uppermost mapped position.

Previous Work

The first geological description of the Cascade Slide was made by Ebenezer Emmons in 1836. He wrote:

. . . The sides of these mountains [Cascade and Pitchoff] are deeply furrowed by slides which have occurred from time to time. The widest is on the south side of the pond [Cascade

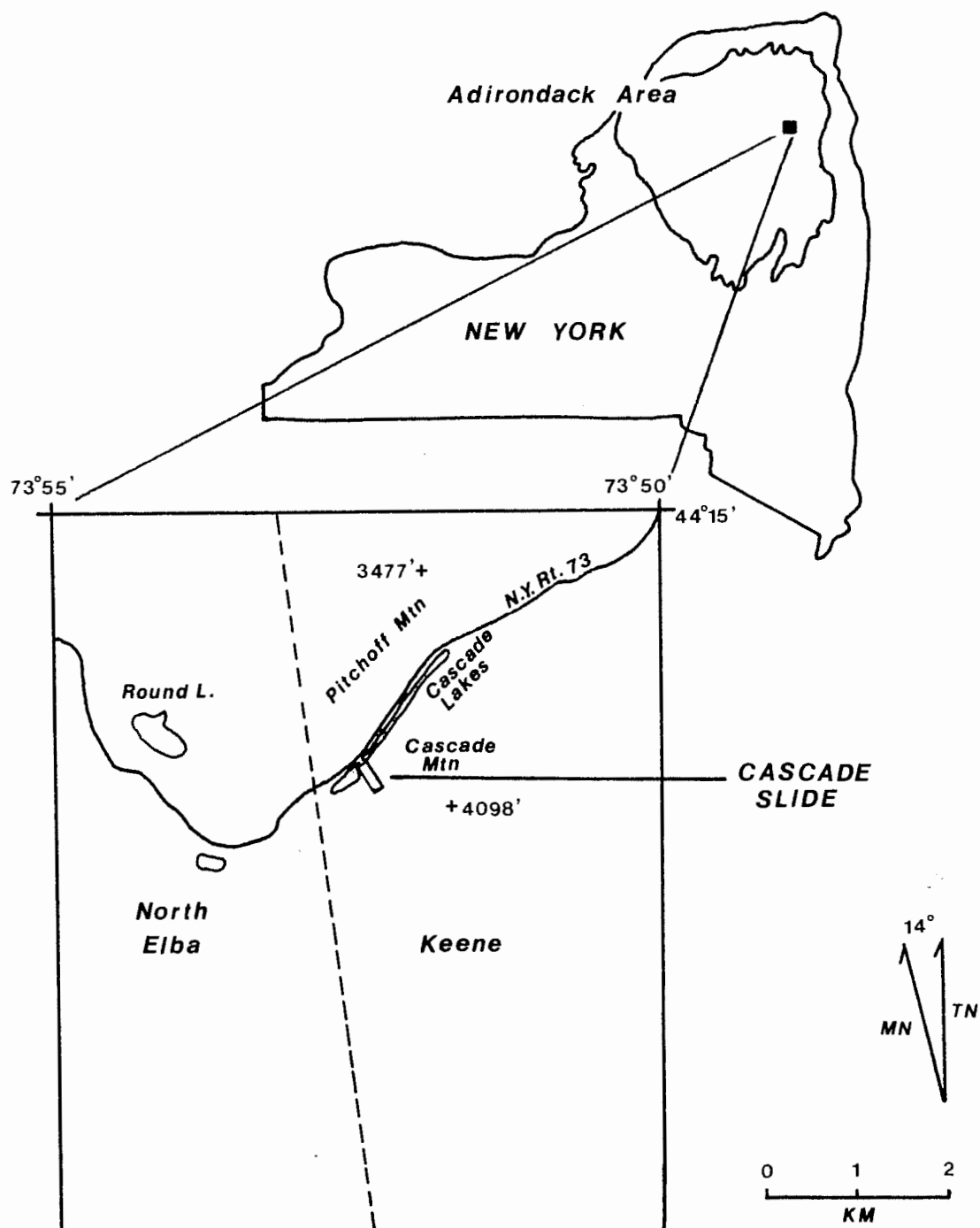


Figure 1. Index map, northeastern part of the Mount Marcy quadrangle, Essex Co., New York.

Lakes] . . . The limestone is the coarse crystalline variety, and generally white. For some distance by the side of the limestone there is a small trap [diabase] dyke, and there the limestone is frequently green. When the surface has been exposed to the air for some time, this color changes to a beautiful blue, a circumstance not easily accounted for. The iron and limestone, as well as the main rock, is cut through by these dykes. In the limestone near the dykes there is a very splendid variety of green coccolite [hedenbergite], together with imperfect crystals of diopside. It contains also phosphate of lime [apatite], garnet, idocrase, and another mineral which we suppose to be a nondescript.

In a second description of the Cascade Slide (1842), Emmons interpreted the calc-silicate as a dike of calcite intruded in the norite [anorthosite], and this time included scapolite in the list of minerals. Hall (1885) mentioned the presence of magnetite in limestone in the neighborhood of the Cascade Lakes. Kemp (1893) located the Cascade Slide on his map of Keene, and considered the whole mass as "doubtless a fragment caught up in the intruded anorthosite."

In recent years the Slide has come under the scrutiny of Dr. H.W. Jaffe, of the University of Massachusetts, and Elizabeth B. Jaffe, who are presently remapping the geology of the Mt. Marcy Quadrangle.

Field Work

In June, 1974, field work commenced with the construction of a base map by the tape and compass method. elevations were computed trigonometrically from leveling data and later checked by altimeter. In July, 1975, two weeks were spent examining the geology and structure of the Slide. Final additions to the geology were made in October of the same year. The accompanying geologic map (plate 1) represents the

synthesis of the data gathered during these field seasons.

Samples for analysis were collected in three parts. Accurately located samples (labelled TM) were gathered during the course of the field work. Some material came from Mr. Spencer Cram, an Adirondack Park ranger, who made available for study his entire collection of specimens from the Slide (labelled SC). Although the precise location of these samples is not known they are unusually fine representatives of the mineral assemblages and are therefore considered. Other samples of Cascade Slide rocks reported on here were collected by Dr. Jaffe, and are so labelled in the text. Samples referred to in this study are located, where possible, on the map.

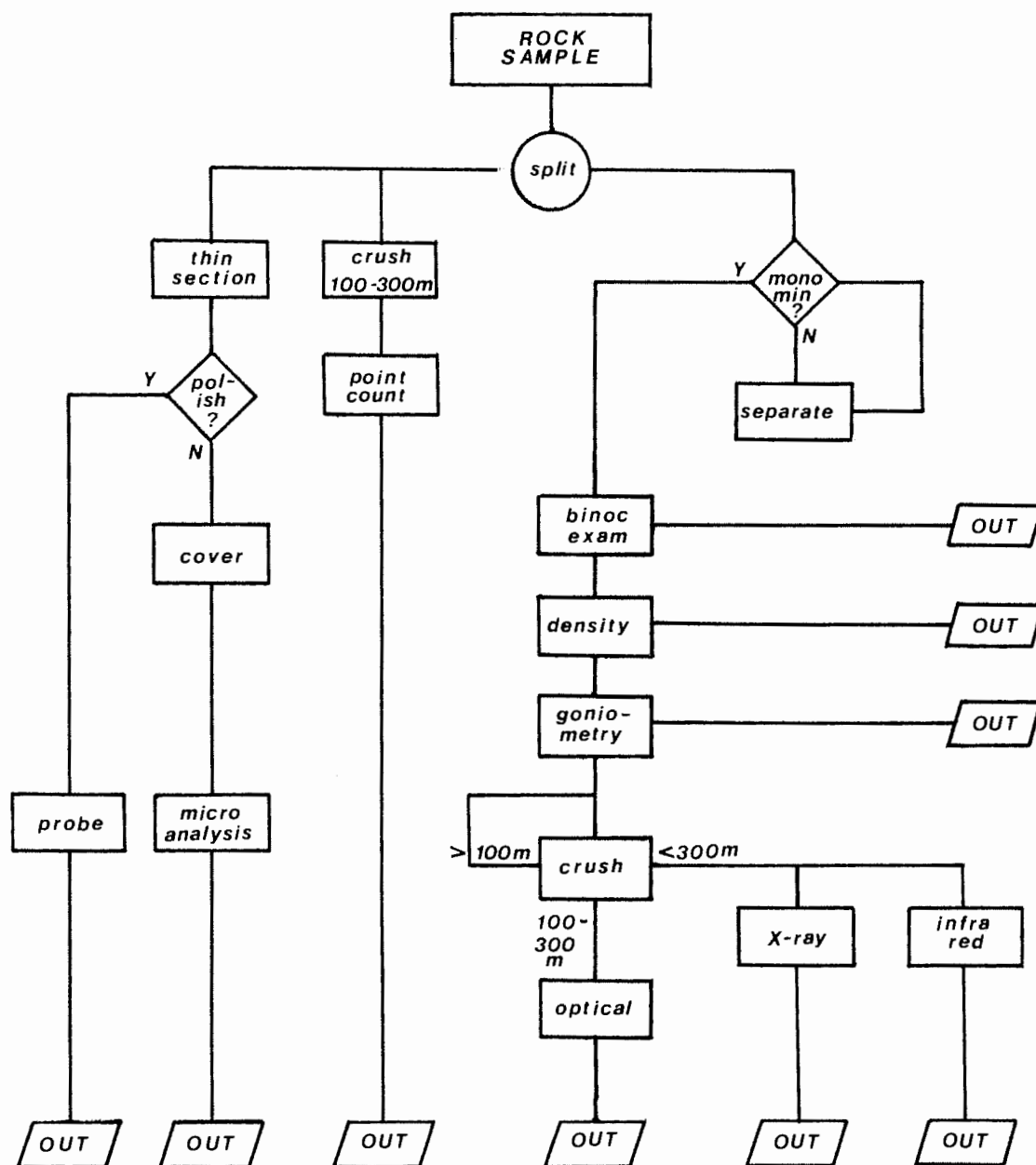
Methods

For analysis, samples were prepared according to the scheme given in figure 2, although not all samples were analysed in every category.

X-ray powder diffraction studies were performed with a Philips Norelco diffraction unit utilizing a 57.3 mm Philips Debye-Scherrer powder camera. This size camera provides a convenient scale of $1^\circ = 1 \text{ mm}$. Throughout, an iron diffraction tube with a manganese filter was employed to obtain monochromatic iron $K\alpha$ radiation. Settings of 45 KV and 10 mA were used. Film patterns were read according to methods described in Azaroff and Buerger (1958), and McKie and McKie (1974). Cubic mineral patterns were indexed directly, all others being compared to patterns reported in the literature and the JCPDS¹ file.

¹ Joint Committee on Powder Diffraction Studies.

Figure 2. Flow chart detailing the sample analysis scheme.



Chemical analyses were performed with an ETEC Mark I Autoprobe (Electron Microprobe). Polished thin sections and grain mounts were carbon coated prior to analysis. Standardization was carried out using standards from the Departmental listing. Care was taken to select standards with elemental concentrations and structures similar to the minerals being analysed. Good results were obtained from the Bence-Albee correction procedure (except for spinel, discussed separately). By broadening the electron beam slightly and decreasing the specimen current it was even possible to attain accurate analyses for fluorine.

Detailed optical analyses and textural investigations were carried out using standard transmitted light petrographic microscopes. Refractive index studies utilized crushed grain mounts (100-200 mesh), as did the whole rock modal analyses. To obtain accurate estimates of mineral content in selected rocks the statistical counting technique of Chayes (1945) was employed. Crystal surfaces were examined with a stereo-microscope. Limited studies of fluorescent inclusions in a calcite sample were done using a Zeiss ultra-violet microscope with dark field condenser.

Goniometry and a detailed study of crystal faces were performed at Amherst College on a goniometer manufactured by Robert Huber Diffraktions-technik. Methods employed are described thoroughly in Terpstra and Codd (1961) and McKie and McKie (1974).

Two samples of calcite were examined by infra-red spectroscopy.

Densities of monomineralic grains were measured with a Berman torsion beam density balance, using toluene as the immersion liquid.

Acknowledgements

This research project was suggested and greatly aided by my thesis advisor, Dr. Howard W. Jaffe. He and his wife, Elizabeth B. Jaffe, introduced me to the field area and provided geological orientation to the problem in the early stages of the investigation. Field expenses and publication costs were underwritten by National Science Foundation Grant GA-31989, to Drs. H.W. Jaffe and Peter Robinson for study of the metamorphic facies in west-central Massachusetts and the Adirondacks. I am particularly indebted to Mr. Spencer Cram of Keene, New York, for supplying many fine study specimens of minerals from the Cascade Slide. Several helpful discussions were carried on with Drs. Stearns A. Morse, Stephen H. Haggerty, and Peter Robinson. William Ranson assisted in examining the phase petrology of the calc-silicate assemblages, and Ruth Kalamarides performed the infra-red absorption analyses. I would also like to thank Dr. C. Cox, of the Microbiology Department, for allowing me to use their ultra-violet microscope, and Dr. J. Klekowski and Mr. D. Poppel, of the Botany Department, for aid in photographing the crystal surface textures. My greatest appreciation, however, must go to my wife, Deborah, field assistant par excellence, who aided in all phases of this investigation.

GENERAL GEOLOGY

The Adirondack Highlands are part of the Adirondack Massif of northeastern New York State. According to Buddington (1939, 1969) this rock mass was formed by the intrusion of a magma of gabbroic anorthosite into a sequence of sedimentary and volcanic strata, locally referred to as the Grenville Series. He infers that the pluton took the shape of a biconvex lens, 3-4 km thick, and was derived from at least two deep seated stocks (extending downward at least 10 km). Closely associated with the now metamorphosed sedimentary and volcanic units is a pyroxene-microperthite gneiss of possible igneous origin.¹

The Adirondack anorthosite series consists of rocks of variable composition, containing plagioclase in the range, An_{30} - An_{50} . The series is subdivided according to the percentage of mafic minerals (Buddington, 1939):

	% mafics
anorthosite	<10
gabbroic anorthosite	10 - 22.5
anorthositic gabbro	22.5 - 35
gabbro, norite	35 - 65
melagabbro	>65

Magnetite-ilmenite ore concentrations are commonly associated with the anorthosite and are used as geothermometers in piecing together the history of the magma (Buddington and Lindsley, 1964). A large ore body, located near Sanford Lake (15 km west of the map area) is mined for the

¹This unit includes rocks classed by Buddington (1939) as pyroxene-quartz syenite, or mangerite, and by de Waard (1968) as mangerite, jotunite, farsundite, and charnockite.

titanium content of the ilmenite by the National Lead Company. Studies are still in progress to determine the exact processes by which differentiation of the anorthosite series occurred.

As the Marcy anorthosite series was emplaced, its rise caused recumbent folds, or nappes, to develop in the overlying country rock. These folds are now seen as stratigraphically discontinuous "screens," or remnants, of the pre-metamorphic stratigraphy. Some contact metamorphism of the country rock undoubtedly occurred, and both the enfolded screens and anorthosite underwent a major regional metamorphism about 1130 m.y. ago (Silver, 1968). One typical sedimentary remnant is the Cascade Slide. It is considered to have originally consisted of layered siliceous or argillaceous dolomites and minor volcanics of the Grenville Series, now enfolded in and metamorphosed with the pyroxene-microperthite gneiss and anorthosite (H.W. Jaffe, pers. comm.). Brown and Engel (1956) in their revision of the Grenville stratigraphy in the northwest Adirondacks describe 650 meters of siliceous dolomites underlain by up to 970 meters of paragneiss.

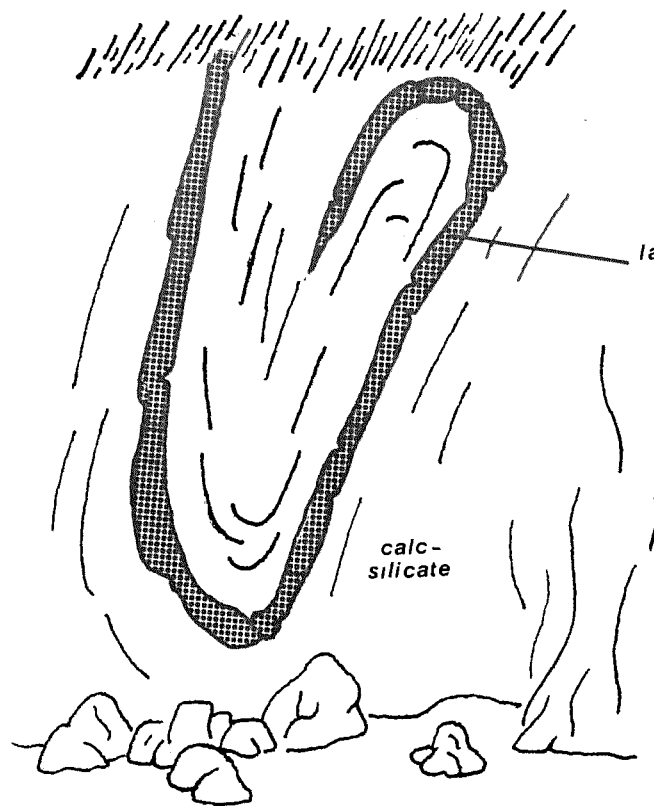
The geologic map (Plate 1) shows the placement of the rock units identified in the Slide. From the contact relationships observed it becomes obvious that the calc-silicate assemblages occur as bands, probably related to original sedimentary layering. No zoning as reported for contact metamorphosed calcareous skarns has been found. Apparent discontinuities between the layers is due to deep erosion following multiple deformations. At present it is impossible to distinguish the original stratigraphic order of the units.

Closely associated with the Cascade Slide calc-silicates, and

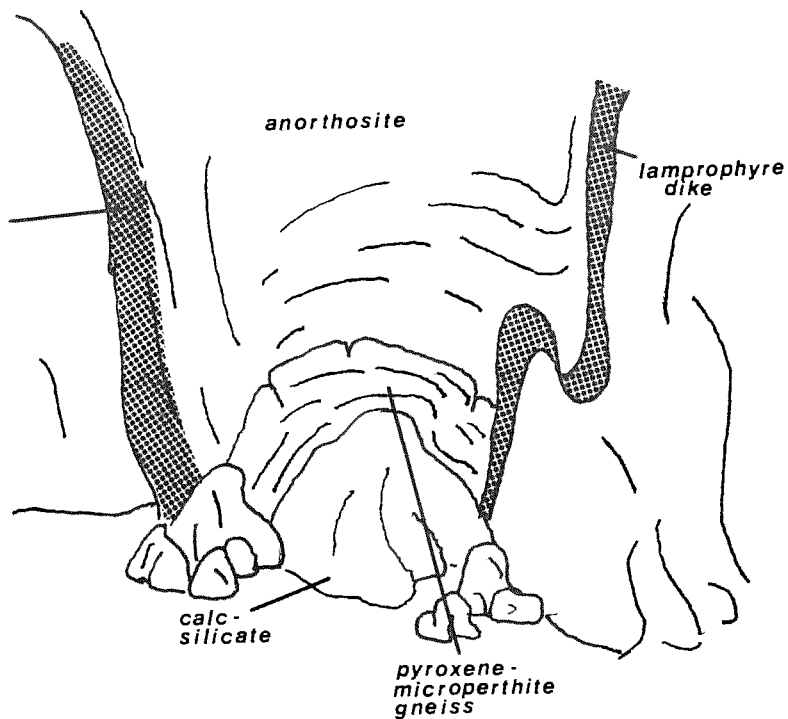
almost universally found between them and the anorthosite is the pyroxene-microperthite gneiss. In places the micro-perthite has been partially to totally altered to scapolite in a metasomatic reaction with the calc-silicate. As a result of detailed mapping it is felt that this gneiss unit represents the metamorphosed equivalent of a volcanic layer (rhyolite/trachyte) associated with the original sedimentary succession overlying the anorthosite. Elsewhere in the Adirondacks a similar rock unit is found in close association with other calc-silicate remnants.

A recumbent fold overturned to the east and plunging roughly NNW is indicated by the repeat of rock units in the Slide. This is the dominant structural feature in the area and is mimicked by other nearby calc-silicate sequences. Cross folds with axes plunging approximately east-west at 20° are considered to represent a second period of folding. There is not enough contrast between the different calc-silicate layers to show up on film so that two sketches of the cross folds observed at the fourth pool are shown in figure 3. Figure 4 is a cartoon showing the relationship of the two major fold sets in the Cascade Slide. The pattern of waterfalls, dropping abruptly from one pool level to the next is probably related to the cross folding. Indeed, at the rock face between the third and fourth pools an eroded sheet of scapolite bearing rock is seen to wrap around the coarse augite marble, creating the fall.

Numerous camptonite and diabase dikes cut across the Slide in an approximate east-west direction ($N80^{\circ}E - S80^{\circ}E$). These dikes appear to be of two distinct ages. Some have been emplaced along planes of weakness in the calc-silicate caused by the cross folding; others, intruded at an earlier time, have been folded right along with the calc-silicate (figure 3).



Fold expressed by lamprophyre dike on the east wall.



Fold in calc-silicate, anorthosite and lamprophyre on the west wall.

Figure 3. Folded rock pattern seen on the walls of the Cascade Slide at the fourth pool (see plate 1 also).

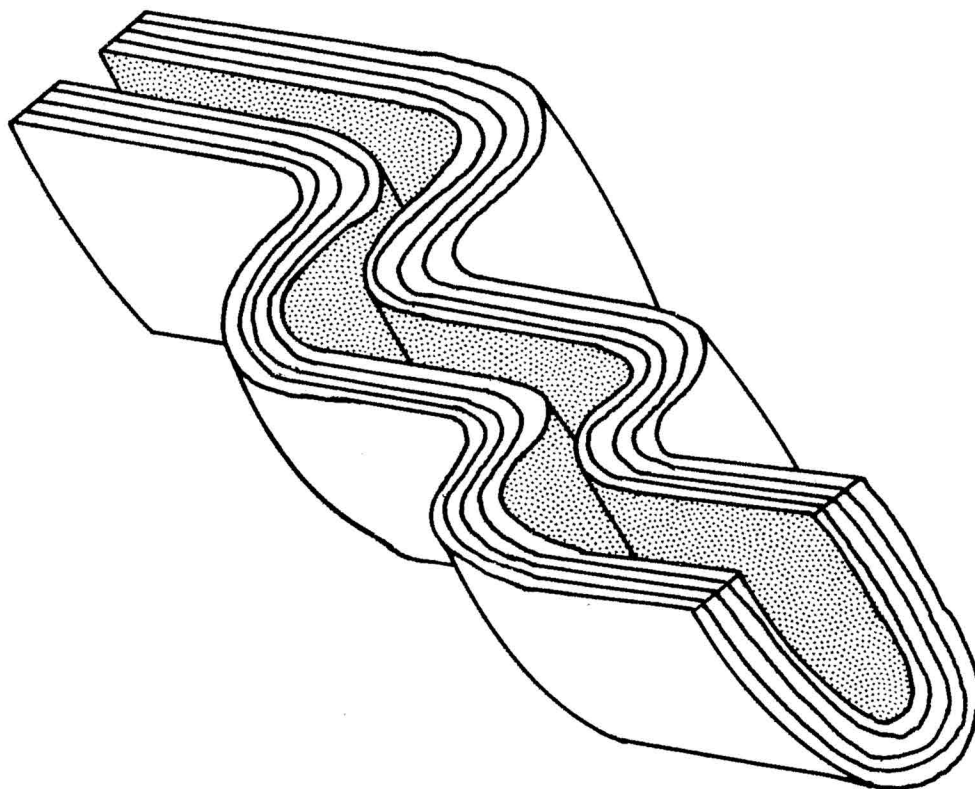


Figure 4. Diagrammatic sketch of the fold pattern observed for the Cascade Slide, looking southwest.

PETROGRAPHY

Several distinct mineral assemblages comprise the Cascade Slide calc-silicate body. These are illustrated on the geologic map (plate 1). Roughly, these assemblages can be thought of as relics of an original layered sedimentary sequence consisting largely of argillaceous and siliceous dolomites. Metamorphism to the pyroxene granulite facies, with attendant metasomatism, has in some places obscured this original layering. In other places the layering is readily visible or may be inferred from contact relations. Differences in both mineral composition and texture distinguish the calc-silicate layers. Modal analyses of the varied calc-silicate rocks are presented in Table 1, and several of the more characteristic assemblages are graphically represented on the ternary diagram of figure 6.

Augite and Monticellite Marble

Perhaps the most striking if not the most widespread rock unit, is a coarse marble (grain size approximately 1-3 mm). Calcite and augite are the ubiquitous components of the marble which may also include major monticellite, magnetite, and vesuvianite. Minor constituents are apatite, forsterite, spinel, harkerite, perovskite, and garnet (not all found together). Generally a layering is present between the different major components of the marble, but the actual contacts are diffuse. A metasomatic migration of ions, probably within a fluid phase, appears to have made gradational boundaries the rule. Typical modal analyses for

Table 1. Estimated and measured modes of calc-silicate rocks from the Cascade Slide. All sample locations are given on Plate 1.
* indicates visual estimates.

	* TM-16	* TM-17	* SC-22	* SC-92	TM-6	TM-18	TM-23	TM-30	* SC-88	SC-33	TM-27
Calcite	62	78	60	70	0.7	-	0.3	-	50	2	6.6
Augite	2	4	20	-	63.3	38	32	48	30	53	16.6
Garnet	-	-	-	-	32.6	-	51	1.6	20	45	44
Monticellite	33	12	-	-	-	-	-	-	-	-	-
Forsterite	1	1	-	-	-	-	-	-	-	-	-
Spinel	1	-	-	-	-	-	-	-	-	-	-
Harkerite	1	-	-	-	-	-	-	-	-	-	-
Scapolite	-	-	-	-	-	54	11.3	44	-	-	-
Vesuvianite	-	5	-	-	-	-	-	-	-	-	-
Wollastonite	-	-	-	-	-	-	-	-	-	-	30
Sphene	-	-	-	-	+	4	0.3	1.3	-	-	-
Apatite	-	-	-	-	-	0.3	-	4.3	-	-	-
Magnetite	-	-	20	-	-	0.6	0.6	-	-	-	-
Graphite	-	-	-	30	-	-	-	-	-	-	-
Hypersthene	-	-	-	-	-	3	-	-	-	-	-
Microperthite	-	-	-	-	-	-	4.3	-	-	-	-
Other	-	-	-	-	3.4	1	-	0.6	-	-	2.6

the marble are given in Table 1 (TM-16, TM-17, SC-22, SC-92). These samples illustrate the wide range of compositions possible within the marble unit. TM-16 and TM-17 contain significant amounts of monticellite, accompanied by spinel or vesuvianite, but with little augite. Figure 5 is a drawing of a typical thin section view of the monticellite-bearing marble, showing textural relationships. SC-22, also part of the marble unit, has abundant augite but no monticellite. Texturally, however, the two marbles are identical, and in the field show continuous gradation from one to another. Neither of these two types show reaction rims around minerals, or zoning, that would indicate disequilibrium (Hyndman, 1971). Occasionally, a grain of monticellite or forsterite may contain inclusions of spinel or graphite, but again without sign of disequilibrium.

SC-92 shows a divergence from the typical marble seen in the Slide. It contains graphite, but no augite or monticellite. Whether the graphite represents original organic material in the Grenville sediments or was derived from a decarbonation reaction involving the calcite is not known.

A significant feature of the coarse marble is the coexistence of forsterite and monticellite in the same rock (figure 5) and indeed in a single grain (H.W. Jaffe, P. Robinson, and R.A. Tracy, in preparation).

Scapolite Gneiss and Granulite

At several locations along the margins of the Slide there are patches of calc-silicate rock containing scapolite. In all instances these are in direct contact with the surrounding pyroxene-microperthite gneiss, suggesting a metasomatic introduction or transfer of sodium, potassium, and perhaps chlorine from the gneiss into the carbonate unit

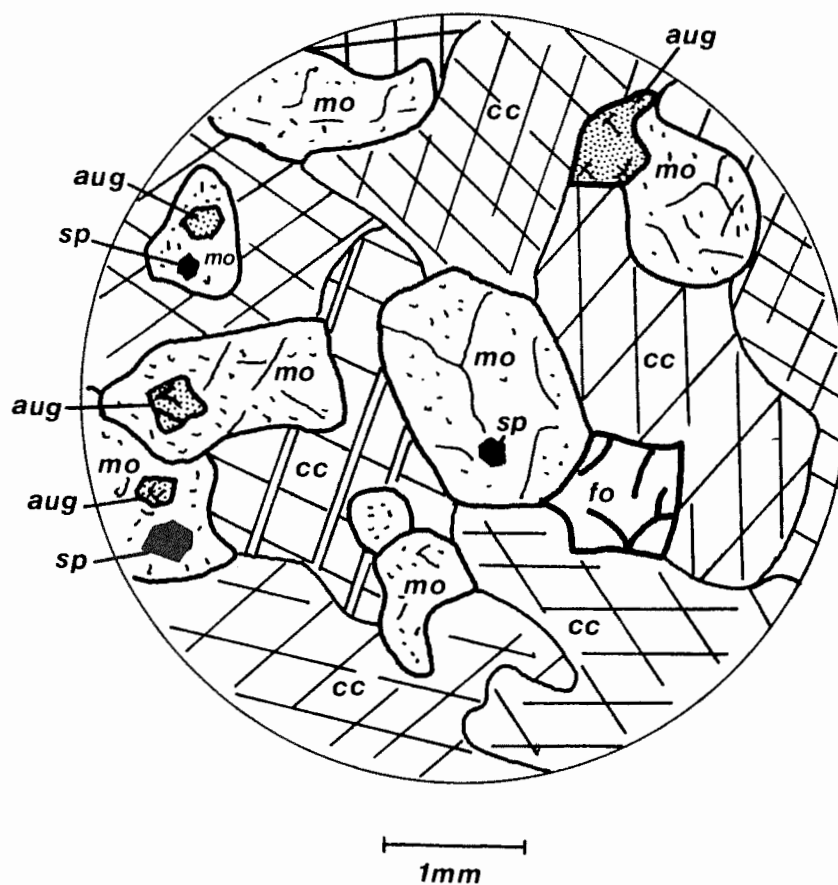
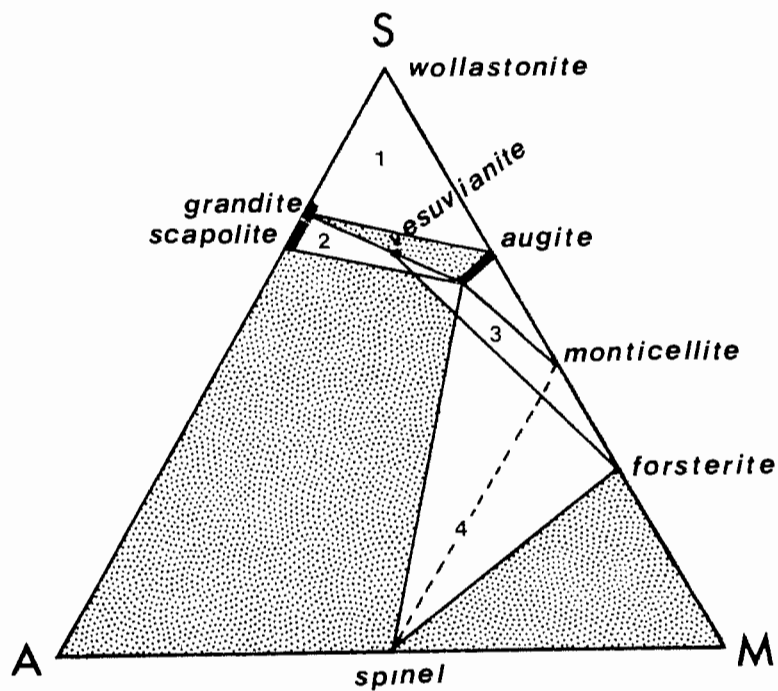


Figure 5. Thin section view of part of specimen Ca-22, monticellite marble, showing monticellite (mo), in contact with forsterite (fo), augite (aug), and calcite (cc). Inclusions of augite and spinel (sp) in monticellite are abundant. Plane polarized light.



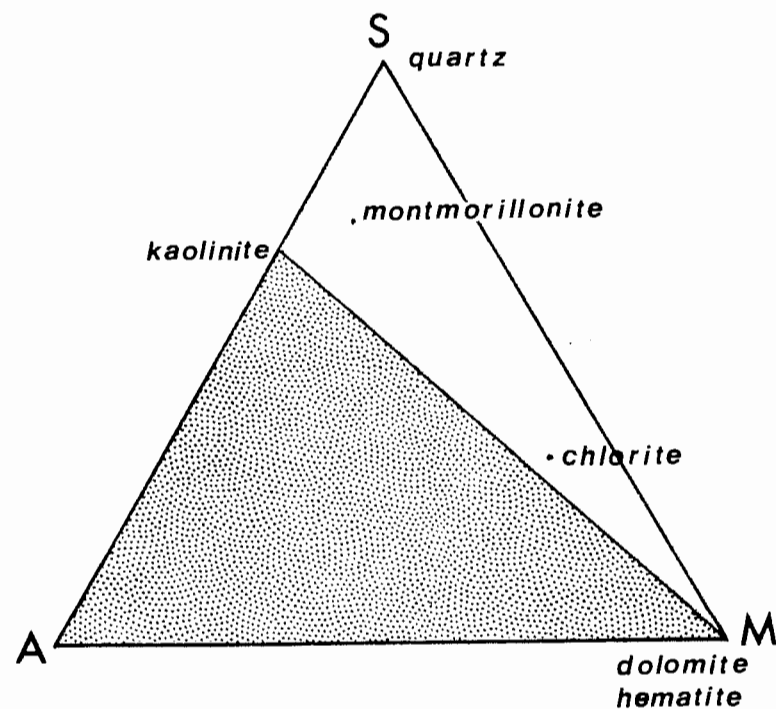
S = SiO_2

A = Al_2O_3

M = $\text{MgO} + \text{FeO} + \text{MnO}$

CaCO_3 , H_2O , F, Cl in excess

grandite = grossular + andradite



Assemblages

1. TM-27, woll.-gross. granulite
2. TM-30, scapolite gneiss
3. TM-17, augite-monticellite marble with vesuvianite
4. TM-16, augite-monticellite marble with spinel

Figure 6. SAM (SiO_2 - Al_2O_3 - MgO) diagrams for argillaceous dolomites metamorphosed in the pyroxene granulite facies at Cascade Slide, Adirondacks, New York.

to form the scapolite. This would probably have occurred during the thermal peak of the metamorphism. Typical modal analyses for the scapolite gneisses are given in Table 1 (TM-18, TM-23, TM-30). The presence of hypersthene and feldspar, and the lack of calcite suggest that the scapolite-bearing assemblages are igneous in origin. Frequently the original igneous texture is maintained. However, near the wall of the third pool (see map, plate 1) a zone of scapolite megacrystals forms a coarse granulite. Single crystals of scapolite range in size from 1 cm long to one with a cross section of 24 cm and an undetermined length (figure 7). Associated with the scapolite are large masses of calcite and occasional augite megacrystals, rimmed by garnet. This granulite zone is also in contact with the pyroxene-microperthite gneiss.

The large crystals are random in growth pattern, but from their size and well developed terminations it appears that they were free growing. This raises the possibility of there once having been a fissure in the rock in which the crystals could grow without interference. Two causes for such a fissure come to mind: tectonic activity associated with the metamorphism, and volumetric change upon metasomatism. The latter possibility is impossible to confirm as the exact nature of the original rock types is unknown, as well as the extent of ion change.

Wollastonite-Garnet Granulite

There are two separate occurrences of wollastonite in the Cascade Slide calc-silicate body. On the far southeastern wall of the Slide there is a band of sugary textured rock composed of wollastonite, diopside, grossular, and minor calcite. A modal analysis for this unit

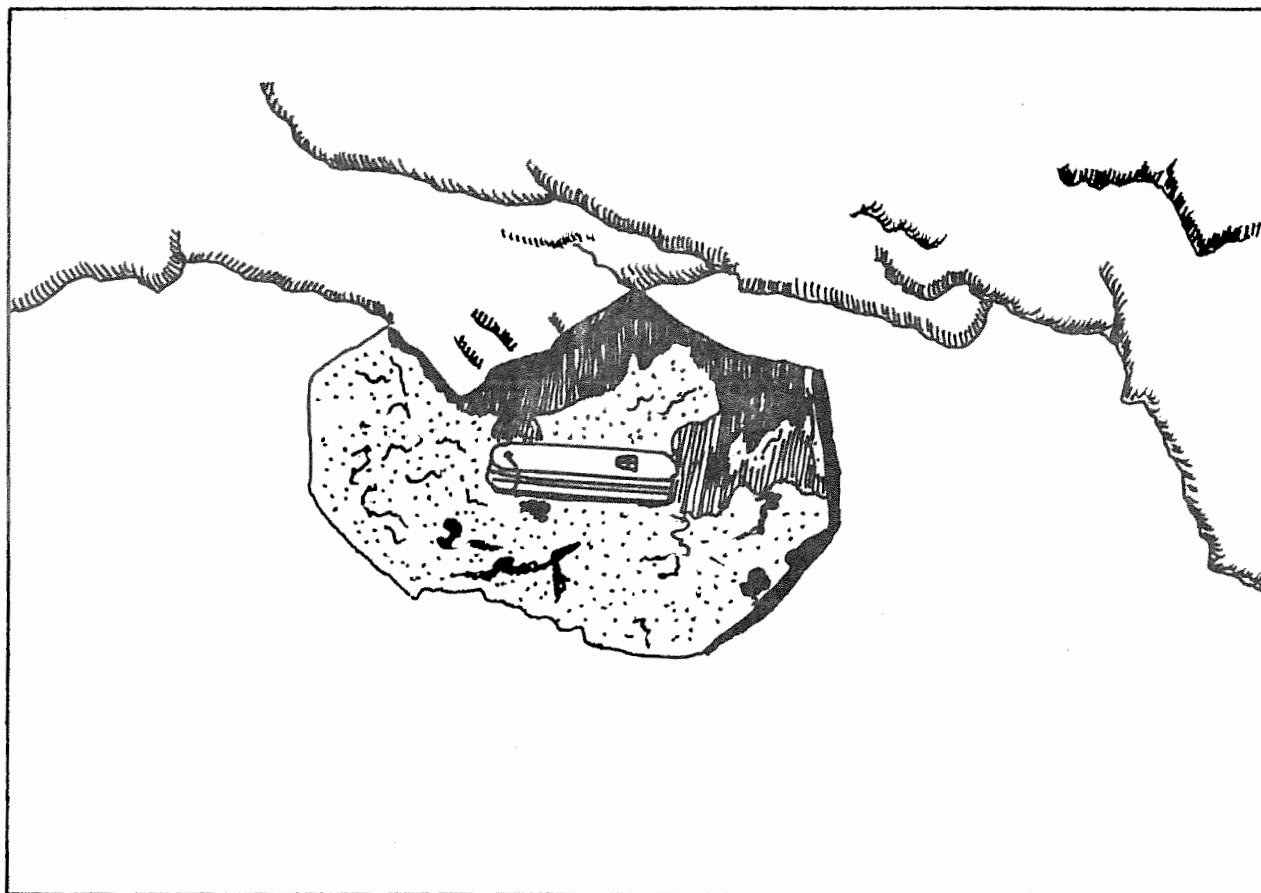
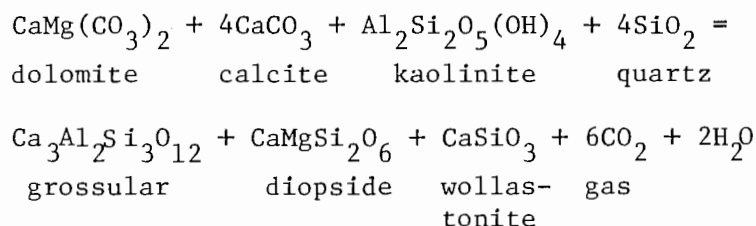


Figure 7. Sketch of a single large crystal of scapolite found at the third pool. The crystal is 24 cm across.

is given in Table 1. It appears to be an equilibrium assemblage with the minerals being heterogeneously mixed and not showing any significant reaction features. Triple junction grain boundaries at 120° are common. Figure 6, a ternary SAM plot shows the stabilized relationship of this assemblage. This type of assemblage is very common in contact metamorphosed skarns, forming only at high temperatures unless P_{CO_2} is decreased.

A non-equilibrium assemblage of the same minerals is found near the fourth pool, within the augite-granulite unit. A large area of massive wollastonite (13 x 13 cm) was found, containing several smaller inclusions of blue calcite (see figure 8). Surrounding the wollastonite is a reaction zone (largely composed of easily weathered wollastonite) giving way to a layer of nearly end member diopside. Beyond the diopside is a thin band of grossular, and finally the more iron rich pyroxenite. This represents a decarbonation reaction of a piece of argillaceous dolomite. Mg and Al appear to have migrated to separate zones on the periphery. The presence of the remaining calcite indicates that there may not have been enough free SiO_2 to convert all the $CaCO_3$ to $CaSiO_3$. A possible reaction is:



Augite Granulite

Probably related to the augite-garnet gneiss is the augite granulite

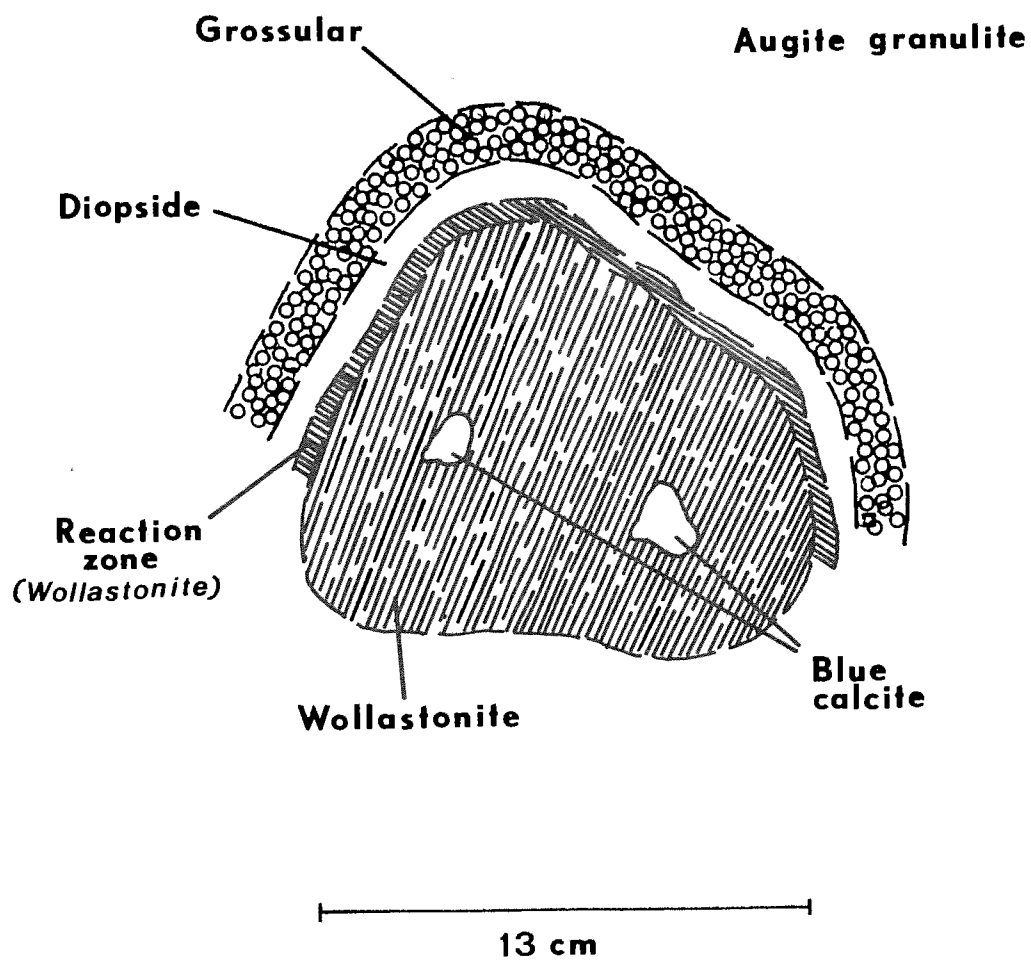


Figure 8. Metasomatic reaction zone involving a dolomite (?) inclusion in the augite granulite.

unit. This is composed primarily of coarse augite, varying amounts of calcite, and finer grained andraditic garnet. The rock is extremely friable, crumbling easily to the touch. It can be differentiated from the augite-garnet gneiss in both the composition of the garnet and its textural appearance. Some parts of the unit have up to 30% garnet; elsewhere this mineral is non-existent. In general the grain size of the augite is 2-4 mm with megacrystals larger than 2 cm occasionally found free growing in pockets. The garnet seldom exceeds 1 mm in size, and it appears that the larger the augite, the less garnet there is with it. Sample modes for the augite granulite are given in Table 1 (SC-88, SC-33).

Augite-Garnet Gneiss

This is a fine-to medium-grained, commonly layered rock (grain size 0.1-1.0 mm) composed almost entirely of augite and garnet. The rock is found throughout the lower part of the Slide, abruptly terminating at the base of the first pool. To the south it is probably gradational into the augite granulite, upstream of the fourth pool. A common feature of this unit is the presence of gneissic banding developed from the separation of augite and garnet into distinct layers, usually 3-4 mm in width. A typical modal analysis measured across the layering is given in Table 1 (TM-6).

The garnet is intermediate between grossular and andradite (based on microprobe analysis). The augite is highly calcic, lying along the diopside-hedenbergite tie line (see figure 15). The lack of calcite is notable and suggests that this unit may be the metamorphic equivalent of

an igneous rather than a calcareous layer in the Grenville succession.

Pyroxene-Microperthite Gneiss and Anorthosite

Surrounding the calc-silicate units is the layer of pyroxene-microperthite gneiss. It appears to exist nearly everywhere between the calc-silicate rocks and the anorthosite. This seems to indicate that the pyroxene-microperthite gneiss was an original layer in the Grenville succession. An extrusive rock of trachytic or rhyolitic composition would most likely yield the present mineralogy. There is a possibility of a genetic relationship to the precursor of the augite-garnet gneiss, such as a differentiated flow, or a basalt and tuff. The pyroxene-microperthite gneiss does not appear to be derived from the anorthosite, at least in this place, as thought by some (de Waard, 1968). Modal analyses of the anorthosite and the pyroxene-microperthite gneiss found near the Slide are given in Table 2, and graphically plotted on ACF and AKF diagrams in Figure 9.

The compositions of both rock types, especially the pyroxene-microperthite gneiss, are observed to vary throughout the mapped area, probably due to metasomatic exchange of ions with the calc-silicate. The fact that the pyroxene-microperthite gneiss is sometimes gradational into the calc-silicate is a further indication of this.

The anorthosite generally contains blue andesine megacrysts (An_{48}) in a groundmass of white andesine (An_{40}) with minor augite (Fe'_{40-55})¹, hypersthene (Fe'_{55}), garnet, ilmenite, magnetite, and hornblende. The

$$^1Fe' = 100(Fe^{+2} + Fe^{+3} + Mn) / (Mg + Fe^{+2} + Fe^{+3} + Mn).$$

Table 2. Measured modes of anorthosite, gabbro of the anorthosite series and pyroxene-microperthite gneiss, from the Cascade Slide region. All sample locations are given on Plate 1.

	PO-1 [*]	TM-19 ^{**}	TM-25 ^{***}
Microperthite	-	72	-
Orthoclase	5.8	-	-
Andesine megacrysts	13.3	-	39.0
Andesine matrix	58.3	-	
Augite	6.5	22	25.6
Hypersthene	3.4	2	10.0
Garnet	3.4	-	18.3
Ilmenite	4.3	0.3	-
Magnetite	0.6	-	4.0
Hornblende	3.6	-	-
Apatite	0.8	-	0.6
Undetermined	-	2	-

* Typical gabbroic anorthosite from roadcut near Cascade Lakes, New York Highway 73. (Jaffe, et al., 1975)

** Typical pyroxene-microperthite gneiss from the Cascade Slide.

*** Gabbro of the anorthosite series found near the margin of the Cascade Slide.

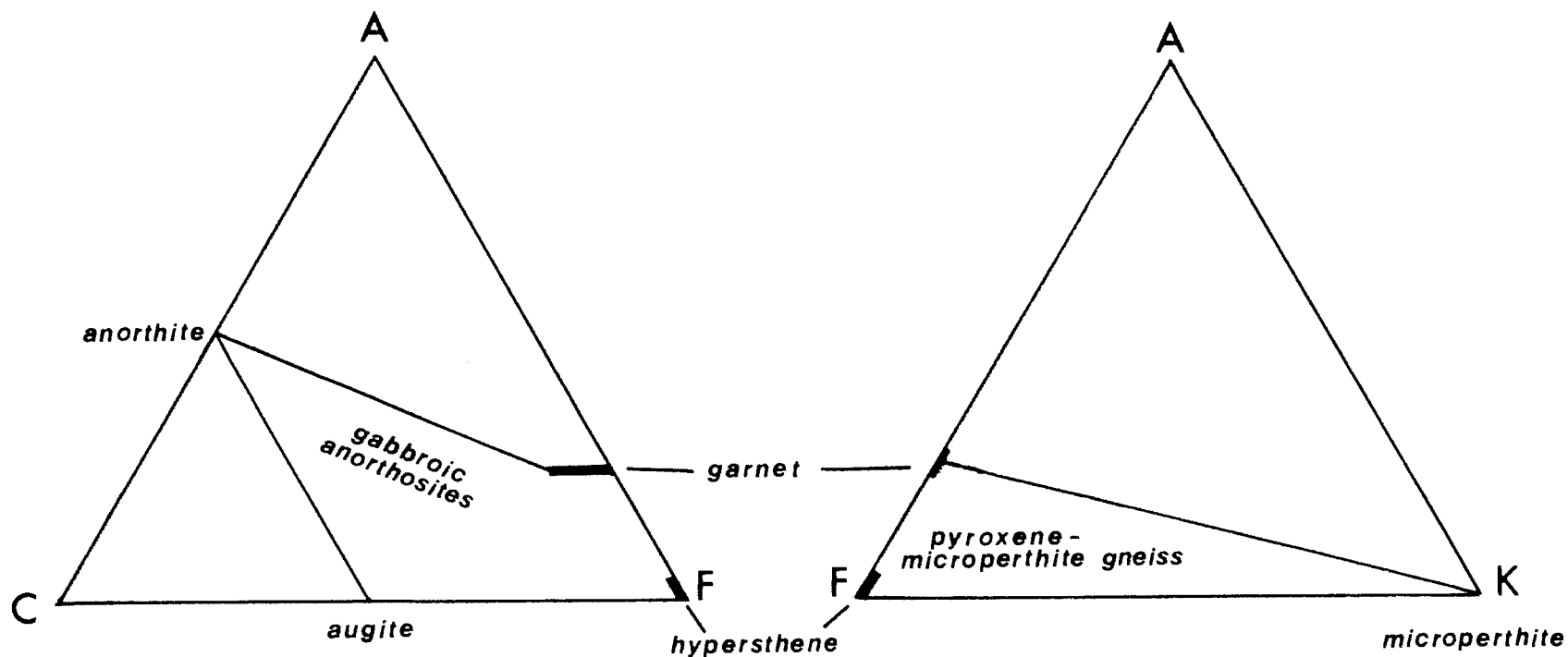
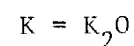
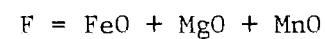
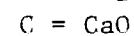
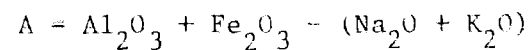


Figure 9. ACF and AKF diagrams for gabbroic anorthosite and pyroxene-microperthite gneiss ("mangerite-charnockite" series) metamorphosed in the pyroxene granulite facies, Cascade Slide area, Adirondacks, New York.



SiO_2 in excess

pyroxene-microperthite gneiss is dominated by microperthite. Hypersthene (Fe'_{40}), augite (Fe'_{35}), garnet, and apatite are the minor constituents.

The petrology of the Cascade Slide poses some interesting geologic problems. Previously mentioned was the coexistence of monticellite and forsterite in the same rock. As perplexing is the very existence of monticellite at all. This mineral is common in contact metamorphosed rocks, but not in regionally metamorphosed ones. On Pitchoff Mountain (immediately north of the Slide) high iron ferrosilite (Fs_{96}) has been described (Jaffe, et al., 1974). The presence of this mineral indicates regional metamorphism under conditions of high pressure, in the neighborhood of 8 kb. At such a pressure, and in the presence of CO_2 , monticellite should not be a stable phase below 1600°C . A small fault does exist between the site of the ferrosilite and the Slide, but there is no indication that movement down it was great enough to cause a large pressure change.

The only way to stabilize monticellite under these conditions is to decrease the activity of CO_2 by means of some diluent. An increase in the activity of H_2O along with F would be the easiest way to accomplish this. However, there are no significant amounts of hydrous minerals in the Slide which would be expected in the presence of water vapor. If water were available in the quantities necessary to allow formation of the monticellite much of the pyroxene should have been converted to amphibole. There is no amphibole present (except as very minor inclusions in some augite megacrystals) in the Slide. There is no evidence for any minerals

in the Slide being relics of previous metamorphisms. There is, however, evidence of a slight retrograde alteration in occasional specimens of the olivine bearing marbles in which forsterite, and to a lesser extent, monticellite grains have been fractured, embayed, and altered to serpentine. Thus, it must be assumed that the major regional metamorphism occurred with pressures that have been estimated from 6.5-8.8 kb at 600°C or 8.8-11.2 kb at 800°C (Jaffe, et al., 1974). Also, some other fluid phase than water, which has left no readily observable trace, must be responsible for lowering the activity of CO₂. In the ensuing discussion of the individual mineral species some possible diluents will be considered.

MINERALOGY

All of the assemblages observed in the Slide are composed of approximately 15 different minerals. Each mineral, however, may occur in several habits depending on the layer in which it is found. The following list describes the properties measured for each mineral type and records the variations observed.

<u>Calcite</u>	CaCO_3 (Z=6)
Rhombohedral	Class: $\bar{3} 2/\underline{m}$
$\epsilon=1.484$	$a=4.98\text{\AA}$
$\omega=1.656$	$c=16.92\text{\AA}$
$\Delta=0.172$	Space Group: $\underline{R\bar{3}c}$
uniaxial (-)	$D_{\text{meas.}}=2.705(\text{SC-19})-2.711(\text{TM-17})$
	H=3
	Cleavage: $\{10\bar{1}1\}$ perfect
	Fluorescence: Deep violet, orange
	fluorescing rod-shaped inclusions
	in SC-19.

Form and Habit: Occurs as massive patches with scapolite megacrystals, as coarse idioblastic grains in the augite marble, as interstitial material in most other assemblages, and as recent flowstone over some augite megacrystals. It breaks showing perfect rhombohedral cleavage.

Color: Generally the calcite is white or very light blue in color. Occasional greenish varieties occur, possibly due to trace amounts of iron. Near the fourth pool, pink (manganian?) calcite was seen but is of very restricted occurrence. The frequent light blue color is probably due to microscopic fluid inclusions. These inclusions are responsible for

causing lower density and refractive indices in SC-19. Calcite is colorless in crushed amounts.

Chemistry: Though nearly pure CaCO_3 , calcite from the Slide shows trace amounts of Al, Mg, Fe, Mn, Li, and Sr. The total of these impurities never amounts to 1 weight percent of the sample.

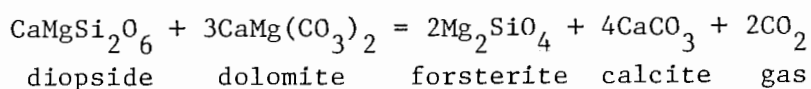
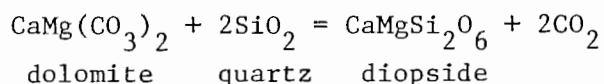
Morphology: The perfect rhombohedral cleavage of the calcite is its most obvious property. Goniometric analysis yields proof of the hexagonal symmetry. Figure 10 is a stereogram showing poles to faces as seen down the hexad axis, c. Figure 11 illustrates the symmetry of calcite observed with the projection in the zone $[10\bar{1}1 : \bar{1}101]$. Interfacial angles measured for the calcite rhombs are:

$$10\bar{1}1 \wedge \bar{1}101 = 77^\circ$$

$$\bar{1}101 \wedge 10\bar{1}1 = 103^\circ$$

X-ray: X-ray analysis shows very good matches between calcite samples from various locations in the Slide and reported powder patterns for synthetic CaCO_3 (Table 3). Minor differences in spacings and occasional extinctions are probably due to a combination of analytical error and the recorded trace impurities. Both the reported crystal class and space group are confirmed by the X-ray, and the crystallographic analysis.

Paragenesis: Calcite formed as a result of metamorphism of the original impure dolomite, possibly by the scheme of Metz and Trommsdorff (1968):



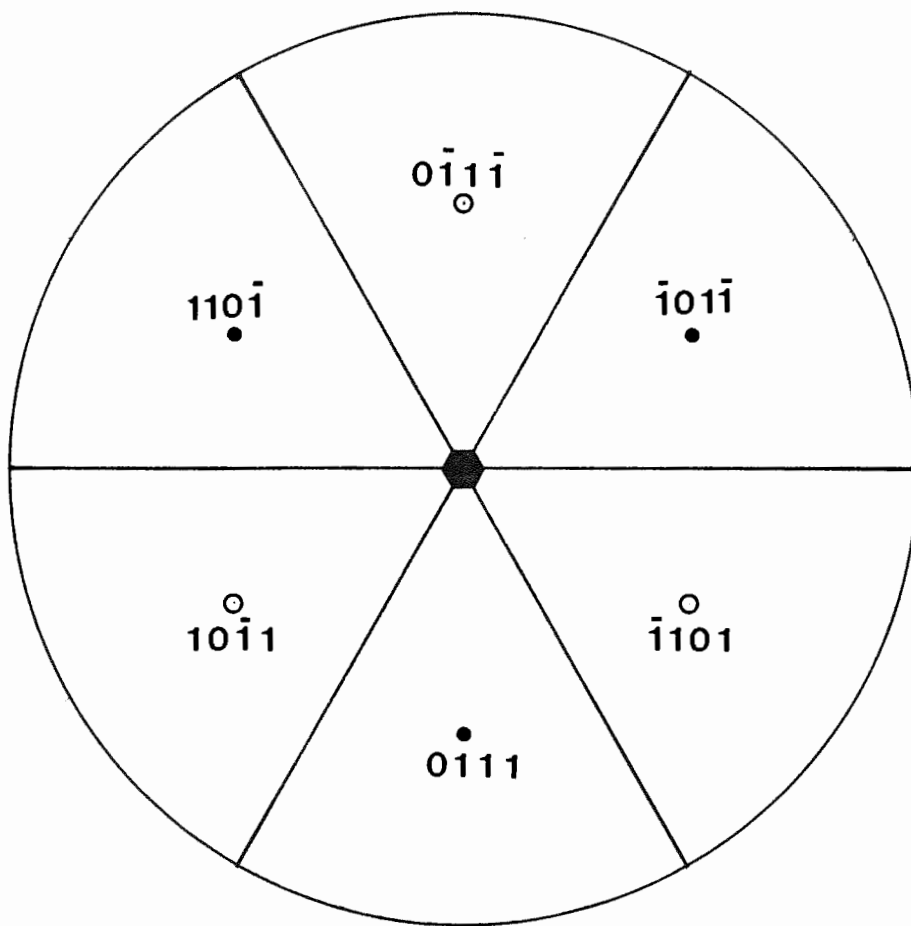


Figure 10. Stereographic projection for calcite, projected along \underline{c} .

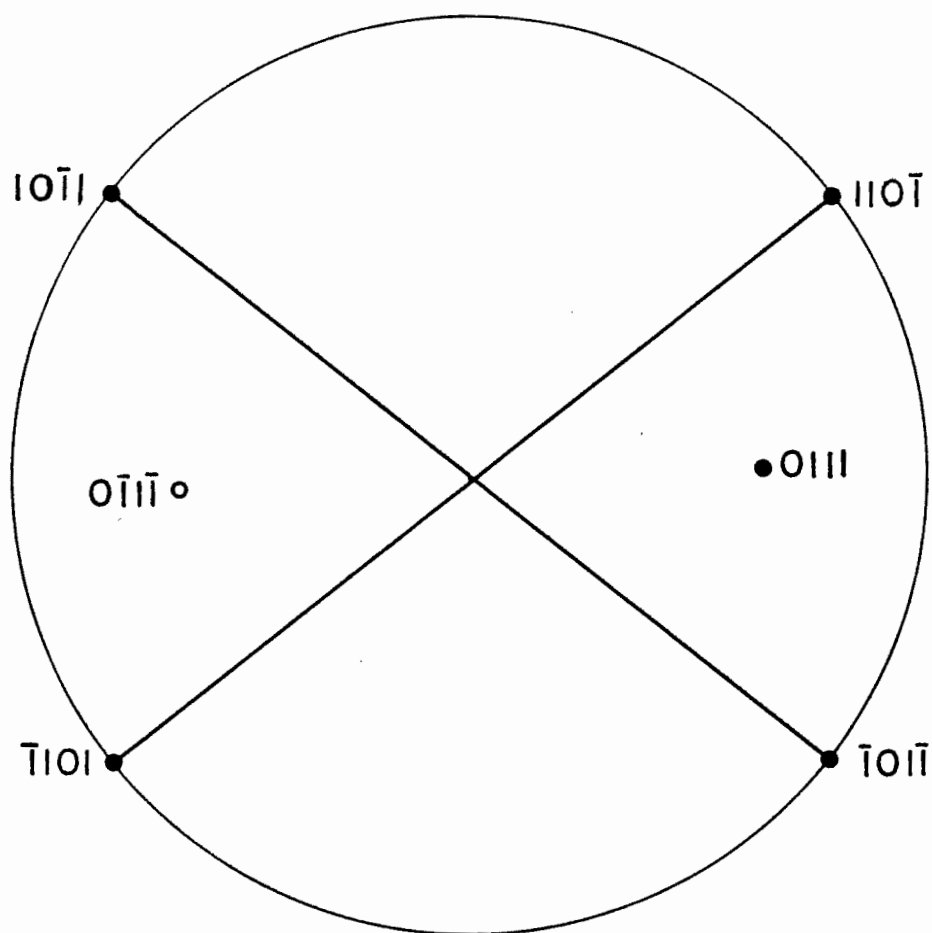


Figure 11. Stereographic projection for calcite, projected in the zone $[10\bar{1}1:\bar{1}101]$.

Table 3. X-ray powder diffraction data for calcite.

SC-19		SC-22		SC-27		Standard*		
I	d	I	d	I	d	I	d	hkl
20	3.81	15	3.80	15	3.79	12	3.86	102
100	3.01	100	3.00	100	2.99	100	3.035	104
		2	2.82	2	2.80	3	2.845	006
20	2.48	20	2.48	20	2.47	14	2.495	110
40	2.27	20	2.27	20	2.26	18	2.285	113
20	2.08	20	2.08	20	2.08	18	2.095	202
						5	1.927	204
40b	1.904	30	1.900	30	1.895	17	1.913	108
50	1.863	10	1.864	20	1.860	17	1.875	116
15	1.618	2	1.620	2	1.616	4	1.626	211
20	1.595	10	1.596			8	1.604	212
				10	1.591	2	1.587	1010
10	1.523	5	1.520	10	1.520	5	1.525	214
						4	1.518	208
10	1.501					3	1.510	119
5	1.467	2	1.468	2	1.468	2	1.473	215
20	1.435	10	1.436	10	1.434	5	1.440	300
10	1.418	7	1.414	7	1.415	3	1.422	0012
5	1.354	2	1.354	2	1.352	1	1.356	217
5	1.333	2	1.335	5	1.331	2	1.339	2010
10	1.293			10	1.291	2	1.297	218
		5	1.275			1	1.284	306
5	1.241			2	1.244	1	1.247	220
17	1.233	5	1.233	10	1.229	2	1.235	1112
10	1.177	5	1.177	10	1.175	3	1.179	2110
20	1.152	10	1.151	20	1.151	3	1.154	314
7	1.140	5	1.141	10	1.138	1	1.142	226
						1	1.124	2111
5b	1.060	5	1.061	10	1.059	1	1.061	2014
						3	1.047	404
30	1.044	50	1.044	50	1.044	4	1.044	138
20	1.035	5	1.033	20	1.034	2	1.035	0116/1115
						1	1.0234	1213
30	1.012	30	1.011	70	1.011	2	1.011	3012
						1	0.9895	231
15	0.9848	10	0.9843	40	0.9846	1	0.9846	322

Unit cell dimensions

	a	c
SC-19	4.97Å	***
SC-22	4.98Å	16.92Å
SC-27	4.97Å	16.80Å
Synthetic	4.99Å	17.06Å

* ASTM Card 5-086
 Ref: Swanson and Fuyat, 1953
 NBS circular 539, Vol. II, 51
 for synthetic calcite.

Fluorescence: Most of the calcite found in the Slide fluoresces at the violet end of the spectrum. However, sample SC-19 was seen to give off an orange light when subjected to short-wave ultraviolet radiation ($<3600\overset{\circ}{\text{A}}$). Upon closer examination it was found that the fluorescence was restricted to tiny rod-like inclusions, randomly arranged throughout the sample. Using an ultraviolet microscope with dark field illumination it was found that the rods were fairly uniform in shape and size. They are approximately 0.05mm in length with a diameter about 1/10th of this value. Some of the rods group together, end to end, to form longer units. Others are surrounded by "halos" of smaller fluorescing trails. Occasionally a calcite grain was seen to exhibit a brilliant yellow-green fluorescence of a diffuse nature. The origin of this particular color is unknown.

Immersion in oil and thin sections of the calcite proved impossible to analyze by fluorescence microscopy as the oil, epoxy, and balsam all fluoresced to an undesirable degree. Water was the only immersion medium that could be employed.

When the fluorescence spectra were examined through an optical spectroscope a continuous band was observed, ranging from approximately $6200\overset{\circ}{\text{A}}$ to $5300\overset{\circ}{\text{A}}$, with the highest intensities in the red-orange and yellow-green regions. D.C. arc spectroscopy of SC-19 showed trace amounts of Fe, Cu, Zn, and Co. None of these impurities has ever been reported as causing orange fluorescence (McDougall, 1952; Gleason, 1960; Pringsheim and Vogel, 1946). Fluorine, a possible center for this color, was not found as the CaF band in the arc, perhaps owing to its low concentration.

The size of the inclusions was too small to allow examination by transmitted light microscopy, therefore, a polished section was prepared for microprobe analyse. Those rods which were intersected by the polished surface proved to be empty tubes, indicating that the fluorescing material was a fluid. Several rods that were unbroken, but very near the surface, were located by a combination of reflected and transmitted light microscopy. In the probe the electron beam was focused on the surface of the calcite just above a rod. As the beam "burned" its way down to the rod the three spectrometers continuously monitored Zn, Cl and F. At the moment of penetration the count for fluorine increased significantly and then diminished, indicating that the rods had contained a fluorine compound which escaped upon breaching. Table 4 records the change in fluorine measured during one run. After penetration the rods no longer fluoresced, confirming the volatile nature of the fluorescent compound.

Table 4

Results of microprobe penetration of fluorine-filled inclusion.

Count period	Counts		
	Zn	Cl	F
1	18	14	10
2	16	13	7
3	16	16	8
4	20	12	16 → penetration occurs
5	26	17	5
6	24	12	5
7	31	22	10
Avg. background counts	44.75	19.25	5.25

A sample of SC-19 and a non-fluorescing calcite from the Slide were examined by an infra-red spectrophotometer. SC-19 has a small, yet significant peak at 17 microns that is missing from the other calcite (Figure 12). This may also represent the unknown fluid phase.

The presence of a fluorine compound as a trapped fluid in the calcite may have wide reaching implications for the petrology of the Cascade Slide. This may be a remnant of the fluid that was the diluent for CO_2 , allowing the formation of monticellite under high pressure conditions.

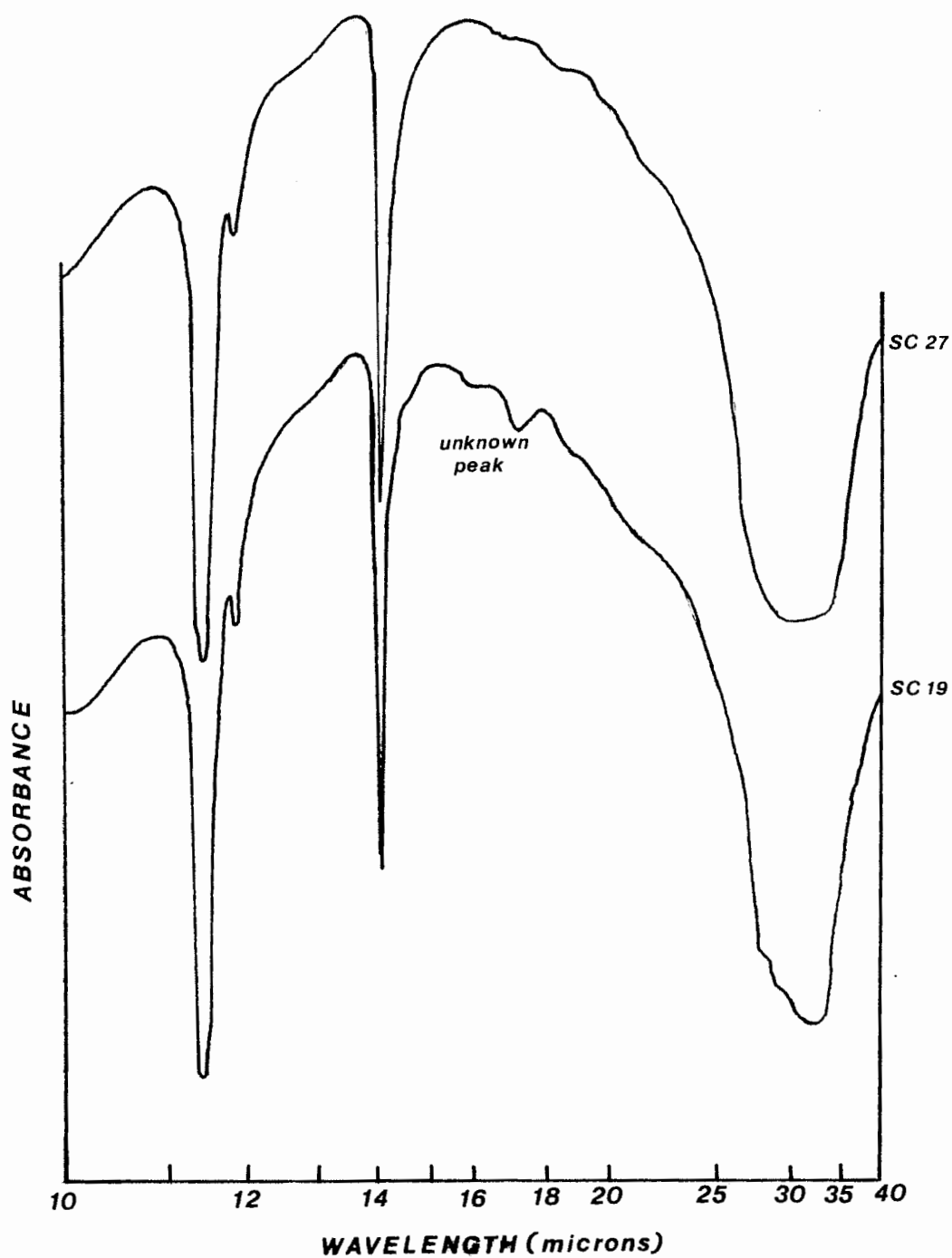
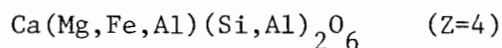


Figure 12. Infra-red absorption spectra of two samples of calcite showing an unknown peak for SC-19 at 17 microns, possibly due to fluid inclusions.

Augite

Monoclinic

Class: $2/\underline{m}$ $\gamma=1.703-1.733$, $Z\wedge c=43^\circ-45^\circ$ Space Group: $\underline{C}2/\underline{c}$ $\beta=1.678-1.713$, $Y=b$ $D_{\text{meas.}}=3.269-3.436$ $\alpha=1.668-1.705$, $X\wedge a=23.8^\circ-30^\circ$ $H=5\frac{1}{2}-6\frac{1}{2}$ $\Delta=0.035-0.028$ Cleavage: $\{110\}\{001\}$ good $2V=65^\circ(+)$ $\beta=105^\circ-105.2^\circ$ $a=9.34-9.44\overset{\circ}{\text{\AA}}$ $r>v$ $b=8.82-8.84\overset{\circ}{\text{\AA}}$ $c=5.02-5.02\overset{\circ}{\text{\AA}}$

Twinning: Sometimes occurs on (100). Crystals also commonly intergrown.

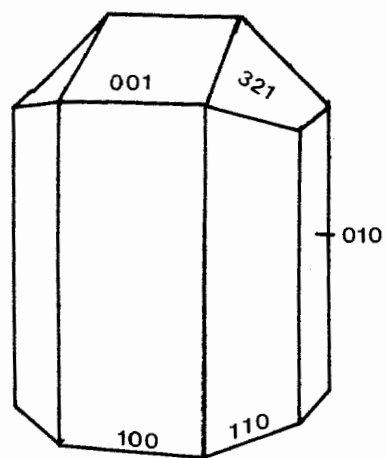
Form and Habit: Augite in the Slide occurs as megacrystals (>1 cm in

length) in the augite granulite, idiomorphic grains (1-3 mm) in the coarse augite marble, and as small equant grains (<1 mm) in the augite-garnet gneiss. It usually forms short prisms, frequently well terminated. In the megacrystals (010) is usually small, giving a cross-section similar to that of an amphibole. The smaller crystals tend to be more regular in their habit with larger development of (010), (111), and (02 $\bar{1}$). Figure 13 illustrates the several varieties of augite morphology seen in the Cascade Slide. Figure 14 is a stereogram of the poles to faces of a typical megacrystal. It shows the common form of these augites which terminate with only an (001) face bounded by strongly developed (321) faces. The stereogram is incomplete due to the distortion of certain crystal surfaces. Interfacial angles measured for the augite are:

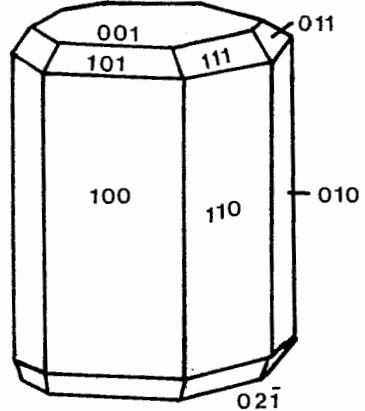
$$(100)\wedge(110)=44^\circ$$

$$(110)\wedge(010)=46^\circ$$

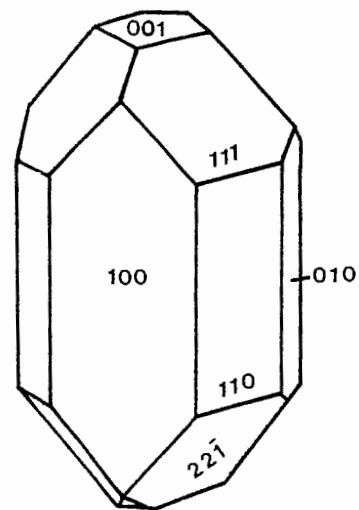
$$(001)\wedge(100)=105^\circ$$



augite megacrystal



augite marble



augite marble

Figure 13. Perspective views of three varieties of augite found in the Cascade Slide.

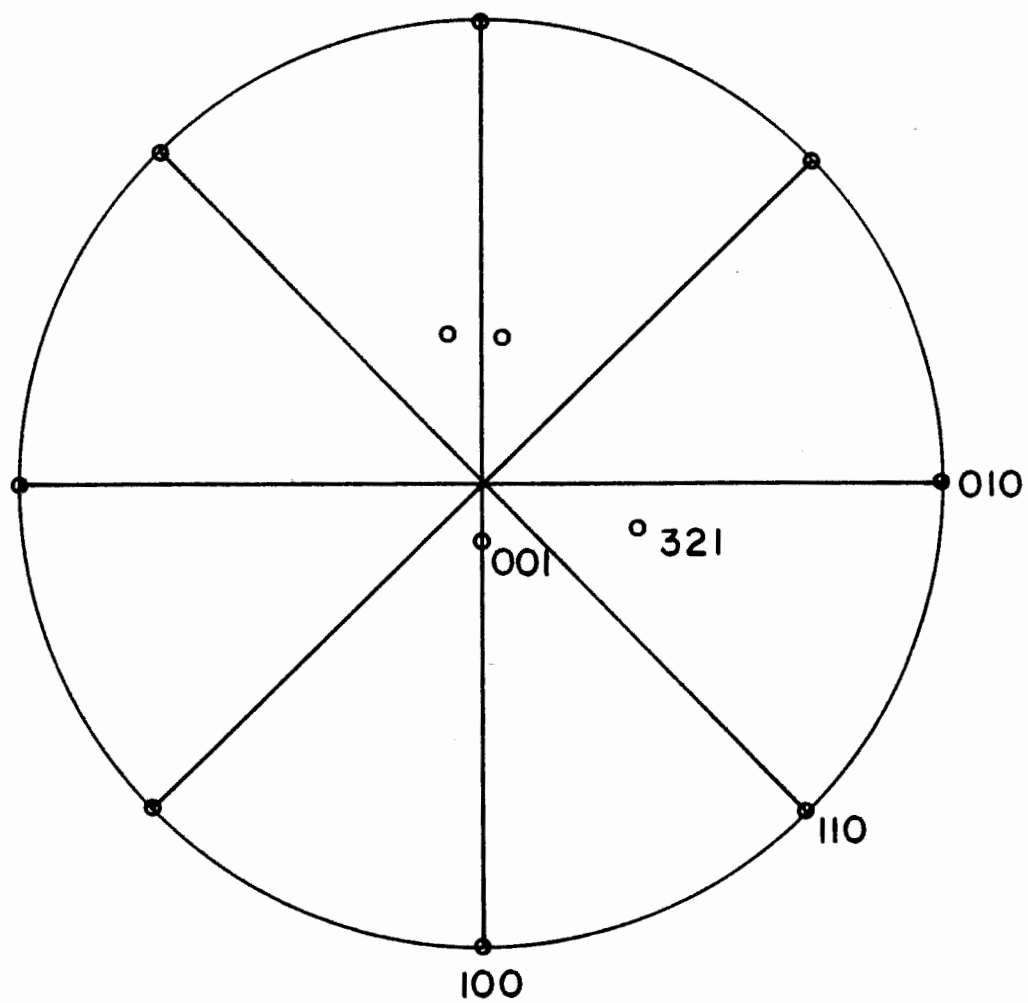


Figure 14. Stereographic projection for augite (SC-38), projected along c .

Color: The color of the augite ranges from pale green for the magnesian varieties to very dark green for the more iron rich. The megacrystals are nearly black in color. Some samples (such as SC-27) show a color variation within individual grains, indicating some zonation. In crushed mounts the augite ranges from colorless to deep green, again depending on the iron concentration. The more strongly colored varieties display a weak pleochroism, with $Z > Y \geq X$.

X-ray: Comparison of X-ray powder diffraction patterns of augite from the Cascade Slide with data reported in the literature indicates a wide range of composition.

Table 5 compares the X-ray patterns of selected augite crystals from the Slide with reported values (JCPDS¹ card 16-701 for hedenbergite). Even with the extinctions, the space group classifications may still be considered C2/c. Minor differences in the d spacings between samples reflect the variations of Mg, Fe, and Al.

Chemistry and Paragenesis: The augites are the most chemically variable species in the Slide. All are very calcic, plotting on or near the diopside-hedenbergite tie line of the pyroxene quadrilateral (Figure 15). This is not unexpected in view of the abundance of Ca available in the area. There is, however, a great deal of variation in the other chemical constituents. Table 6 gives electron microprobe analyses for several augites, not adjusted for ferric iron. Mg and Fe vary with location in the Slide. All of the megacrystals and occasional augites from the coarse marble are iron-rich with $100(\text{Fe}+\text{MnO})/$

¹Joint Committee on Powder Diffraction Studies.

Table 5. X-ray powder diffraction data for augite

SC-5		SC-22		SC-29		Standard*	
I	d	I	d	I	d	I	d
						20	6.45 110
				2	4.67	10	4.70 200
				2	4.41	10	4.45 020
10	3.20	10	3.20	20	3.21	20	3.24 220
100	2.97	100	2.97	100	2.97	100	2.97 22 $\bar{1}$
10	2.87	10	2.87	10	2.87	10	2.87 130?
						30	2.56 13 $\bar{1}$
70b	2.48	80	2.50	80	2.51	50	2.53 11 $\bar{2}$ /20 $\bar{2}$
						10	2.51 11 $\bar{2}$ /221
5	2.29	5	2.29	7	2.30	10	2.32 311
5b	2.21	5	2.21	7	2.21	20	2.22 022/221
2	2.15					10	2.16 330
10	2.12	5	2.12	10	2.12	30	2.13 33 $\bar{1}$
2	2.09					20	2.10 42 $\bar{1}$
5	2.03	5	2.03	7	2.03	10	2.04 041
10	2.00			10	2.00	10	1.99 402/240
1	1.964			2	1.958	10	1.87
2	1.825			2	1.836	10	1.79
						10	1.76
10	1.745	5	1.745	20	1.751	30	
1	1.710						
40	1.620	20	1.618	50	1.621	30	1.63
						20	1.61
						10	1.58
				10	1.544	10	1.55
5	1.522					10	1.52
5	1.503			7	1.502	20	1.50
5	1.440					30	1.44
15	1.422	10	1.421	10	1.425		
10	1.404	3	1.404	5	1.406		
1	1.389						
10	1.328	5	1.327	10	1.330		
2	1.311			2	1.316		
10b	1.278	5	1.278	5	1.283		
7	1.262	3	1.265	5	1.264		
7	1.248	3	1.244	5	1.249		
2b	1.215			2	1.214		
2b	1.174			2	1.175		
2b	1.146			2	1.147		
20b	1.073	20b	1.072	50	1.074		
10	1.066	10	1.063	10	1.066		
5	1.052			7	1.053		
2	1.045			2	1.044		
				2	1.030		
				2	1.017		
				2	1.009		
				2	1.004		
				2	0.9956		
5	0.9804			10	0.9807		

* ASTM Card 16-701
 Ref: Neuman and
 Bergstol, Geol. Min.
 Museum, Oslo, Norway.

Table 5. (Cont'd.)

SC-34		SC-37		SC-106		Standard*		
I	d	I	d	I	d	I	d	
						20	6.45	110
		1	4.72			10	4.70	200
		1	4.42			10	4.45	020
10	3.16	10	3.21	25	3.24	20	3.24	220
		10	2.94					
100b	2.94	100	2.97	100	2.97	100	2.97	221
		10	2.87	30	2.87	10	2.87	130?
						30	2.56	131
70b	2.52	80	2.51	20	2.55	50	2.53	002/202
						10	2.51	112/221
				100	2.39?			
10	2.28	5	2.30	5	2.28	10	2.32	311
10	2.20	5	2.21	5	2.19	20	2.22	022/222
				2	2.14	10	2.16	330
10b	2.09	10	2.12	5	2.12	30	2.13	331
		2	2.10	2	2.09	20	2.10	421
		5	2.04	10	2.04	10	2.04	041
10b	1.996	10	2.01	10	1.995	10	2.02	402/240
						10	1.99	
5	1.953	2	1.963					
7	1.816			5	1.820	10	1.87	
						10	1.79	
10	1.731	10	1.745	15	1.748	30	1.76	
10	1.654							
50	1.616	20	1.622	40	1.619	30	1.63	
						20	1.61	
						10	1.58	
		2	1.547			10	1.55	
10	1.515	5	1.525	5	1.519	10	1.52	
7	1.496	5	1.506	5	1.500	20	1.50	
				2	1.485	30	1.44	
20	1.415	10	1.426	40	1.420			
15	1.396	5	1.405	10	1.403			
20	1.321	10	1.328	10	1.325			
5	1.287	10	1.282	10	1.281			
10	1.274	5	1.261	10	1.261			
10	1.241	10	1.250	10	1.244			
5	1.208			5	1.212			
7	1.167	2	1.175	2	1.172			
7	1.148	2	1.148	2	1.147			
60b	1.069	20	1.075	25	1.075			
20	1.061	10	1.066	10	1.066			
10	1.052	2	1.053					
10	1.041	2	1.044	5	1.040			
10	1.028	2	1.024	5	1.030			
7	1.015			5	1.016			
3	1.006			5	1.004			
3	1.002			5	1.000			
3	0.9996	2	0.9953	5	0.9902			
10	0.9810	5	0.9806	10	0.9783			

Table 5. (Cont'd.)

TM-10		TM-13		Standard*		
I	d	I	d	I	d	
				20	6.45	110
				10	4.70	200
2	4.41			10	4.45	020
		5	3.31			
15	3.19	10	3.18	20	3.24	220
100	2.97	100	2.94	100	2.97	22 $\bar{1}$
20	2.88	10	2.84	10	2.87	130?
				30	2.56	13 $\bar{1}$
70b	2.49	90	2.48	50	2.53	002/20 $\bar{2}$
				10	2.51	11 $\bar{2}$ /221
10	2.29	10	2.28	10	2.32	311
10	2.20	10	2.20	20	2.22	022/22 $\bar{2}$
5	2.15			10	2.16	330
10	2.12			30	2.13	33 $\bar{1}$
5	2.10	20	2.10	20	2.10	42 $\bar{1}$
10	2.03	15	2.03	10	2.04	041
10	2.00			10	2.02	40 $\bar{2}$ /240
5	1.960	15	1.990	10	1.99	
		5	1.954			
10	1.827	10	1.822	10	1.87	
				10	1.79	
10	1.743	25	1.738	30	1.76	
30	1.624	30	1.63			
		70	1.614	20	1.61	
				10	1.58	
2	1.560			10	1.55	
5	1.542	5	1.520	10	1.52	
5	1.503	5	1.497	20	1.50	
		5	1.477	30	1.44	
30	1.420	30	1.418			
20	1.404	15	1.401			
2	1.390					
10b	1.327	20	1.323	Unit cell dimensions (Å)		
10	1.278	15	1.275			
		5	1.256	a	b	c
10	1.246	5	1.244	SC-5	-	4.96
5	1.211	5	1.226	SC-22	-	5.00
		5	1.170	SC-29	9.34	5.02
5	1.148	5	1.147	SC-34	-	5.04
30	1.071	70	1.072	SC-37	9.44	5.02
10	1.065	20	1.063	SC-106	-	5.10
10	1.054	20	1.052	TM-10	-	4.98
5	1.042	15	1.042	TM-13	-	4.96
5	1.029	10	1.028	Standard	9.85	5.26
		10	1.015	(hedenbergite)		
10	1.005	5	1.006			
		5	1.002			
10	0.9915	5	0.9923			
10	1.9788	5	0.9843			

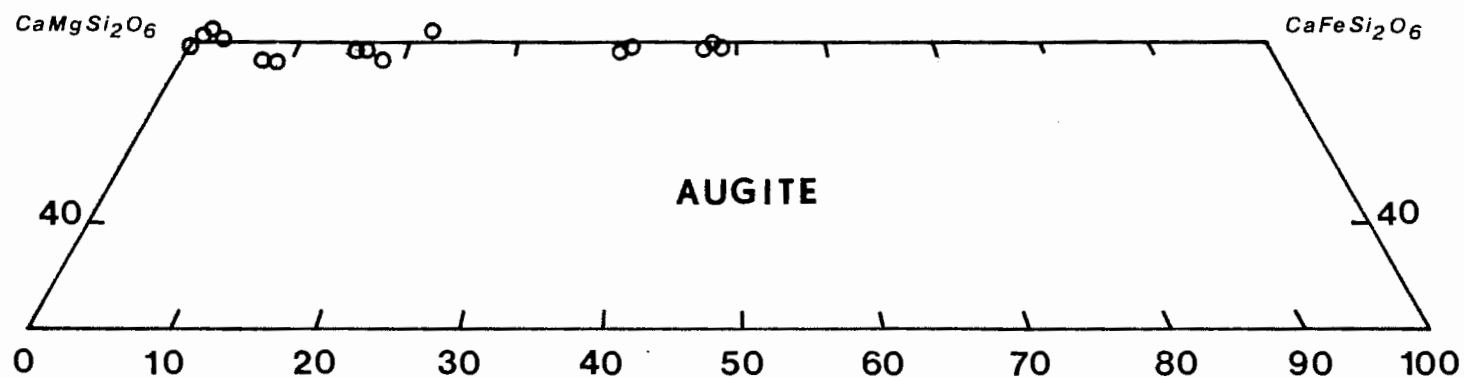


Figure 15. Part of the pyroxene quadrilateral showing the composition of Cascade Slide augites along the diopside-hedenbergite join.

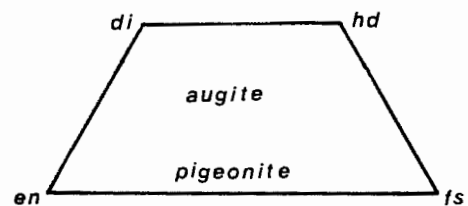


Table 6. Electron microprobe analyses of augite
(not corrected for Fe⁺³)

	SC-5	SC-5	SC-22	SC-22	SC-106	SC-106	SC-27	SC-27	SC-29	SC-29
SiO ₂	51.54	50.65	53.37	53.81	55.10	54.42	52.47	52.37	50.52	50.07
Al ₂ O ₃	1.36	2.38	1.34	1.31	0.30	0.13	2.38	1.42	3.34	3.18
TiO ₂	0.00	0.07	0.00	0.00	0.15	0.00	0.13	0.00	0.24	0.26
Cr ₂ O ₃	0.00	0.07	0.00	0.02	0.03	0.00	0.06	0.00	0.00	0.02
FeO	13.03	13.62	2.35	2.26	2.78	2.54	1.25	0.92	14.15	14.41
MgO	10.20	9.67	17.47	17.16	17.64	16.96	17.71	17.92	8.29	8.40
MnO	0.34	0.22	0.06	0.07	0.11	0.00	0.05	0.09	0.33	0.34
CaO	23.98	23.44	25.70	25.98	24.73	24.75	25.87	25.31	23.52	23.38
Na ₂ O	<u>0.26</u>	<u>0.44</u>	<u>0.00</u>	<u>0.00</u>	<u>0.06</u>	<u>0.06</u>	<u>0.00</u>	<u>0.00</u>	<u>0.53</u>	<u>0.46</u>
	100.61	100.56	100.29	100.61	100.83	98.86	99.92	99.03	100.92	100.52
γ =	1.725									
β =	1.707		1.6836		1.6790		1.6784		1.7113	
α =	1.698									
D =	2.965		3.276				3.269		3.436	

Table 6. (Cont'd.)

	SC-5	SC-5	SC-22	SC-22	SC-106	SC-106	SC-27	SC-27	SC-29	SC-29
<u>Formula units based on 6 oxygens</u>										
Si	1.96	1.93	1.94	1.95	1.99	2.00	1.91	1.95	1.92	1.92
Al	0.04	0.07	0.06	0.05	0.01	0.00	0.09	0.05	0.08	0.08
Al	0.02	0.07	0.00	0.01	0.00	0.00	0.01	0.01	0.07	0.06
Ti	0.00	0.00	0.00	0.00	0.00	0.02	0.00	0.00	0.00	0.00
Cr	0.00	0.00	0.00	0.00	0.00	0.00	0.00	0.00	0.00	0.00
Fe	0.41	0.43	0.07	0.07	0.08	0.08	0.04	0.03	0.45	0.46
Mg	0.58	0.55	0.95	0.93	0.95	0.93	0.96	0.98	0.47	0.48
Mn	0.01	0.00	0.01	0.02	0.00	0.00	0.00	0.00	0.01	0.01
Ca	0.98	0.96	1.00	1.01	0.96	0.97	1.01	0.99	0.96	0.96
Na	0.02	0.03	0.00	0.00	0.00	0.00	0.00	0.00	0.04	0.03
*en	58.6	56.1	93.1	93.0	92.2	92.1	96.0	97.0	51.1	51.1
**fs	41.4	43.9	6.9	7.0	7.8	7.9	4.0	3.0	48.9	48.9
***wo	49.7	49.5	49.5	50.2	48.2	49.0	50.2	49.5	51.1	50.5

$$*en = 100Mg / (Fe+Mg)$$

$$**fs = 100Fe / (Fe+Mg)$$

$$***wo = 100Ca / (Ca+Fe+Mg)$$

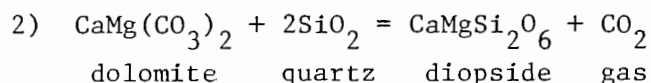
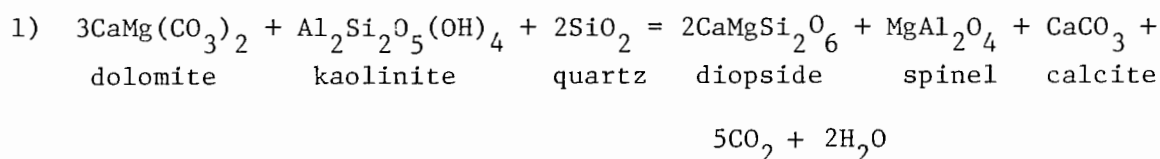
Table 6. (Cont'd.)

	SC-34	SC-34	SC-37	SC-37	TM-10	TM-10	SC-76	TM-13	TM-13	TM-14
SiO ₂	49.01	49.01	50.00	49.14	53.09	54.03	53.96	50.01	52.69	52.24
Al ₂ O ₃	6.67	5.03	3.35	3.29	1.90	2.48	0.74	3.98	2.55	3.24
TiO ₂	0.82	0.69	0.26	0.26	0.07	0.05	0.00	0.35	0.21	0.12
Cr ₂ O ₃	0.00	0.03	0.04	0.06	0.00	0.00	0.08	0.03	0.06	0.00
FeO	6.04	6.35	14.18	14.43	1.29	1.66	1.74	9.28	4.95	2.42
MgO	12.92	13.06	8.17	8.86	17.32	16.70	17.57	11.61	14.63	16.29
MnO	0.10	0.12	0.26	0.26	0.06	0.05	0.20	0.15	0.16	0.04
CaO	24.68	24.66	23.03	23.67	25.71	25.76	25.71	24.49	25.01	25.72
Na ₂ O	<u>0.09</u>	<u>0.06</u>	<u>0.52</u>	<u>0.45</u>	<u>0.00</u>	<u>0.00</u>	<u>0.00</u>	<u>0.33</u>	<u>0.08</u>	<u>0.00</u>
	100.82	99.01	99.81	100.42	99.49	100.88	100.00	100.23	100.34	100.07
γ =	1.721		1.726		1.699		1.694			
β =	1.697		1.705		1.674		1.6801	1.7034		1.6862
α =	1.691		1.697		1.667					
D =										

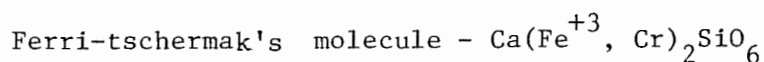
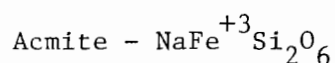
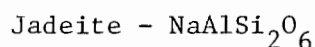
Table 6. (Cont'd.)

	SC-34	SC-34	SC-37	SC-37	TM-10	TM-10	SC-76	TM-13	TM-13	TM-14
<u>Formula units based on 6 oxygens</u>										
Si	1.82	1.84	1.92	1.89	1.94	1.94	1.96	1.88	1.94	1.91
Al	0.18	0.16	0.08	0.11	0.06	0.06	0.03	0.12	0.06	0.09
Al	0.11	0.06	0.07	0.04	0.02	0.04	0.00	0.06	0.05	0.05
Ti	0.11	0.02	0.00	0.00	0.00	0.00	0.00	0.01	0.00	0.00
Cr	0.00	0.00	0.00	0.00	0.00	0.00	0.00	0.00	0.00	0.00
Fe	0.19	0.20	0.46	0.46	0.04	0.05	0.05	0.29	0.15	0.07
Mg	0.71	0.73	0.47	0.51	0.94	0.90	0.95	0.65	0.80	0.89
Mn	0.00	0.00	0.01	0.01	0.00	0.00	0.00	0.00	0.00	0.00
Ca	0.97	0.99	0.95	0.98	1.01	1.00	1.00	0.99	0.98	1.01
Na	0.00	0.00	0.04	0.03	0.00	0.00	0.00	0.02	0.00	0.00
en	78.9	78.5	50.5	52.6	95.9	94.7	95.0	69.1	84.2	92.7
fs	21.1	21.5	49.5	47.4	4.1	5.3	5.0	30.9	15.8	7.3
wo	51.9	51.6	50.5	50.2	50.8	51.3	50.0	51.3	50.8	51.3

(Fe+MnO+MgO) as high as 50. All other augites are generally magnesium-rich to the point of being nearly pure diopside. Al is the most important minor constituent, substituting for both Si in the tetrahedral sites and Mg and Fe in the octahedral positions. Al abundance varies from less than 1% to greater than 6% by weight. There is no observed correlation between Al and variations in any other ion. Other minor elements present are Ti, Cr, Mn, Na, and very minor K. None of these impurities ever amounts to more than 1 weight percent of the pyroxene. Possible reactions for the formation of the augite from an aluminous and siliceous dolomite are:



Iron analysed by the probe has been reported as total iron, not as ferric and ferrous. In order to get an idea of the amount of ferric iron present in each analysis it is necessary to apply some sort of correction. Cawthorn and Collerson (1974) reported a recalculation scheme which breaks an augite analysis into percentages of various hypothetical pyroxene end members. They propose that all augites may be thought of as containing varying amounts of the following molecules;



Titanium-tschermak's molecule - $\text{CaTiAl}_2\text{O}_6$

Tschermak's molecule - $\text{CaAl}_2\text{SiO}_6$

Wollastonite - CaSiO_3

Enstatite - $\text{Mg}_2\text{Si}_2\text{O}_6$

Ferrosilite - $\text{Fe}_2\text{Si}_2\text{O}_6$

By sequentially "using up" ions to create these molecules, as illustrated in Table 7, one can account for all the analyzed elements. When Fe^{+3} is not determined directly it is found that some total iron is left after a recalculation. By reiterating the procedure using the remaining iron as ferric iron a perfect balance can be achieved. Table 7 gives the adjusted analyses of selected augites as percentages of the various end members. It is from these calculations that the relative abundances of wollastonite, enstatite, and ferrosillite were derived for plotting in Figure 20. It must be remembered that this recalculation scheme gives only a suggestion of the true amount of Fe^{+3} in the augite.

The dispersion technique of Merwin (1912) was applied to several samples of augite. The results are given in Table 8 as the mean enstatite (en) composition of the augite, derived from optical composition curves (unpublished) by a computer program of S.A. Morse. The optically derived compositions can be compared with the compositions from the microprobe analysis (Table 6). The largest differences are noted for those augites with abundant Al^{+3} or Fe^{+3} which cause the measured refractive indices to deviate from the ideal.

At first it was thought that there must be observable zoning in

Table 7. Recalculation of augite compositions by the method of Cawthorn and Collerson (1974).

Example: SC-5 (with 4.02 cations/6 oxygens)									mole %
	Si	Al	Ti	Fe ⁺³ ,Cr	Fe ⁺² ,Mn	Mg	Ca	Na	
Comp.	1.96	0.06	0.00	0.0	0.42	0.58	0.98	0.02	
Jadeite	1.92	0.04			0.42	0.58	0.98	0.00	2.0
CATs	1.90	0.00			0.42	0.58	0.96		2.0
Woll.	0.94				0.42	0.58	0.00		48.0
Ens.	0.36				0.42	0.00			29.0
Fs.	0.00				<u>0.06</u>				<u>21.0</u> 102.0

Reiteration using total iron remainder as Fe⁺³

Comp.	1.96	0.06	0.00	0.06	0.36	0.58	0.98	0.02	
Jadeite	1.92	0.04		0.06	0.36	0.58	0.98	0.00	2.0
Fe ⁺³ CATs	1.89	0.04		0.00	0.36	0.58	0.95		3.0
CATs	1.87	0.00			0.36	0.58	0.93		2.0
Woll.	0.94				0.36	0.58	0.00		46.3
Ens.	0.36				0.36	0.00			28.8
Fs.	0.00				0.00				<u>17.9</u> 100.0

Table 7. (Cont'd.)

	SC-22	SC-106	SC-27	SC-29	SC-34	SC-37	SC-76	TM-10	TM-13	TM-14
Jadeite				3.0		4.0				
Fe ⁺³ CATs	4.0		1.5	2.5	1.5	4.0	2.0	0.5		3.0
Ti CATs					2.0					
CATs	3.0	0.5	3.0	5.5	12.5	5.5	1.5	5.0	5.5	7.0
Woll.	46.1	48.5	47.1	44.0	40.5	43.1	48.4	47.4	46.5	45.3
Ens.	46.6	46.7	47.9	24.0	35.5	23.7	47.6	45.1	40.2	44.3
Fs.	0.0	4.0	0.0	21.0	8.0	19.6	0.5	2.0	7.5	0.5

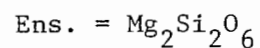
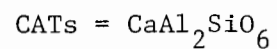
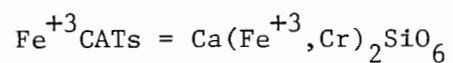
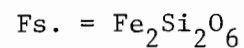
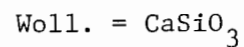
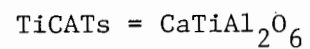
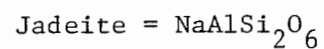


Table 8. Results of dispersion analysis for
Cascade Slide augite.

Sample	en* chem	en** mean	std. dev.	mean Beta R.I.	Sample type
TM-10	94.7	89.9	1.7	1.6830	au
SC-22	93.1	89.1	1.4	1.6836	au
SC-101	n.d.	96.9	1.2	1.6782	pyx
SC-106	92.2	95.7	1.3	1.6790	pyx
TM-13	69.1	60.3	1.9	1.7034	au
TM-14	92.7	85.3	2.4	1.6862	au
SC-5	56.1	46.9	2.4	1.7126	mxl
SC-29	51.1	48.7	2.3	1.7113	mxl
TM-15	n.d.	94.6	1.3	1.6798	gdw
TM-27	n.d.	93.3	3.5	1.6807	gdw
SC-76/1	n.d.	42.9	1.9	1.7153	gdw
SC-76/2	n.d.	51.4	2.0	1.7094	gdw
SC-76/3	95.0	94.1	1.2	1.6801	gdw
SC-34	78.5	60.5	1.4	1.7032	mxl
SC-37	n.d.	45.8	3.0	1.7133	mxl
SC-27/1	97.0	96.7	0.5	1.6784	au
SC-27/2	n.d.	92.9	1.2	1.6810	au

au = augite marble; pyx = augite granulite; mxl = augite megacrystal
gdw = wollastonite-grossular granulite

* en from microprobe analysis (Table 6)

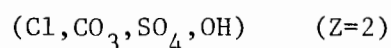
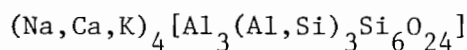
** en from optical composition curves for augite (unpublished) by
computer program of S.A. Morse.

the augites of the Cascade Slide, especially in the large megacrystals. Dispersion analyses of samples SC-27 and SC-76 (Table 8) gave a variation in the mean beta refractive index of up to 0.035. Variation is also reflected in those samples with a standard deviation for the mean enstatite composition of greater than 2.0. Electron microprobe analyses of both single grains and across a large crystal (Table 9) showed no systematic zoning, only random variations in composition. The megacrystal, however, did contain numerous inclusions. Two large patches of calcite are readily visible at the center of the crystal. Corroded grains and stringers of garnet occur throughout the crystal. Several grains of an optically positive amphibole (pargasite?) were seen in thin section but could not be located under the microprobe. All other megacrystals examined showed similar inclusions, leaving open to question the type of parent rock from which they grew.

Table 9. Electron microprobe traverse across an augite megacrystal (SC-38). Traverse points are approximately 2 mm apart.

	#1 (rim)	#2	#3	#4	#5 (core)
SiO ₂	47.874	47.720	49.800	49.657	48.928
Al ₂ O ₃	4.676	4.944	2.944	3.140	3.436
TiO ₂	0.485	0.398	0.311	0.064	0.242
*FeO	16.683	15.160	13.930	14.405	14.840
MnO	0.271	0.304	0.106	0.341	0.359
MgO	7.183	7.592	8.797	8.620	8.461
ZnO	0.427	0.336	0.260	0.367	0.413
CaO	22.388	23.215	23.371	23.003	23.494
Na ₂ O	0.00	0.00	0.00	0.00	0.00
K ₂ O	<u>0.032</u>	<u>0.043</u>	<u>0.031</u>	<u>0.044</u>	<u>0.059</u>
	100.019	97.710	99.553	99.645	100.234
Formula units per 6 oxygens					
Si	1.865	1.856	1.922	1.920	1.891
Al	0.135	0.144	0.078	0.080	0.109
Al	0.079	0.082	0.056	0.063	0.047
Ti	0.014	0.011	0.009	0.001	0.007
Fe	0.543	0.493	0.450	0.466	0.480
Mn	0.008	0.010	0.003	0.011	0.011
Mg	0.417	0.440	0.506	0.497	0.487
Zn	0.012	0.009	0.007	0.010	0.011
Ca	0.935	0.968	0.967	0.053	0.973
K	0.001	0.002	0.001	0.002	0.002

* Ferric and ferrous iron not differentiated.

Scapolite

Tetragonal

Class: $4/\underline{m}$ $\epsilon=1.549-1.552$ Space Group: $\underline{I}4/\underline{m}$ $\omega=1.575-1.583$ $D_{\text{meas.}}=2.68-2.79$

uniaxial(-)

 $H=5\frac{1}{2}-6$ $\frac{\epsilon+\omega}{2}=1.562-1.567$ Cleavage: $\{100\}\{110\}$ Perfect $\Delta=0.026-0.031$

Fluorescence: Usually deep purple

 $a=11.92-12.12\overset{\circ}{\text{\AA}}$

under short wave u.v. Some varieties

 $c=7.52-7.54\overset{\circ}{\text{\AA}}$

fluoresce yellow-orange.

Form and Habit: Scapolite crystals in the Slide are most distinctive as large, prismatic megacrystals (>2 cm long), occasionally growing to an extremely large size. One crystal seen on the margin of the third pool measured 23 cm in cross section (Figure 7); its length could not be determined. Scapolite also occurs as subhedral grains (1-3 mm) in calc-silicate rock altered from mangerite. Large crystals show good development of (110) and a slightly reduced development of (100). Terminations are (111) pyramidal. The stereogram in Figure 16 illustrates the tetragonal nature of the crystals. A perspective drawing of a typical megacrystal (Figure 17) shows the well-developed terminations. It should be noted that the larger scapolite crystals have re-entrants which create uneven surfaces.

Color: In outcrop the scapolite crystals weather a chalky buff color. On a fresh break they appear translucent gray. Scapolite is colorless in thin section.

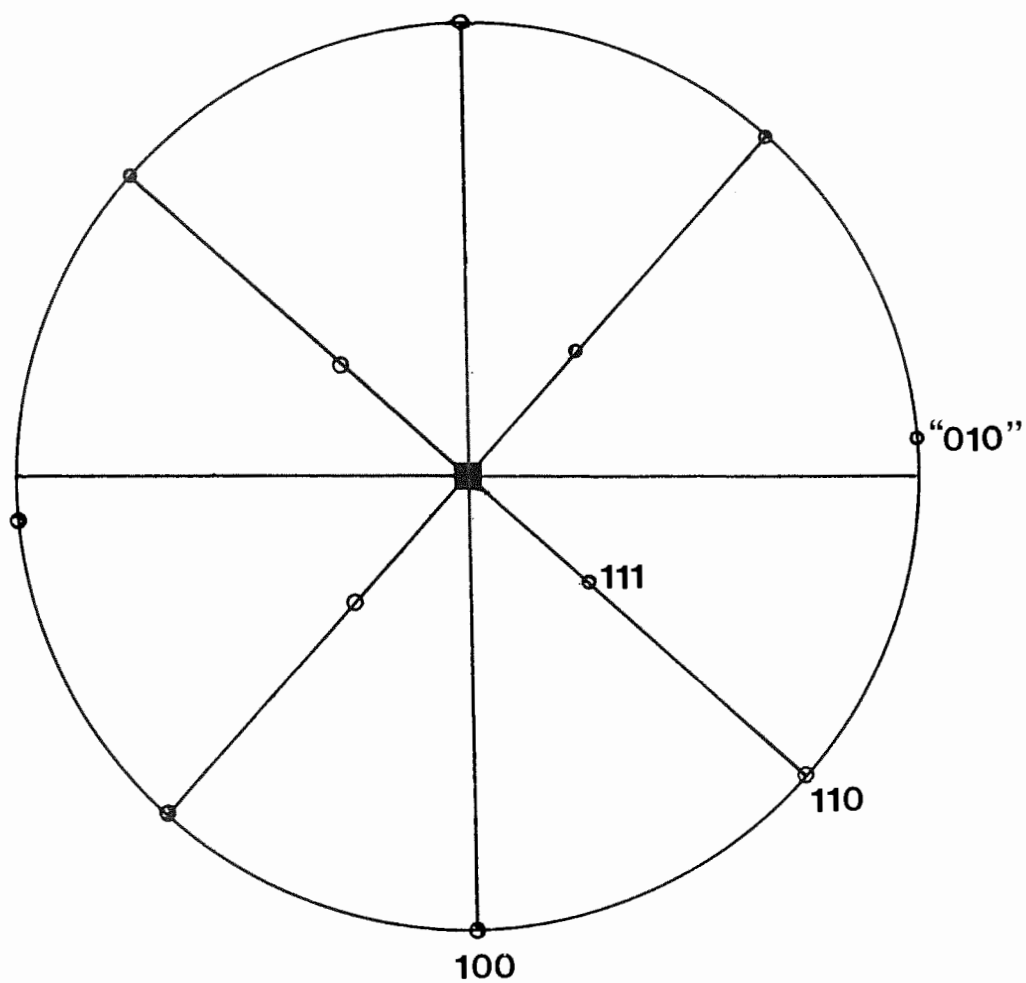


Figure 16. Stereographic projection for scapolite, projected along c . (010) appears offset due to measurements made on reentrants on the crystal faces.

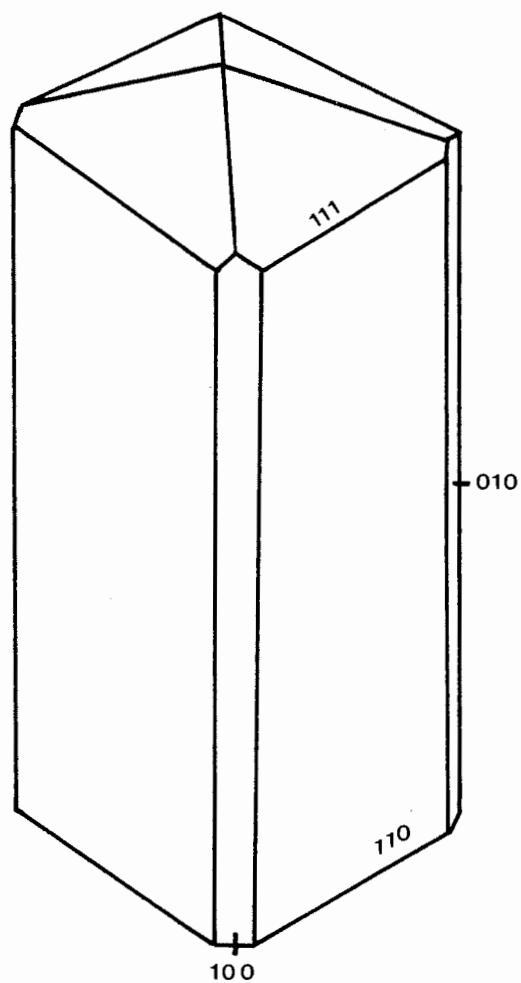


Figure 17. Perspective drawing of a Cascade Slide scapolite megacrystal showing tetragonal morphology and well developed (111) terminations.

X-ray: X-ray powder diffraction patterns for the Cascade Slide scapolite did not match well with those reported in the JCPDS file. However, a very good match was obtained with a pattern reported by Gibbs and Bloss (1961) for scapolite from Grenville, Quebec (Table 10) which probably represents a closer similarity in chemical composition. The indexed lines give a body-centered tetragonal lattice without screws or glides.

Chemistry and Paragenesis: Though a part of a chemically complex species, the scapolites from the Slide show very little chemical variations. Optically they represent the mizzonite range of composition (50-60% meionite end member), but their $\text{CaO}/(\text{CaO} + \text{Na}_2\text{O})$ ratio (see Figure 18) places them much closer to the meionite end (75-85%). This discrepancy is probably caused by substitution of the CO_3 molecule which would greatly affect the indices of refraction. Kelly (1974) also noticed a similar discrepancy in scapolites from a metasomatic zone in Keene Valley, 10 km southeast of the Slide.

Probe analyses of several scapolites are given in Table 9. Because CO_2 and H_2O could not be determined on the microprobe, all of the analytical summations are low. Accordingly, formulas were calculated on a basis of 16 cations rather than on a basis of 24 oxygens. With the exception of SC-2/1, all show little variation in chemistry. SC-2/1 is a decomposed megacrystal showing the development of very fine diopside crystals on its surface. The higher Na and lower Ca values reported indicate a closer association of this sample to the nearby pyroxene-microperthite gneiss. The rest of the scapolite analyses are very calcic, with limited Na. This is probably due to the limited

Table 10. X-ray powder diffraction data for scapolite.

SC-1		SC-2		SC-14		KS-1		Standard*		hkl
I	d	I	d	I	d	I	d	I	d	
30	6.06			10	5.97	15	5.96	5	8.6	110
		10	5.73					20	6.087	200
		10	5.46							
5	4.41	2	4.33	2	4.43	2	4.36	5	4.422	211
								5	4.306	220
40	3.82	40	3.80	50	3.82	30	3.78	45	3.846	310
		5	3.51					10	3.577	301
100	3.46	100	3.40	100	3.43	100	3.42	95	3.465	112
								10	3.21	202
80	3.07			90	3.06	80	3.06	75	3.085	321
								55	3.043	400
		20	2.87					5	2.869	330
2	2.84							5	2.843	222
								5	2.750	411
								5	2.721	420
50	2.69	50	2.65	50	2.68	40	2.67	100	2.700	312
1	2.38	1	2.42					5	2.387	510
10	2.32	10	2.29	10	2.31	10	2.30	15	2.317	431
								15	2.287	332
2	2.20	2	2.18					5	2.209	422
						10	2.15	15	2.164	521
10b	2.14	5	2.13	20	2.13			20	2.142	303
2	2.08	1	2.07	2	2.07	5	2.07	5	2.086	530
10	2.02	5	2.00	10	2.01	10	2.01	10	2.019	512
								15	1.933	611
20b	1.920							30	1.923	620
		20	1.909	20	1.905	15	1.911	15	1.918	413
10	1.886			20	1.880	5	1.883	15	1.893	004
								10	1.843	541
1	1.830							5	1.827	532
2	1.759							10	1.764	631
				2	1.750	2	1.752	5	1.752	503
5	1.719	5	1.708	5	1.712	5	1.710	5	1.721	710
2	1.686	1	1.672					5	1.687	640
2	1.632	5	1.621			2	1.624	5	1.632	721
2	1.604	5	1.582			2	1.600	5	1.607	404
10	1.564	5	1.554	5	1.559	5	1.559	15	1.567	613
5	1.516			5	1.511	2	1.511	5	1.518	
5	1.479									
5	1.470	5b	1.467	5	1.469	2	1.464	10	1.472	732
1	1.450							5	1.459	505
5	1.433	2	1.427	5	1.428	2	1.428			
2	1.415	2	1.408			2	1.411			
								5	1.381	325

Table 10. (Cont'd.)

SC-1		SC-2		SC-14		KS-1		Standard*		hkl
I	d	I	d	I	d	I	d	I	d	
20b	1.373	20	1.367	5	1.368	30	1.367	15	1.376	822
								5	1.349	624
5	1.343	2	1.341	2	1.340	2	1.342	5	1.344	910
5	1.325	2	1.319	5	1.323	2	1.323	5	1.325	653

Unit Cell dimensions (\AA)

	a	c
SC-1	12.12	7.544
SC-2	?	? (Generally smaller than SC-14)
SC-14	11.94	7.520
KS-1	11.92	7.532
Stand.*	12.174	7.572

* Gibbs and Bloss, 1961, Am. Min. 46:1493.

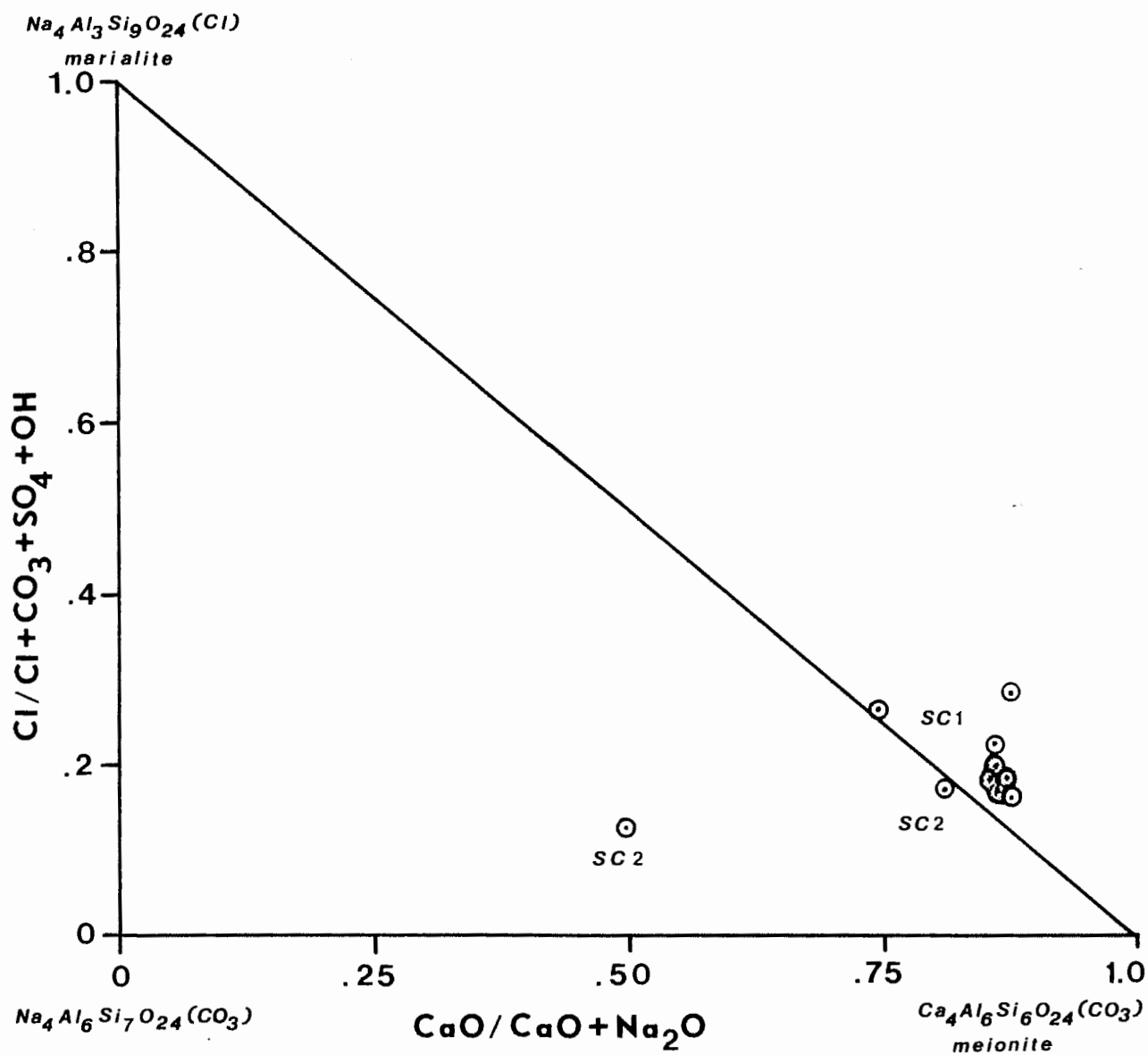


Figure 18. Plot of CaO/Na₂O against Cl concentration in Cascade Slide scapolite.

availability of Cl^- and SO_4^{-2} in the Slide and the overwhelming abundance of CO_2 . Substantial K is also reported in the chemical analyses and is undoubtedly related to the alteration of the microperthite.

Scapolite from nearby deposits (Kelly, 1974) shows very little variation in chemistry from those found in the Slide. This supports the hypothesis (Jaffe, pers. comm.) that the various calc-silicate units in this part of the Adirondacks were originally part of the same Grenville sedimentary sequence.

Like the augite megacrystals, the large scapolites show no systematic zonation from core to rim. Table 11 gives the results of a probe traverse across a crystal 1.5 cm in cross section (SC-1). Minor variations do occur, and a rise in Ca percentage is seen near the center of the traverse. This is due to the fact that SC-1 is cored by pink calcite which is a source of the Ca.

Most of the scapolite fluoresces deep purple under short wave ultraviolet radiation. Those which occasionally fluoresce yellow-orange may do so because of the presence of manganese (a common center for orange fluorescence). The fluorine compound described in the section on calcite was not found in any of the scapolites.

Table 11. Electron microprobe analyses of
Cascade Slide scapolite.

	SC-1/1	SC-1/2	SC-1/3	SC-1/4	SC-1/5	SC-1/6	SC-1/7	SC-1/8	SC-2/1	SC-2/2
SiO ₂	47.53	44.90	45.11	45.01	45.42	44.72	45.14	44.66	50.55	47.44
Al ₂ O ₃	24.71	28.23	29.24	28.33	28.50	28.27	29.08	28.13	21.02	24.76
MgO	0.00	0.04	0.00	0.01	0.07	0.01	0.00	0.00	0.00	0.10
FeO	0.02	0.08	0.14	0.13	0.09	0.08	0.03	0.10	0.10	0.10
Na ₂ O	5.44	2.83	2.80	2.71	2.87	3.00	3.00	3.13	9.59	3.54
CaO	15.46	17.63	18.23	17.92	17.26	17.51	17.80	18.05	9.35	15.13
K ₂ O	0.80	1.13	1.19	1.14	1.08	1.06	0.90	0.85	1.14	1.71
S	0.01	0.01	0.01	0.02	0.002	0.02	0.02	0.01	0.03	0.03
F	0.00	0.00	0.00	0.00	0.00	0.00	0.00	0.00	0.03	0.00
Cl	<u>1.65</u>	<u>0.95</u>	<u>0.92</u>	<u>0.78</u>	<u>0.84</u>	<u>0.93</u>	<u>0.91</u>	<u>0.99</u>	<u>1.02</u>	<u>1.19</u>
	95.62	95.80	97.65	96.05	96.13	95.60	96.88	95.92	92.83	94.00
ω =	1.583								1.575	
ε =	1.552								1.549	
<u>Formula units based on 16 cations</u>										
Si	7.255	6.899	6.798	6.896	6.945	6.876	6.846	6.845	7.668	7.432
Al	4.447	5.113	5.194	5.117	5.138	5.124	5.200	5.082	3.759	4.573
Mg	0.000	0.009	0.000	0.002	0.016	0.002	0.000	0.000	0.000	0.024
Fe	0.003	0.010	0.017	0.017	0.016	0.010	0.004	0.013	0.013	0.013
Na	1.611	0.844	0.819	0.805	0.851	0.894	0.882	0.930	2.820	1.075
Ca	2.529	2.903	2.944	2.941	2.828	2.884	2.893	2.965	1.519	2.540
K	0.156	0.222	0.228	0.223	0.211	0.209	0.175	0.166	0.221	0.343
S	0.003	0.003	0.003	0.006	0.000	0.006	0.005	0.003	0.008	0.008
F	0.000	0.000	0.000	0.000	0.000	0.000	0.000	0.000	0.008	0.000
Cl	0.427	0.247	0.237	0.203	0.218	0.242	0.234	0.257	0.263	0.316

<u>Garnet</u> (var. grossular/ andradite)	$\text{Ca}_3(\text{Fe}^{+3}, \text{Al}_2[\text{SiO}_4]_3)$ (Z=8)
Isometric	Class: $4/\underline{m} \bar{3} 2/\underline{m}$
n variable	Space Group: $\underline{\text{Ia}}3\underline{\text{d}}$
1.740-	$D_{\text{meas.}} = 3.599$ (gross.)
1.760 for grossularitic types	3.650 (and.)
1.867 } 1.840 }	$H = 6\frac{1}{2} - 7$
for melanite in CL-1	Cleavage: None

Form and Habit: Garnet occurs as equant grains in practically every assemblage in the Slide. These grains are usually small (1-3 mm). Most of the garnets appear to take the form of trapezohedrons, though this is often difficult to determine due to rounding and distortion of the crystal faces.

Color: The garnets range in color from nearly colorless to honey brown for the grossularitic types, and yellow-green (topazalite) to nearly black for the andraditic types. Ti-rich andradite (melanite) is black in color. In grain mounts and thin sections the garnet takes on a paler version of its macroscopic color.

X-ray: All X-ray powder diffraction patterns for garnet from the Cascade Slide give a body-centered cell with an a glide in the plane (001), a diamond glide in the plane (11 $\bar{0}$), and a three-fold symmetry axis perpendicular to (111). Variations in the unit cell dimensions depend largely on the $\text{Fe}^{+3} : \text{Al}^{+3}$ ratio. Although three sets of unit cell values are given for each sample (Table 12), the most accurate value is probably that derived from an average of the three strongest back reflection lines: $d = \underline{1040}$, $\underline{1042}$, and 880. The largest cell, that of

Table 12. X-ray powder diffraction data for garnet

SC-19		SC-37		SC-76		TM-14		hkl
I	d	I	d	I	d	I	d	
						2	4.15	
50	2.95	40	2.92	70	2.95	50	2.95	400
100	2.65	100	2.62	100	2.64	100	2.64	420
5	2.52	10	2.49	5	2.51	5	2.53	332
30	2.42	20	2.39	40	2.41	45	2.42	422
10	2.32	10	2.31	10	2.32	10	2.32	431
10	2.17	10	2.14	15	2.17	10	2.16	?
20	1.928	30	1.908	40	1.923	25	1.928	611
5	1.881			2	1.878	2	1.883	620
10	1.712	10	1.705	20	1.714	10	1.719	444
30	1.652	40	1.636	60	1.648	40	1.648	640
80	1.591	80	1.575	90	1.587	100	1.593	642
10	1.490	10	1.477	10	1.486	10	1.491	800
20	1.333	20	1.323	20	1.330	20	1.333	840
30	1.303	40	1.291	20	1.298	20	1.303	842
20	1.272	20	1.262	20	1.270	20	1.273	664
5	1.257	10	1.248					930
10	1.206	5	1.196	5	1.202	10	1.208	941
		5	1.162	2	1.169			862
50	1.110	70	1.100	80	1.106	70	1.111	<u>1040</u>
50	1.092	70	1.083	70	1.088	70	1.092	<u>1042</u>
		5	1.074					?
50	1.058	70	1.049	60	1.054	70	1.058	880
5	0.9984	40	0.9891	30b	0.9952	40b	0.9988	?

Unit cell dimensions (\AA)

	\bar{a}	a^*	$a(800)$	
SC-19	11.90	11.96	11.92	
SC-37	11.80	11.86	11.82	\bar{a} = avg. of all lines
SC-76	11.87	11.92	11.89	a^* = avg. of lines <u>1040</u> , <u>1042</u> and 880
TM-14	11.90	11.97	11.93	
TM-15	11.86	11.89	11.86	$a(800)$ = a from line 800
SC-67		11.87	11.68	
SC-88		11.98	11.94	

Table 12. (Cont'd.)

TM-15		SC-67		SC-88		hkl
I	d	I	d	I	d	
50	2.95	70	2.80	50	2.97	400
100	2.65	100	2.53	100	2.64	420
5	2.53	5	2.42	5	2.54	332
25	2.41	50	2.32	30	2.43	422
10	2.33	5	2.23	5	2.33	431
10	2.16	10	2.09	10	2.18	?
25	1.914	40	1.870	20	1.932	611
		5	1.826	5	1.884	620
10	1.708	15	1.672	10	1.717	444
20	1.644	40	1.611	30	1.654	640
80	1.584	80	1.554	70	1.596	642
5	1.483	20	1.460	10	1.493	800
		1	1.441			?
15	1.326	20	1.313	20	1.335	840
20	1.295	25	1.282	20	1.305	842
10	1.267	20	1.255	15	1.275	664
		1	1.242			930
5	1.200	5	1.192	10	1.208	941
3	1.165					862
80	1.104	70	1.101	60	1.113	<u>1040</u>
60	1.086	70	1.084	60	1.094	<u>1042</u>
60	1.051	50	1.051	40	1.059	880
15	0.9921	20	0.996	20	1.000	

SC-88, belongs to an andraditic garnet from the pyroxenite zone. H.W. Jaffe (pers. comm.) has found titanian andradite from the calcite-augite marble with $a=12.04\text{\AA}$, by far the largest cell edge yet reported for garnet from the area. The smallest cell belongs to SC-37, a grossularitic variety. SC-67 has a distorted cell (compare the average value with that for $hkl=800$). This is due to the abundance of Ti in that particular sample.

Chemistry: Seven garnets were analyzed by electron microprobe (Table 13).

All but one were found to be intermediate in composition between grossular and andradite. The exception (SC-50) is an almandine from the anorthositic gabbro. For garnet from the Slide the variation in Al and Fe^{+3} is shown in Figure 19. There is no apparent correlation of garnet type with any particular rock unit. The most andraditic varieties occur in both the augite marble and the augite granulite. SC-67 and SC-37 are both associated with augite megacrystals. Higher Al values, however, are frequently, but not exclusively, associated with the wollastonite-bearing assemblages.

Ferric corrections for the probe analyses were performed using a FORTRAN program devised by J. Berg (pers. comm.)¹. The program assumes perfect stoichiometry of the mineral and calculates a formula based on a set number of oxygen atoms (in this case 24). Deviations from this stoichiometry are assumed initially to be caused by ferric iron and the amount of the deviation is recalculated as Fe_2O_3 . Some garnet analyses were returned with a small negative amount of FeO reported. This was due to the assumption in the program of a constant 24 oxygens

¹Department of Geology, University of Massachusetts.

Table 13. Electron microprobe analyses of Cascade Slide garnet
(corrected for Fe⁺³).

	SC-67 (rim)	SC-67 (core)	SC-50	TM-8	SC-88 (core)	SC-88 (rim)	TM-15 (rim)	TM-15 (core)	TM-27	SC-37
SiO ₂	34.67	35.29	38.43	37.36	36.37	36.72	38.77	38.55	38.98	38.82
Al ₂ O ₃	8.98	8.67	21.17	12.88	5.96	5.94	15.17	16.06	15.25	16.74
TiO ₂	4.33	4.39	0.00	0.92	0.51	0.53	1.09	1.09	0.75	0.41
Fe ₂ O ₃	15.98	16.46	0.65	13.24	23.21	22.54	8.67	7.70	8.84	6.40
FeO	0.00	0.00	28.63	0.00	0.02	0.16	0.00	0.12	0.38	5.34
MnO	0.07	0.12	1.07	0.03	0.12	0.11	0.14	0.19	0.22	0.48
MgO	1.29	1.33	3.28	0.54	0.52	0.32	0.58	0.61	0.34	0.30
CaO	33.77	34.24	8.07	35.21	33.44	33.91	36.13	35.65	35.92	31.55
Na ₂ O	0.09	0.03	0.00	0.00	0.00	0.02	0.00	0.00	0.00	0.00
K ₂ O	0.00	0.01	0.00	0.00	0.01	0.00	0.00	0.00	0.01	0.00
ZnO	0.11	0.00	0.06	0.00	0.00	0.00	0.00	0.00	0.03	0.00
	99.29	100.54	101.36	100.18	100.16	100.25	100.55	99.97	100.72	100.04
a =					11.98		11.89			11.86
D =	11.87			3.830	3.650					3.599
Formula units based on 24 oxygens										
Si	5.61	5.64	6.01	5.87	5.94	5.99	5.98	5.96	6.01	6.04
Al	0.39	0.36	0.00	0.13	0.06	0.01	0.02	0.04	0.00	0.00
Al	1.32	1.27	3.90	2.25	1.09	1.13	2.74	2.89	2.77	3.07
Ti	0.53	0.53	0.00	0.11	0.06	0.07	0.13	0.13	0.09	0.05
Fe ⁺³	1.95	1.98	0.08	1.56	2.85	2.76	1.01	0.89	1.03	0.75
Fe ⁺²	0.00	0.00	3.74	0.00	0.003	0.02	0.00	0.02	0.05	0.70
Mn	0.01	0.02	0.14	0.004	0.02	0.02	0.00	0.02	0.03	0.06
Mg	0.31	0.32	0.76	0.13	0.13	0.08	0.13	0.14	0.08	0.07
Ca	5.85	5.87	1.35	5.93	5.85	5.92	5.97	5.91	5.94	5.26
Na	0.03	0.01	0.00	0.00	0.00	0.006	0.00	0.00	0.00	0.00
K	0.00	0.002	0.00	0.00	0.002	0.00	0.00	0.00	0.002	0.00
Zn	0.01	0.00	0.007	0.00	0.00	0.00	0.00	0.00	0.003	0.00

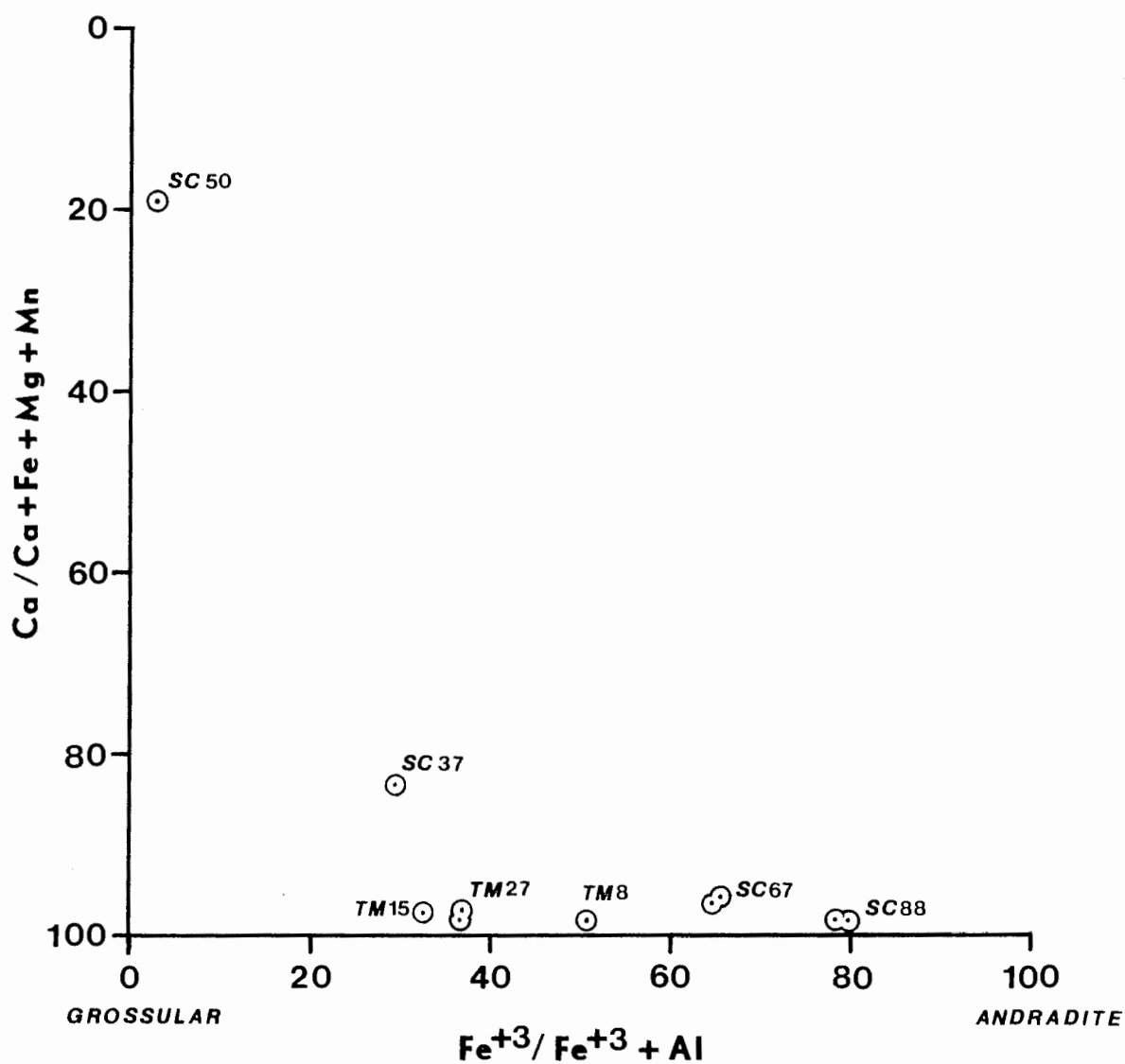


Figure 19. Plot of Ca concentration against Fe^{+3}/Al for Cascade Slide garnet.

for each sample. The presence of (OH) instead of oxygen, or any defects in the structure would cause the computer to register a negative value rather than zero if no ferrous iron were present. Rather than include the negative results in the table, it was decided to place FeO at zero in these cases, leaving all the iron in the ferric state.

Sample SC-37 (Figure 19) found on the surface of an augite megacrystal, has the highest percentage of ferrous iron of any but the anorthositic garnet. This may reflect a deficiency of Ca caused by the growth of the augite. SC-67 also deviates from the other garnets in its chemistry. In this case Mg and Ti are higher than expected, and are not entirely accounted for by a decreased Ca percentage. Throughout the Slide garnet has a higher calcium content than usually reported for grossular and andradite (Deer, Howie, and Zussman, 1966), once again reflecting the highly calcic aspect of the area.

Several garnet crystals were probed to determine the presence of systematic chemical zonation. The results (given as core and rim in Table 13) support random rather than systematic chemical inhomogeneity.

Attempts to apply a recalculation scheme to the garnets similar to the one of Cawthorn and Collerson (1974) for augite proved unsuccessful. In all cases excess silica and calcium resulted.

WollastoniteCaSiO₃ (Z=6)

Triclinic

Class: $\bar{1}$ $\gamma=1.629-1.631$, Z Λ aSpace Group: $P\bar{1}$ $\beta=1.627-1.628$, Y Λ b=3°D_{meas.}=2.619 $\alpha=1.615-1.619$, X Λ c

H=4½ - 5

 $\Delta=0.014-0.012$

Cleavage: {100} Perfect

2V=44°-60°(-)

{001}{ $\bar{1}02$ } Good

r>>v

OAP (100)

a=15.24A°

b=7.28A°

c=6.94A°

Form and Habit: Wollastonite from the Cascade Slide occurs either in massive patches or as fine crystals (<1 mm) in the wollastonite-diopside-grossular rock. It breaks readily into fine acicular fragments along the perfect (100) cleavage. However, it was impossible to obtain any single crystals in a form applicable to goniometry. In both grain mounts and thin sections there was no evidence of twinning. Inclusions, probably of augite, are common.

Color: Wollastonite in the Slide appears chalky white on a weathered surface and is thus easily distinguished from the associated calcite. On a fresh fracture it appears translucent gray or white and is distinguished from fresh scapolite only by its cleavage. Wollastonite is colorless in crushed mounts and thin sections.

X-ray and Optical: The X-ray powder diffraction patterns for the various samples of wollastonite examined are consistent with the space group $P\bar{1}$, the only symmetry element being a center of symmetry. The X-ray

analyses of the wollastonite most closely match the indexed pattern of Hutton (1971) of material from Harrisville, New York (Table 14). Some similarities in X-ray powder diffraction data for Cascade Slide wollastonites and that reported for para-wollastonite (Table 15) were also observed. However, using only a 57.3 mm camera, the data are not clear enough to confirm any correlation.

Under the microscope it was impossible to locate grains in immersion mounts which would yield $X\lambda_c$ and $Z\lambda_a$. This is due to the perfect (100) cleavage.

Chemistry: All the samples of wollastonite examined by microprobe approximate pure CaSiO_3 . Impurities amount to little over 0.5 weight percent of an analysis (Table 16). The most notable impurity is Zn which apparently substitutes for Mg and Fe.

Table 14. X-ray powder diffraction data for wollastonite.

SC-3		SC-8		SC-76		Standard*		hkl
I	d	I	d	I	d	I	d	
						20	7.67	200
						10	5.03	?
		2	4.63			10	4.31	21 $\bar{1}$
3	3.93			2	3.98			
20	3.75	30	3.80	20	3.78	40	3.785	400
						10	3.685	31 $\bar{1}$
20	3.44	30	3.47	20	3.45	40	3.48	002
						1	3.36	?
20	3.27	30	3.27	30	3.26	40	3.29	20 $\bar{2}$
						10	3.13	12 $\bar{1}$
20	3.04	25	3.07	20	3.06	20	3.055	202
100	2.92	100	2.93	100	2.94	100	2.96	310/50 $\bar{1}$
						20	2.787	32 $\bar{1}$
3	2.67	2	2.69	5	2.69	20	2.7055	402
5	2.54	5	2.54	5	2.53	30	2.54	600
10	2.44	10	2.44	10	2.46	50	2.46	112
10	2.32	10	2.32	10	2.32	40	2.335	003/520/32 $\bar{2}$
10	2.25	10	2.28	10	2.28	30	2.281	601/20 $\bar{3}$
10	2.15	15	2.15	20	2.17	60	2.170	602/322/521
5	2.07			3	2.08	1	2.083	40 $\bar{3}$
5	2.00	2	2.00	5	2.00	20	2.009	52 $\bar{2}$
				3	1.962	10	1.970	602
5	1.896			3	1.903	10	1.907	800
3	1.856			3	1.862	10	1.874	?
						1	1.845	?
3	1.812	5	1.821	3	1.821	5	1.825	040
2	1.778			2	1.788	1	1.7845	
10	1.743	3	1.749	3	1.744	40	1.7465	
20	1.703	10	1.713	20	1.710	70	1.713	
						1	1.686	
						1	1.652	
15	1.590	10	1.595	15	1.595	60	1.5985	
7b	1.524					10	1.527	
						1	1.512	
7	1.476	5	1.475	2	1.475	30	1.4725	
7	1.448	5	1.449	5	1.452	30	1.454	
						10	1.4285	
10	1.378					10	1.385	
3	1.336	7	1.358	10	1.356	30	1.358	
3	1.336	2	1.339	3	1.337			
						10	1.322	
						1	1.298	
2	1.275					1	1.281	
3	1.259	5	1.263	3	1.261	20	1.265	
5	1.234	2	1.237			10	1.2385	
10	1.208	5	1.211	10	1.210	20	1.210	
		2	1.184			10	1.187	
10	1.170	5	1.170	7	1.171	20	1.1715	

Table 14. (Cont'd.)

SC-3		SC-8		SC-76		Standard*		hkl
I	d	I	d	I	d	I	d	
10	1.135			5b	1.137	10	1.1465	
10b	1.102	2	1.104	5	1.103	10	1.1395	
10b	1.089	2	1.091	5	1.091	20	1.105	
						30	1.092	

Unit cell dimensions (\AA)

	a	b	c
SC-3	15.24	7.248	6.96
SC-8	15.24	7.284	6.96
SC-76	15.18	7.284	6.96
std.	15.256	7.300	7.005

* Hutton, 1971, Am. Min. 56:589.

Table 15. X-ray powder diffraction data for wollastonite and parawollastonite.

Wollastonite			Parawollastonite		
I	d	hkl	I	d	hkl
40	7.7	200	40	7.7	200
10	4.05	h11	5	4.37	h11
80	3.83	400	80	3.83	400
80	3.52	002	5	3.73	h11
5	3.40	h11	80	3.52	002
80	3.31	20 $\bar{2}$	80	3.31	20 $\bar{2}$
5	3.16	11 $\bar{1}$	5	3.16	12 $\bar{1}$
30	3.09	202	30	3.09	202
100	2.97	310	100	2.97	320
10b	2.80	31 $\bar{1}$	10b	2.80	32 $\bar{1}$
10	2.72	40 $\bar{2}$	10	2.72	40 $\bar{2}$
		11 $\bar{2}$			12 $\bar{2}$
30	2.55	600	30	2.55	600
		112			122
60	2.47	402	60	2.47	402
		003			003
40	2.33	510	40	2.33	520
		312			
		60 $\bar{1}$			60 $\bar{1}$
40	2.29	20 $\bar{3}$	40	2.29	20 $\bar{3}$
		60 $\bar{2}$			60 $\bar{2}$
60	2.18	31 $\bar{2}$	60	2.18	32 $\bar{2}$
5	2.08	40 $\bar{3}$	5	2.08	40 $\bar{3}$
20	2.01	51 $\bar{2}$	20	2.01	52 $\bar{2}$
20	1.98	602	20	1.98	602
20	1.91	800	20	1.91	800
20	1.88		20	1.88	
10	1.86	020	10	1.86	
60	1.83		60	1.83	040
5	1.80		5	1.80	
5	1.79		5	1.79	
40	1.75		40	1.75	
60	1.72		60	1.72	
40	1.602		40	1.602	
10	1.531		10	1.531	
5	1.515		5	1.515	
20b	1.478		20b	1.478	
30	1.455		30	1.455	
5	1.426		5	1.426	
5	1.387		5	1.387	
30	1.358		30	1.258	
10	1.332		10	1.332	
5	1.312		5	1.312	
			5	1.295	
			10	1.273	

* ASTM Cards 19-249, 10-489

Ref: Heller and Taylor, 1956, Crystal data for the calcium silicates, London.

Table 16. Electron microprobe analyses of Cascade Slide wollastonite.

	SC-8	SC-76
SiO ₂	52.38	52.63
Al ₂ O ₃	0.15	0.25
MgO	0.01	0.00
FeO	0.10	0.06
MnO	0.14	0.11
TiO ₂	0.00	0.00
ZnO	0.22	0.18
K ₂ O	0.05	0.05
Na ₂ O	0.00	0.00
CaO	<u>48.87</u>	<u>47.63</u>
	100.92	100.91
γ =		1.631
β =		1.628
α =		1.619
D =		2.619
Formula units based on 18 oxygens		
Si	5.973	6.031
Al	0.020	0.033
Mg	0.001	0.000
Fe	0.009	0.005
Mn	0.013	0.010
Ti	0.000	0.000
Zn	0.018	0.015
K	0.007	0.007
Na	0.000	0.000
Ca	5.974	5.852

<u>Monticellite</u>	CaMgSiO_4 (Z=4)
Orthorhombic	Class: $2/\underline{m} \ 2/\underline{m} \ 2/\underline{m}$
$\gamma=1.650-1.656$, Z=a	Space Group: <u>Pb</u> nm
$\beta=1.645-1.650$, Y=c	$D_{\text{meas.}}=3.058$
$\alpha=1.641-1.642$, X=b	$H=5\frac{1}{2}$
$\Delta=0.009-0.014$	Cleavage: none
$2V=84^\circ-82^\circ(-)$	$a=4.816\overset{\circ}{\text{\AA}}$
$r>v$	$b=10.84\overset{\circ}{\text{\AA}}$
OAP=(001)	$c=6.28\overset{\circ}{\text{\AA}}$

Form and Habit: Monticellite occurs as 1-3 mm, equant grains solely in the coarse marble. Most crystals have rounded edges and restricted growth surfaces. However, from examination of a large number of grains it is apparent that the ideal crystal form is that shown in Figure 20. This is similar to models illustrated in Deer, Howie, and Zussman (1966) and Tröger (1971), but with (010) enlarged. Although there is no visible cleavage in the monticellite, there is a frequent irregular fracture subparallel to (001).

Color: Monticellite ranges from brownish to transparent colorless. When colorless it is impossible to distinguish from the less common olivine. The brown color is a weathering phenomenon due to the iron present in the mineral. This same coloration has been noted by other researchers (Tilley, 1951; Woodford, et al., 1941). Monticellite is colorless in immersion mounts.

X-ray: The X-ray powder diffraction pattern for monticellite gives a primitive lattice (P), a b glide in the plane (100), an n glide in plane (010), and three mirror planes (100), (010), and (001). The

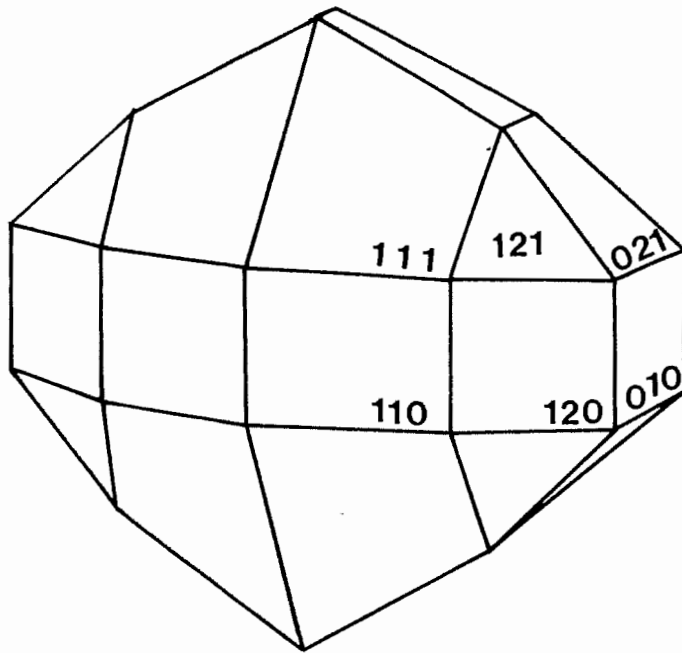


Figure 20. Idealized perspective drawing of a typical Cascade Slide monticellite crystal (TM-16). (010) shows larger development than illustrated in Tröger.

unit cell dimension calculated from the pattern is slightly smaller than that reported in Table 17.

Chemistry: Monticellite is one of the only mineral species from the Slide to have had both wet chemical and probe analyses performed on it. Results of the two techniques are compared in Table 18. The two analyses differ by an insignificant amount. All reported samples of monticellite come from the same location in the Slide (near TM-11 on the map), and are undoubtedly comparable. The substantial amount of iron in the mineral (3-4%) is probably the cause of the brown weathering color. It is interesting to note that Fe replaces Mg in the monticellite rather than concentrating elsewhere in the same rock. The iron content of coexisting forsterite is commonly lower than that in monticellite.

Table 17. X-ray powder diffraction data for monticellite.

TM-11		60-JCL-1		Standard*		hkl
I	d	I	d	I	d	
10	5.42	10	5.45	70	5.54	020
				30	4.41	110
30	4.10	25	4.15	80	4.18	021
5	3.82	5	3.80	70	3.84	101
70	3.59	90	3.61	100	6.62	120
				70	3.18	002
10	3.14	20	3.16	50	3.15	121
5	2.99					
20	2.89	30	2.92	80	2.929	130
		5	2.75	50	2.762	040
100	2.64	100	2.65	100	2.658	131
70	2.56	80	2.58	100	2.578	112
5	2.50	5	2.53	70	2.534	041
30	2.38	30	2.39	80	2.391	122/140
				60	2.346	210
5	2.19	10	2.21	60	2.204	211/220
				30	2.150	132
5	2.08	5	2.09	50	2.082	221/042
2	2.00	5	2.01	50	2.011	150
10	1.905	5	1.914			
				50	1.828	123
100	1.809	100	1.815	100	1.811	222/240
2	1.768	5	1.771			
2	1.738	5	1.743	60	1.744	241
5	1.712	10	1.720	70	1.716	133
				60	1.697	152
5	1.665	10	1.682	60	1.680	043
80	1.590	80	1.598	70	1.593	143
5	1.535	5	1.544			
10	1.497	10	1.503	60	1.499	170
				50	1.416	312
15	1.384	15	1.388	60	1.385	322
5	1.355	5	1.359			
5	1.326	5	1.330			
		10	1.295			
10	1.268	10	1.273			
		1	1.250			
		2	1.229			
10	1.204	10	1.205			
7	1.168	10	1.170			
		10	1.128			
5	1.117	10	1.119			

Table 17. (Cont'd.)

TM-11		60-JCL-1		Standard*		
I	d	I	d	I	d	hkl
		5	1.105			
20	1.093	40	1.096			
5	1.082					
20b	1.044					
5	1.034					
5	1.009					
5	0.9953					
20	0.9840					

Unit cell dimensions (\AA)

	a	b	c
TM-11	4.816	10.84	6.34
60-JCL-1	4.828	11.00	6.45
Standard	4.815	11.08	6.37

* ASTM card 19-240

Ref: U.S. Steel Co., Ltd.

Swinden Labs, Rotherham, 1967.

Table 18. Chemical analyses of Cascade Slide monticellite.

	60-JCL-1*	Ca-22**
SiO ₂	36.99	37.72
TiO ₂	0.04	0.03
Al ₂ O ₃	0.47	0.09
Fe ₂ O ₃	0.15	
FeO	4.12	3.56
Cr ₂ O ₃		0.07
CaO	34.68	35.27
MgO	22.62	22.71
MnO	0.33	0.36
Na ₂ O	0.01	
K ₂ O		0.02
H ₂ O(+)	0.57	
H ₂ O(-)	<u>0.30</u>	
	100.28	99.83

Formula units based on 4 oxygens

Si	0.9765	1.001
Al	0.015	0.002
Al		0.002
Ti	0.0008	
Cr		0.001
Fe ⁺³	0.0029	
Fe ⁺²	0.0909	0.079
Mn	0.0074	0.008
Mg	0.8899	0.899
Ca	0.9810	1.003
Na	0.0005	

* Analysis by Japan Chemistry Research Institute, June, 1973.

** Electron microprobe analysis.

<u>Olivine</u> (var. forsterite)	$(\text{Mg,Fe})_2\text{SiO}_4$ (Z=4)
Orthorhombic	Class: $2/\underline{m}$ $2/\underline{m}$ $2/\underline{m}$
$\gamma=1.681$, Z=a	Space Group: <u>Pbnm</u>
$\beta=1.660$, Y=c	$D_{\text{meas.}} = \text{n.d.}$
$\alpha=1.644$, X=b	H=7
$\Delta=0.037$	$a=4.84\overset{\circ}{\text{\AA}}$
$2V=82^\circ(+)$	$b=10.05\overset{\circ}{\text{\AA}}$
	$c=5.88\overset{\circ}{\text{\AA}}$

Form and Habit: Olivine occurs as small, equant grains (1-2 mm in size) in the augite marble. It is less abundant than assumed at the start of this project. In hand specimen the olivine is colorless and is thus indistinguishable from the transparent monticellite, except under the microscope. Occasional inclusions of graphite or magnetite parallel to c have been reported (H.W. Jaffe, pers. comm.).

Color: Olivine is colorless and transparent in both hand specimen and crushed mount. When serpentized it may appear gray to blackish.

X-ray: A powder diffraction pattern was made of olivine from sample Ca-22Fo (obtained from H.W. Jaffe). In this sample there is extensive evidence of serpentization of the forsterite. Care was taken to select only the most unaltered grains for analysis. However, it appears that some alteration has occurred in even the most transparent grains. Numerous d lines are missing or are offset from those reported for forsterite by Sahama (Table 19).

Chemistry: The Cascade Slide olivine from sample Ca-22 Fo is nearly pure forsterite, with only 3.5% total iron (Table 20). Al, Mn, and Ca total less than 1 weight percent and make up the only analyzed impurities.

Table 19. X-ray powder diffraction data for forsterite.

Ca-22Fo		Standard*		
I	d	I	d	hkl
		50	5.10	020
		10	4.30	110
50	3.81	70	3.883	021
		10	3.723	101
		10	3.496	111
10	3.42	20	3.478	120
10	3.17	10	3.007	121
100	2.94	10	2.992	002
5	2.85			
40	2.74	60	2.768	130
5	2.66			
5	2.58			
		70	2.512	131
100	2.48	100	2.458	112
70	2.43			
		5	2.383	200
		20	2.347	041
		10	2.316	210
		40	2.269	122
10	2.23	30	2.250	140
5b	2.14	10	2.161	220/211
5b	2.02	5	2.032	132
5	1.914	20	1.876	150
5	1.856	5	1.175	151
10	1.823	40	1.750	222
100	1.736	10	1.740	240
5	1.710	10	1.731	123
5	1.662	10	1.671	241
40b	1.611	10	1.636	061
5	1.559	10	1.634	232
5	1.516	20	1.619	133
10	1.491	5	1.590	152
10	1.470	20	1.497	004
10	1.416	20	1.479	062
10	1.416	10	1.397	170/233
10	1.384	5	1.388	312
20	1.343	20	1.351	322
5	1.324	10	1.316	134
5	1.307			
5	1.288			
5	1.274			
5	1.256			
5	1.241			
5	1.183			
5	1.162			
5	1.154			
5	1.097			
20	1.073			
10	1.061			
10	1.051			
20	1.035			

* ASTM card 7-74
 Ref: Sahama, Rept. of Invest., 4408
 U.S. Dept. of Int., Bur. of Mines

Unit cell dimensions (Å)

	Ca-22Fo	Standard
a =	4.84	4.758
b =	10.05	10.207
c =	5.88	5.988

Table 20. Electron microprobe analyses of
forsterite (Ca-22Fo)*

		Formula units based on 4 oxygens	
SiO ₂	42.07	Si	1.103
Al ₂ O ₃	0.05	Al	0.001
TiO ₂	0.00	Ti	0.000
Cr ₂ O ₃	0.00	Cr	0.000
FeO	3.47	Fe	0.069
MnO	0.33	Mn	0.006
MgO	52.49	Mg	1.885
CaO	0.34	Ca	0.008
	<hr/> 98.75		

$$\gamma = 1.681$$

$$\beta = 1.660$$

$$\alpha = 1.644$$

$$2V = 82 (+)$$

* Microprobe analysis by

R.J. Tracy.

<u>Vesuvianite</u>	$\text{Ca}_{10}(\text{Mg,Fe})_2\text{Al}_4\text{Si}_9\text{O}_{34}(\text{OH,F})_4$ (Z=4)
Tetragonal	Class: $4/\underline{m}$ $2/\underline{m}$ $2/\underline{m}$
$\omega=1.714$	Space Group: \underline{P} $4/\underline{nnc}$ (ideal)
$\epsilon=1.711$	$D_{\text{meas.}}=3.176$
$\Delta=0.003$	H=6 - 7
$2V=\pm 10^\circ(-)$ (anomalous)	Cleavage: none visible
$a=15.48\overset{\circ}{\text{\AA}}$	
$c\approx 11.83\overset{\circ}{\text{\AA}}$	

Form and Habit: Vesuvianite crystals are frequently well formed as stubby prisms with well developed (110) and (011) faces. Figure 21 shows the most common crystal form seen in the vesuvianite. In some crystals (100)^(110) is not 45° , possibly giving rise to the anomalous bi-axiality. Figure 22 is a stereographic projection of a vesuvianite crystal in the zone [110:011]. This orientation occurred because of the rounded and indistinct face development of the sample which made alignment difficult.

Color: All vesuvianite examined is a very dark brown in hand specimen and golden brown in crushed mounts.

X-ray: The X-ray powder diffraction pattern for TM-17 (Table 21) is indicative of a primitive cell. However, lines indicating the four-fold axis are missing. This may mean that the actual structure is pseudo-tetragonal and slightly orthorhombic.

Unit cell dimensions are close to those reported in Dana (1959).

Chemistry: There is variable chemistry within even one sample of vesuvianite as seen in the three analyses of TM-17 (Table 22). However, the elements present are only those expected. Some Ti, Mn, and Zn

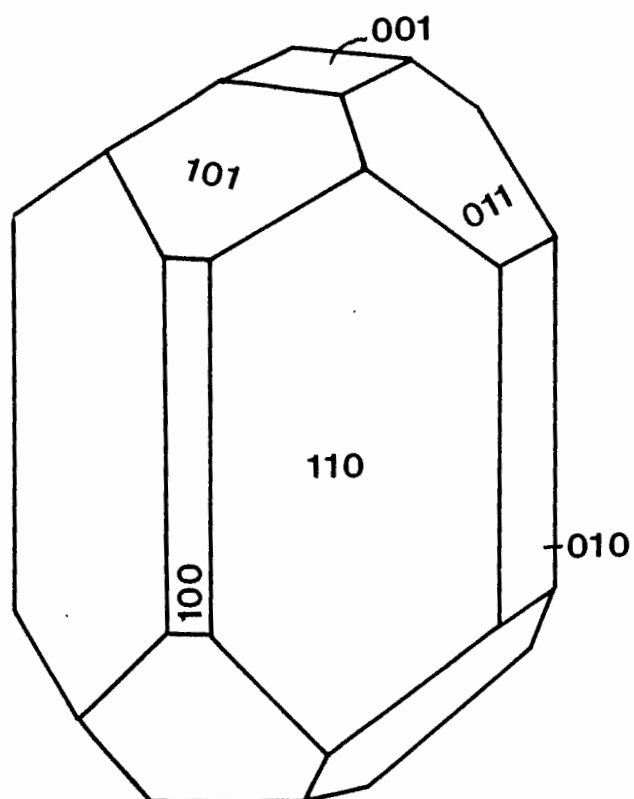


Figure 21. Perspective drawing of Cascade Slide vesuvianite.

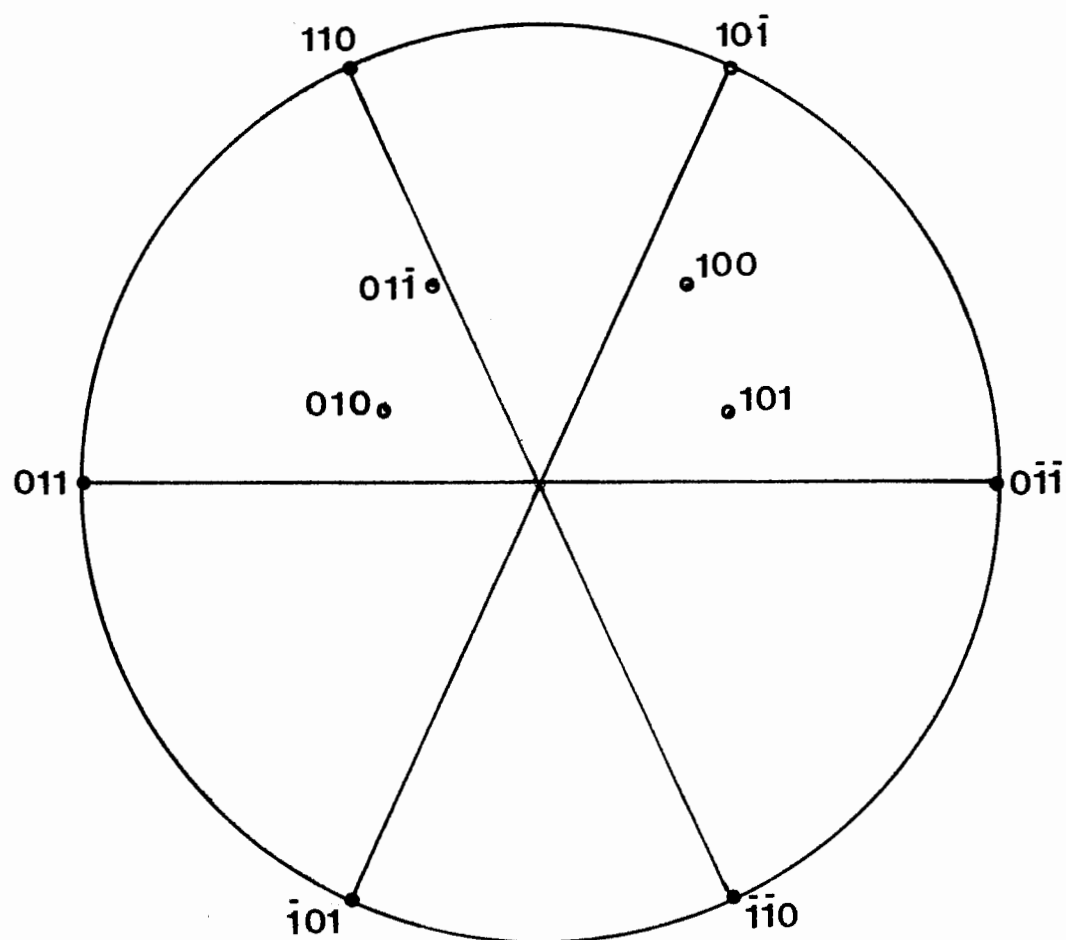


Figure 22. Stereographic projection for Cascade Slide vesuvianite, projected in the zone $[110:011]$.

Table 21. X-ray powder diffraction data for vesuvianite.

TM-17		Standard*		
I	d	I	d	hkl
		5	11.0	110
		10	5.09	211
		5	4.69	202
		20	4.03	222
5	3.47	20	3.469	420/322
		10	3.244	402
40b	3.00	20	3.054	313/510
		5	2.999	431/422
		40	2.946	004
100	2.74	100	2.752	204/440
50	2.58	80	2.593	600/522
10	2.46	50	2.452	620
5	2.32	10b	2.332	
5	2.26	10	2.194	
5	2.08	30	2.122	
5	2.07			Unit cell dimensions (Å)
		10b	1.997	
5	1.932	5	1.960	a c
5	1.895	10	1.882	TM-17 15.48 11.72
5	1.854			Standard 15.58 11.93
		5	1.793	
		20	1.762	
		5	1.679	
		30	1.662	
20	1.628	60	1.621	* ASTM card 11-145
20	1.591	5	1.568	Ref: Domanska, Nedoma and
		10	1.556	Zabinski, Min. Mag. 37:343-348.
		5	1.539	
5	1.529	5	1.525	
		10	1.495	
		5	1.476	
		10	1.387	
		5	1.374	
2	1.357	10	1.345	
5	1.331	20	1.297	
7	1.302			
		10	1.280	
5	1.271	10b	1.264	
5	1.152			
20	1.110	10b	1.104	
20	1.090	5b	1.074	
10	1.057	5	1.030	
		5	1.021	
		5	1.004	

Table 22. Electron microprobe analyses of
Cascade Slide vesuvianite (TM-17).

	TM-17/1	TM-17/2	TM-17/3
SiO ₂	35.69	36.01	36.22
Al ₂ O ₃	12.86	13.72	14.15
MgO	4.52	4.50	4.57
FeO	3.68	3.50	3.83
MnO	0.00	0.02	0.07
TiO ₂	0.00	1.12	1.13
ZnO	0.00	0.01	0.13
K ₂ O	0.01	0.00	0.00
CaO	34.77	35.33	35.15
F	0.44	0.84	0.71
Cl	<u>0.23</u>	<u>0.20</u>	<u>0.22</u>
	92.20	95.25	96.18

$$\omega = 1.714$$

$$\varepsilon = 1.711$$

$$D = 3.176$$

Formula units based on 25 cations

Si	8.948	8.954	8.690
Al	3.803	4.022	4.002
Mg	1.689	1.668	1.633
Fe	0.771	0.728	0.768
Mn	0.000	0.0003	0.014
Zn	0.000	0.0001	0.023
Ti	0.000	0.209	0.203
Ca	9.341	9.413	9.036
K	0.002	0.000	0.000
F	0.349	0.66	0.539
Cl	0.098	0.081	0.089

are found to substitute for Ca, as does the excess Mg and Fe. Problems occur upon analysis of the volatile constituents. Analyzed Cl and F amount to only a maximum of 1 weight percent of the mineral, or only $3/4$ out of 4 possible formula units. Some other volatile, negatively-charged constituent must be present in the vesuvianite. The hydroxyl radical is the most likely choice although only little if any water ever existed during the metamorphism of the Slide. The fluid found in the fluorescing rods in the blue calcite might also be contained in the vesuvianite. A final possibility is some type of hydrocarbon, although this cannot be determined at the present time.

<u>Apatite</u> (var. Fluorapatite?)	$\text{Ca}_5(\text{PO}_4)_3(\text{OH}, \text{F}, \text{Cl}, \text{SO}_4)$	(Z=2)
Hexagonal	Class: $6/\bar{m}$	
$\omega=1.635$	$a=9.69\overset{\circ}{\text{\AA}}$	Space Group: $P6_3/m$
$\epsilon=1.632$	$c=6.85\overset{\circ}{\text{\AA}}$	$D_{\text{meas.}}=3.091$
$\Delta=0.003$		H=5
uniaxial (-)	Cleavage: none visible	

Form and Habit: Cascade Slide apatite occurs as small (1 mm) idiomorphic crystals within certain restricted parts of the augite marble. A perspective drawing, Figure 23, compares the morphology of the Slide apatite with that illustrated in Troger (1971). The lack of a well developed termination is shown also in Figure 24. A stereographic projection (Figure 25) demonstrates the nearly perfect hexagonal symmetry of this mineral. Interfacial angles are constant at $120^\circ \pm 0.5^\circ$ (or 60° between poles to faces).

Color: All apatites so far observed are transparent and sky blue in color, with an occasional gradation into green. Emmons reported blue apatite of a large size from the Slide in 1842, but these have long since been either buried or carried off by collectors. In crushed mounts the apatite is colorless.

X-ray and Optical: Optically, the apatite is a fluorapatite, distinguished by low indices of refraction and very low birefringence (Deer, Howie, and Zussman, 1966). However, the X-ray powder pattern, and especially the unit cell dimensions deviate to some degree from those reported for fluorapatite (Table 23). This may indicate the presence of an ion, such as Sr^{+2} or a trivalent lanthanide, e.g., La^{+3} in sites normally occupied by Ca^{+2} . These might expand the cell but keep the

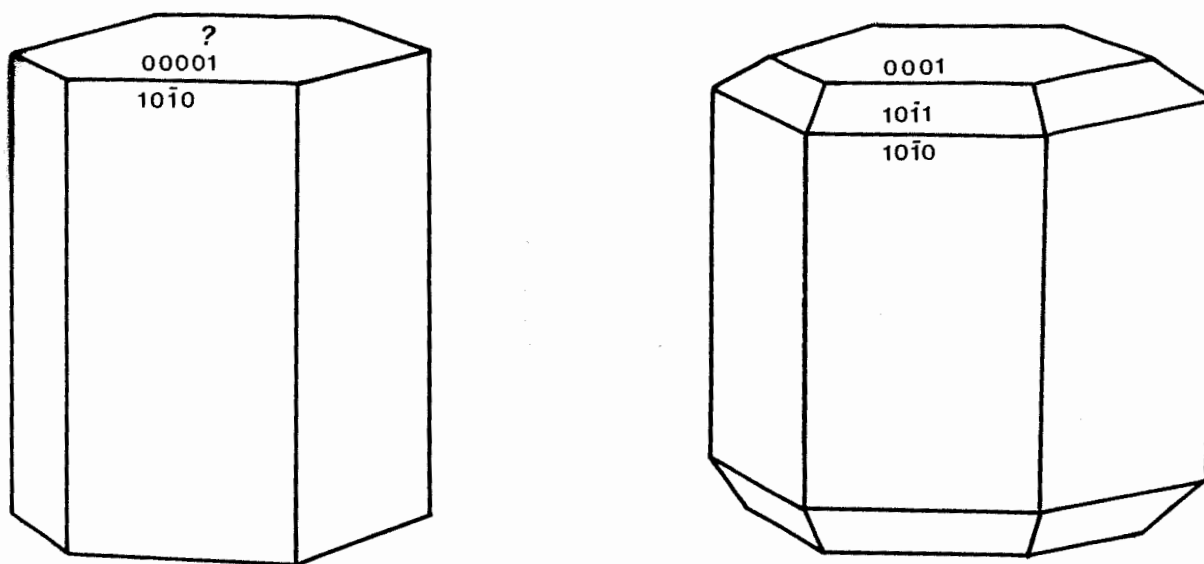


Figure 23. Perspective drawing of Cascade Slide apatite (left) and that illustrated in Tröger (right). Note lack of terminations developed on the Cascade Slide sample.

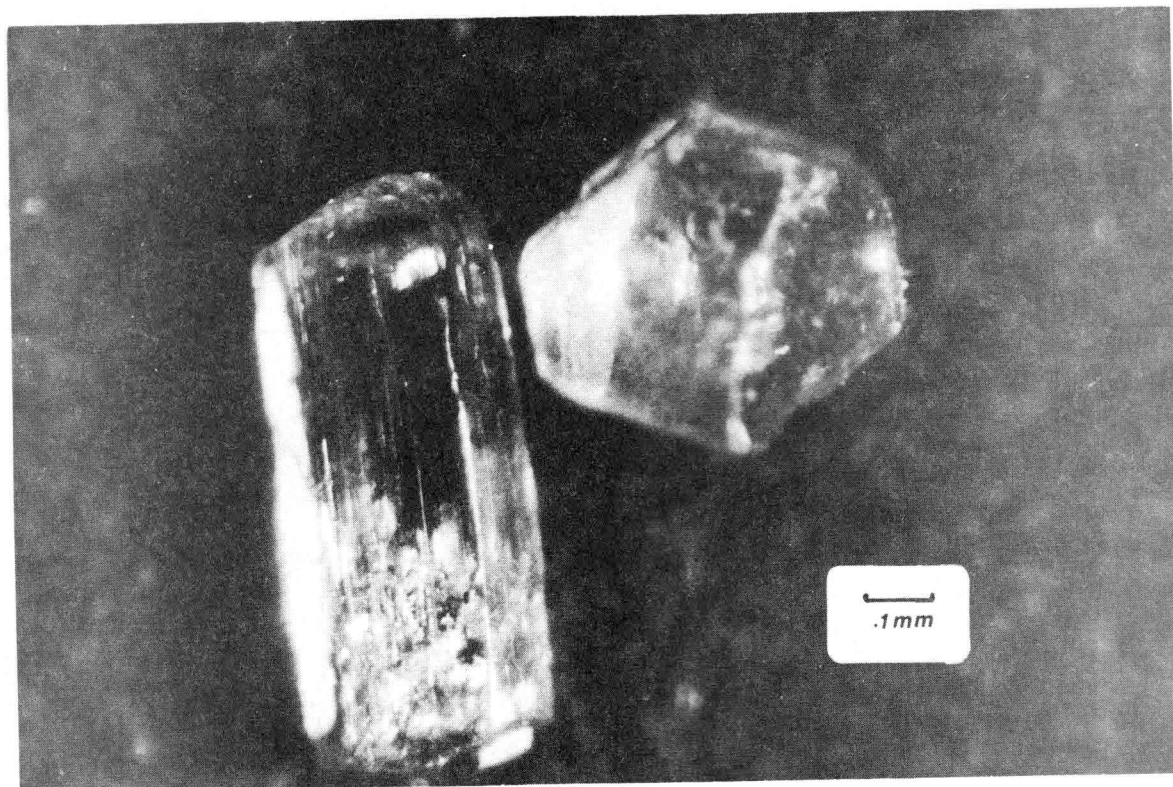


Figure 24.- Photomicrograph of typical apatite crystals found in the coarse augite marble. Crystals are approximately 1 mm in diameter.

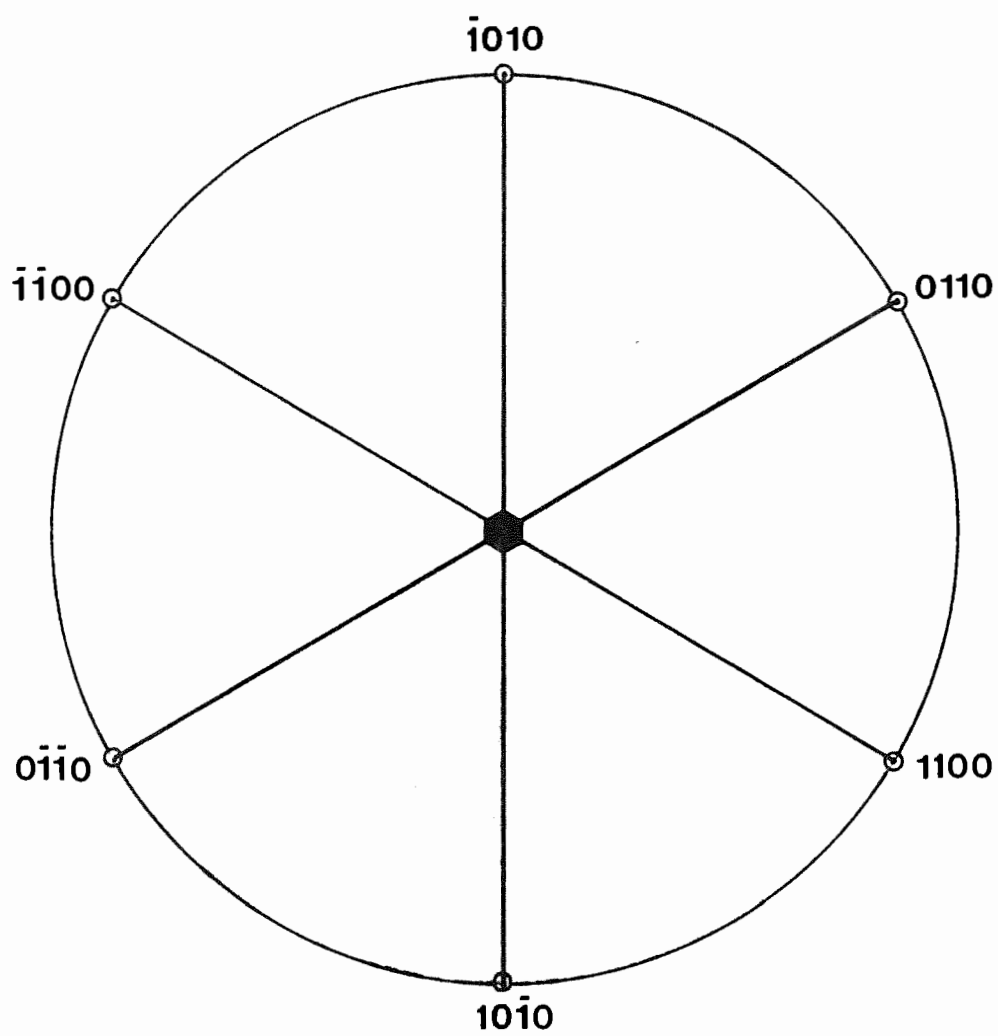


Figure 25. Stereographic projection for Cascade Slide apatite, projected along c .

Table 23. X-ray powder diffraction data for apatite.

SC-18		Standard*		
I	d	I	d	hkl
		8	8.12	100
		4	5.25	101
1	4.27	1	4.68	110
2	4.02	8	4.05	200
2	3.83	8	3.87	111
2	3.62	1	3.49	201
40	3.40	40	3.44	002
5	3.13	14	3.16	102
10	3.03	18	3.06	210
100	2.78	100	2.80	211
		55	2.77	112
70	2.68	60	2.70	300
30	2.61	30	2.62	202
2	2.51	6	2.51	301
2	2.27	8	2.28	212
30	2.24	20	2.25	310
		4	2.21	221
5	2.13	6	2.14	311
		4	2.12	302
5	2.05	6	2.06	113
		2	2.03	400
2	1.984	4	1.997	203
30	1.927	25	1.937	222
10	1.877	14	1.884	312
		4	1.862	320
50	1.824	30	1.837	213
10	1.794	16	1.797	321
10	1.770	14	1.771	410
10	1.738	14	1.748	402
10b	1.713	16	1.722	004
		1	1.684	104
5	1.633	6	1.637	322
2	1.603	4	1.607	313
2	1.574	2	1.580	501
		1	1.562	330
2	1.528	6	1.534	420
2	1.520	4	1.524	331
10	1.498	4	1.497	421

Table 23. (Cont'd.)

SC-18		Standard*		
I	d	I	d	hkl
10	1.468			
10	1.445			
7	1.425			
5	1.401			
2	1.343			
5	1.311			
2	1.299			
10	1.277			
10	1.254			
20b	1.232			
10	1.217			
5	1.187			
10	1.155			

* Fluorapatite

Ref: NBS Mono. 25, Sec. 3/22 (1964).

Unit cell dimensions (Å)

	a	c
SC-18	9.69	6.85
standard	9.38	6.89

indices of refraction low.

The X-ray pattern is consistent with a primitive lattice. Extinctions in 001 indicate a $\bar{6}_3$ hexad screw axis parallel to \underline{c} , with a translation of $c/2$. The gross morphology demonstrates the existence of three mirror planes perpendicular to the three diad axes.

<u>Titanite</u> (sphene)	$\text{CaTiSiO}_4(\text{O,OH,F})$ (Z=4)
Monoclinic	Class: $2/\underline{m}$
All indices above the range of available oils.	Space Group: $\underline{C}2/\underline{c}$
Δ =very high	D=n.d.
$2V=35-40^\circ$ (est.) (+)	$H=5-5\frac{1}{2}$
$X\Lambda a \approx 21^\circ$	$a=5.56\overset{\circ}{\text{A}}$
$Y=b$	$b=n.d.$
$r \gg v$	$c=6.28\overset{\circ}{\text{A}}$

Form and Habit: Titanite is occasionally found as large crystals (0.5-1.0 cm) on the surface of augite megacrystals. In the case of SC-52 several crystal faces are well developed but could not be analyzed by goniometer due to the intimate association of the augite. Titanite is also found as a minor constituent in the augite-garnet gneiss, the augite marble, and the pyroxene-microperthite gneiss.

Color: Titanite displays a yellow-brown or red-brown macroscopic color and a characteristic adamantine luster. It is pale brown and weakly pleochroic in crushed mounts.

Discussion: The analyzed X-ray powder diffraction pattern for the mineral shows a smaller cell size than reported by Zachariasen (see Table 24). The titanite lattice is \underline{c} face centered with a \underline{c} glide in the (001) plane.

Titanite is a very minor constituent of the Slide. It usually occurs in the presence of augite, and may form from titanaugite in the presence of excess silica. The large observed optic axial angle, $2V$, indicates a low Ti and generally high Fe^{+3} content (Deer, Howie,

Zussman, 1966, p.18). Substitution of chromium, rare earth elements, and niobium reported by Jaffe (1947) may also produce a similar increase in the axial angle.

<u>Graphite</u>	C (Z=4)
Hexagonal	Class: $6/\underline{m} \ 2/\underline{m} \ 2/\underline{m}$
Opaque	Space Group: $\underline{P}6_3/\underline{mmc}$
$a=2.460\overset{\circ}{\text{\AA}}$	$H=1\frac{1}{2}$
$c=6.690\overset{\circ}{\text{\AA}}$	

Graphite from a piece of float found in the Slide has been confirmed by X-ray diffraction analysis (Table 26). It occurs with calcite in a rock texturally resembling the augite marble. It has not been observed in place and is not considered of great importance in the Slide.

Table 24. X-ray powder diffraction data for titanite.

SC-52		Standard		hkl
I	d	I	d	
5	4.77	30	4.93	$\bar{1}11$
85	3.14	100	3.233	111/002
85	2.92	90	2.989	$\bar{2}02$
5	2.78	5	2.841	200
100	2.55	90	2.595	$\bar{2}21/022$
		5	2.362	$\bar{1}13/220$
20	2.24	30	2.273	112/ $\bar{1}32$
		5	2.225	131
		20	2.101	$\bar{3}12$
20	2.03	40	2.058	$\bar{3}11$
		10	1.972	221
2	1.921	10	1.945	$\bar{3}13$
		5	1.848	$\bar{2}04/310$
3	1.784	10	1.802	042/ $\bar{2}41$
		20	1.741	$\bar{3}32$
		10	1.725	240
10	1.681	30	1.703	$\bar{2}24$
15	1.625	40	1.643	$\bar{3}33$
10	1.543	20	1.554	151/241
5	1.515	10	1.527	043/ $\bar{1}34$
10	1.481	40	1.494	133
		40	1.418	400
20b	1.409	20	1.409	
10	1.338	20	1.344	
10	1.297	20	1.306	
10	1.266	10	1.275	
7	1.219	5	1.227	
2	1.140	10	1.132	
15	1.127	5	1.117	
20	1.104	10	1.107	
15b	1.074	5	1.077	
3	1.052			
15b	1.040	5	1.042	
		5	1.030	
10b	1.014	5	1.015	
10b	0.9963	5	0.999	

Unit cell dimensions (\AA)

	a	b	c
SC-52	5.56	?	6.28
Standard	6.549	8.682	7.435

* ASTM card 11-142

Ref: Zachariasen, 1930, Z. Krist., 73:7.

<u>Magnetite</u>	$\text{Fe}^{+2}\text{Fe}^{+3}_2\text{O}_4$ (Z=8)
Cubic	Class: $4\bar{3}2/m$
Opaque	Space Group: $\text{Fd}\bar{3}m$
$a=8.384\text{\AA}$	$D_{\text{meas.}}=4.891$
	$H=7\frac{1}{2}$

Form and Habit: Magnetite occurs as equant grains in the augite marble.

These grains do not display easily measured faces and are readily fractured.

Color: Magnetite is opaque, black in both hand specimen and crushed mount.

Discussion: The identity of this mineral was confirmed by X-ray powder diffraction analysis. The pattern (Table 25) is compatible with the space group $\text{Fd}\bar{3}m$, and there are no striking irregularities.

The dominant diagnostic feature of the magnetite is its magnetism. By this property magnetite has been confirmed in several samples of augite marble. The occurrence of magnetite and magnesian augite together in the same rock must reflect the level of f_{O_2} (oxygen fugacity) at the time of formation.

Table 25. X-ray powder diffraction data for magnetite.

I	d	I	d	hkl	
10	4.74	8	4.85	111	
50	2.92	30	2.967	220	
5	2.68				
100	2.50	100	2.532	311	Unit cell dimensions (Å)
5	2.40	8	2.424	222	
45	2.08	20	2.099	400	SC-22 a = 8.384
15	1.701	10	1.715	422	Standard a = 8.396
20	1.609	30	1.616	511	
90	1.476	40	1.485	440	
		2	1.419	531	* ASTM card 19-629
5	1.323	4	1.328	620	Ref: NBS Mono. 25, Sec.
15	1.276	10	1.281	533	5, 31 (1967).
5	1.261	4	1.266	622	
10	1.209	2	1.212	444	
25	1.120	4	1.122	642	
70	1.090	12	1.093	731	
40	1.048	6	1.050	800	
15	0.9896	2	0.9896	822	

Table 26. X-ray powder diffraction data for graphite.

SC-92		Standard*		hkl	
I	d	I	d	hkl	
5	3.42				
100	3.29	100	3.36	002	
10	3.13				
		10	2.13	100	Unit cell dimensions (Å)
5	2.01	50	2.03	101	
50	1.662	80	1.678	004	a c
		10	1.544	103	SC-92 2.460 6.670
10	1.225	30	1.232	110	Standard 2.463 6.714
10	1.152	50	1.158	112	
		5	1.138	105	
10	1.115	20	1.120	006	* ASTM card 23-64
		5	1.054	201	Ref: Ferguson, Berry, and
		40	0.994	114/106	Thompson, GSA Mem. 85, 23.
		10	0.481	008	
		40	0.829	116	
		5	0.801	211	

<u>Spinel</u>	$(\text{Mg, Fe, Zn})\text{Al}_2\text{O}_4$ (Z=8)
Cubic	Class: $4/\underline{m} \quad \bar{3} \quad 2/\underline{m}$
n=1.760	Space Group: $\underline{\text{Fd}}3\text{m}$
a=8.104Å ^o	D=n.d.
	H=7½-8
	Cleavage: none

Form and Habit: Spinel occurs as small crystals (<1 mm) in the coarse monticellite-augite marble. It appears to develop a dodecahedral habit, occasionally modified by more complex forms. Intergrown crystals, possibly twins, are sometimes observed.

Color: The spinel is always very dark green, almost black in both hand specimen and lighter green in crushed mount.

X-ray: X-ray powder diffraction analysis (Table 27) shows the Cascade Slide spinel to have a face centered cubic cell, with a d glide in the plane (001), and typical cubic symmetry. The measured unit cell size of 8.104Å^o is normal for spinel (Deer, Howie, and Zussman, 1966, p. 424).

Chemistry: Microprobe analyses of spinel from the Slide (Table 28) show the presence of large amounts of Zn and Fe, substituting for Mg in the tetrahedral site. Analyses of TM-16 sum very high and are probably the result of poor standardization for both Zn and Al. The Ca-22 analysis has a much better sum and can be considered a closer approximation to the actual composition.

Table 27. X-ray powder diffraction data for spinel.

TM-16		Gahnite*		Hercynite**		Spinel***		hkl
I	d	I	d	I	d	I	d	
10	4.58	3	4.67	20	4.69	35	4.66	111
2	2.99							?
50	2.84	84	2.861	60	2.87	40	2.858	220
2	2.66							300
100	2.42	100	2.438	100	2.45	100	2.437	311
		1	2.335			4	2.335	222
40	2.01	8	2.021	80	2.02	65	2.02	400
		10	1.855					331
7	1.646	24	1.650	16	1.64	10	1.650	422
2	1.595							?
80	1.551	40	1.556	40	1.56	45	1.5554	511
100	1.428	43	1.429	80	1.43	55	1.4289	440
2	1.277	6	1.278			4	1.278	620
10	1.234	9	1.233	12	1.23	8	1.233	533
		1	1.219			2	1.2187	622
5	1.168	1	1.167	8	1.17	6	1.1666	444
2	1.132	1	1.1322			2	1.132	711
20	1.082	9	1.0803	4	1.08	6	1.0802	642
80	1.055	12	1.0525	16	1.05	12	1.0524	731
40	1.013	4	1.0104	8	1.01	8	1.0104	800

Unit cell dimensions (\AA)

TM-16 $a = 8.104$

Gahnite $a = 8.0848$

Hercynite $a = 8.119$

Spinel $a = 8.0831$

* ZnAl_2O_4 Ref: Swanson and Fuyat, NBS Cir. 539, Vol. II, 38.

** FeAl_2O_4 Ref: Dow Chemical artificial sample.

*** MgAl_2O_4 Ref: NBS Mono. 25, Sec. 9.

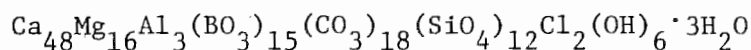
Table 28. Electron microprobe analyses of Cascade Slide spinel.

	TM-16	Ca-22
SiO_2	0.11	0.00
Al_2O_3	66.67	62.50
MgO	22.71	22.22
FeO	7.38	7.66
MnO	0.20	0.12
TiO_2	0.00	0.00
ZnO	13.69	6.47
K_2O	0.01	0.00
Na_2O	0.00	0.23
CaO	0.01	0.00
Cr_2O_3	0.00	0.13
	<u>110.78</u>	<u>99.33</u>

Formula units based on 4 oxygens (Ca-22)

Si	0.00
Al	1.898
Mg	0.853
Fe	0.165
Mn	0.003
Ti	0.000
Zn	0.123
K	0.000
Na	0.012
Ca	0.000
Cr	0.003

* Probe analysis by R.J. Tracy.

Harkerite

Cubic

Class: $4/\underline{m} \bar{3} 2/\underline{m}$

n=1.656

Space Group: $\text{?m}\underline{3}\underline{m}$ a=29.52Å^o (approx.)

Cleavage: none

Fluorescence: bright pink
under short wave U.V.

Form and Habit: Harkerite occurs as chalky white, indistinct patches (1-3 mm) in the calcite-augite marble. Because of its restricted development it is easily mistaken for calcite, from which it is distinguished by its lack of cleavage.

Color: The harkerite is always opaque, white in hand specimen. In crushed mount it is colorless and isotropic, although a few grains may appear fibrous and weakly birefringent.

X-ray: Harkerite was first identified in material from the Slide by H.W. Jaffe (pers. comm.). He noticed an isotropic phase resembling hydrogrossular but slightly different in character. Upon X-ray examination it was found that the mineral was actually harkerite (Table 29). The powder pattern measured for the mineral is almost identical to that reported and named by Tilley (1951) from Scawt Hill in the Broadford area, Isle of Skye. This is remarkable considering the complex nature of its chemistry. Unfortunately the reflection lines become too large in value to easily allow a determination of the space group. With the exception of the 710 reflection, the indexing of diffraction lines suggests a Face-centered (F) cubic lattice. If the 710 index is reliable, then the lattice must be considered Primitive cubic (P).

Chemistry: No chemical analysis has yet been attempted on the Cascade Slide harkerite. Because of the presence of boron and water it appears

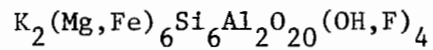
Table 29. X-ray powder diffraction data for harkerite.

CL-1h		Standard*		hkl
I	d	I	d	
20	5.24	70	5.22	440
		40	4.45	622
		20	4.17	710
		20	3.84	731
		20	3.69	800
		20	3.61	733
		20	3.58	820
10	3.38	60	3.39	662
		20	3.30	840
5	3.21	40	3.24	911
		20	3.15	644
70	3.02	60	3.01	844
10	2.99	20	2.97	933
		20	2.95	
10	2.84	60	2.84	
		20	2.81	
		40	2.66	
100	2.61	100	2.61	Unit cell dimensions (Å)
		20	2.53	
30	2.48	20	2.50	CL-1h a = 29.52 (approx.)
		40	2.46	
		20	2.39	Standard a = 29.53
		20	2.37	
10	2.34	40	2.33	* Ref: Tilley, 1951, Min. Mag.
10	2.26	20	2.25	Vol. 29.
5	2.20	20	2.22	
		20	2.16	
50	2.12	80	2.13	
5	2.07	60	2.07	
		20	2.03	
		20	2.00	
5	1.972	60	1.97	
5	1.907	40	1.92	
50	1.842	90	1.84	
		20	1.82	
5	1.782	20	1.80	
5	1.733	60	1.74	
5	1.698	60	1.70	
5	1.655	60	1.65	
20	1.503			
10	1.310			
10	1.302			
5	1.166			
5	1.063			
5	0.9926			
5	0.9868			

that wet chemistry will be more applicable than a microprobe investigation.

Although it looks like calcite in hand specimen, and only occurs as small grains, the harkerite has the advantage of fluorescing brilliant pink under short wave ultra-violet radiation. The cause of this fluorescence is unknown, but it makes identification of the mineral in a sample very easy.

Harkerite is usually found rimming grains of augite and monticellite. A further detailed investigation of this second reported occurrence of harkerite is in progress.

Phlogopite

Trigonal or
Monoclinic

D=2.818

Form and Habit: Crystals are slight platy, but formed around diopside, are jagged in appearance. Because of the perfect basal cleavage a detailed optical analysis was not attempted.

Color: Phlogopite is golden brown in hand specimen and pheochrioc yellow to yellow-brown in crushed mount.

Phlogopite was found in a piece of float which contained only diopside as an accompanying phase. Because this assemblage was never seen in place in the Slide no detailed analysis was made. Initial X-ray results (Table 30) indicate that the phlogopite may have either a monoclinic, 1M, or trigonal, 3T, structure. Further analysis is necessary to determine which. The X-ray pattern also matches that reported for lepidolite (1M). However, D.C. arc spectroscopy revealed only K and Mg as major constituents, with Li absent. Thus, the match with the lepidolite pattern was simply fortuitous, demonstrating that X-ray data alone may yield inconclusive or misleading results.

Table 30. X-ray powder diffraction data for phlogopite.

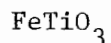
SC-106		3T Standard*			1M Standard*		
I	d	I	d	hkl	I	d	hkl
20	9.46	100	10.13	003	100	9.94	001
2	4.91	25	5.022	006	8	5.02	002
		10	4.596	100	6	4.588	020
10	4.49	10	4.558	101	6	4.553	110
7	3.86	4	3.941	104	4	3.923	111
10	3.58	8	3.663	105	8	3.654	11 $\bar{2}$
		45	3.408	106	20	3.39	022
100	3.30	100	3.354	009	100	3.348	003
10	3.08	35	3.148	107	10	3.144	11 $\bar{2}$
5	2.93	20	2.917	108	8	2.916	11 $\bar{3}$
10	2.84	14	2.710	109	4	2.708	023
		10	2.643	111	8	2.642	130/201
50	2.58	30	2.618	012	30	1.614	200/13 $\bar{1}$
10	2.48	50	2.511	001 $\bar{2}$	16	2.513	004
40	2.40	18	2.429	11 $\bar{5}$	16	2.429	13 $\bar{2}$ /201
2	2.28	4	2.293	201	4	2.290	22 $\bar{1}$
50	2.15	20	2.170	118	16	2.169	13 $\bar{3}$ /202
50	1.990	100	2.009	001 $\bar{5}$	30	2.011	005
2	1.890	6	1.907	111 $\bar{1}$	4	1.909	13 $\bar{4}$ /203
60	1.660	35	1.673	111 $\bar{4}$	16	1.673	13 $\bar{5}$
70	1.526	25	1.535	300	16	1.534	060
2	1.465						
2	1.434						
40	1.352						
15	1.321						

Unit cell dimensions

	a	b	c
SC-106(3T)	4.578	-	29.85
SC-106(1M)	5.16	9.156	9.950
Standard(3T)	4.605	-	30.135
Standard(1M)	5.228	9.204	10.055

* ASTM cards 10-492 and 10-495

Ref: Smith and Yoder, 1956, Min. Mag. 31:209-222.

Ilmenite

Trigonal

Class: $\bar{3}$

Opaque

Space Group: $R\bar{3}$

Not found in place in the Slide, ilmenite probably derives from ore concentrations in the anorthosite. Sample SC-49 was examined by reflected light microscopy and found to contain lamellae of hematite which in turn contain rod-shaped inclusions of spinel. The X-ray pattern (Table 31) shows lines due to the hematite in the ilmenite.

Table 31. X-ray powder diffraction data for ilmenite.

SC-49		Standard*		hkl
I	d	I	d	
40	3.68	50	3.73	102
5	2.95			
100	2.71	100	2.74	104
80	2.52	85	2.54	110
30	2.21	70	2.23	113
5	2.09			
50	1.910	85	1.86	204
80	1.711	100	1.72	116
5	1.627	50	1.63	108
30	1.497	85	1.50	214
30	1.462	85	1.47	300
15	1.337	70	1.34	1010
10	1.265	60	1.27	314
5	1.205	30	1.20	2010
7	1.182	60	1.18	314
15	1.151	70	1.15	226
15	1.115	70	1.12	2110
20	1.073	70	1.07	
5	1.049			318
5	1.003	30	1.00	1014
		50	0.978	2013/324
		70	0.970	410
		70	0.960	3110
		85	0.921	2014
		70	0.913	

Unit cell dimensions

a = 5.06 Å
c = ? SC-49

a = 5.523 Å
c = ? Std.*

* ASTM card 3-0781
Ref: U.S. Steel Co.
Sheffield.

<u>Perovskite</u>	$(\text{Ca}, \text{Na}, \text{Fe}^{+2}, \text{Ce})(\text{Ti}, \text{Nb})\text{O}_3$ (Z=4)
orthorhombic monoclinic, or pseudo-cubic	Class: $2/\underline{m} \ 2/\underline{m} \ 2/\underline{m}$ (?) Space Group: <u>Pnma</u> (?)
n > 2.00	D _{meas.} = 4.036
a = 6.054 Å	H = 5½
b = 7.820 Å	
c = 5.452 Å	

Perovskite occurs as small (<1 mm), dark brown to black equant crystals in the coarse augite marble. Owing to a lack of crystals with well developed faces a morphological description was not attempted.

The ideal structure of the mineral is cubic, but with substitution of minor elements into the true formula, CaTiO_3 , distortion occurs. Deer, Howie, and Zussman (1966) call the structure monoclinic; Roberts et al. (1974) list it as being orthorhombic. The pattern measured by H.W. Jaffe (Table 32) appears to be primitive orthorhombic with an n glide in the plane (001).

Perovskite has only been found in the Cascade Slide in pieces of float. It occurs in the augite marble in association with calcite, monticellite, vesuvianite, and harkerite.

Table 32. X-ray powder diffraction data for perovskite.

I	d	I	d	hkl
30	3.815	14	3.824	101/020
10	3.37	3	3.423	111
20	3.027			
10	2.88	40	2.719	200
100	2.726	100	2.701	121/002
		2	2.413	102
20	2.325	4	2.313	211
		7	2.303	031
		2	2.050	221
60	1.930	50	1.911	040
		2	1.860	230
		3	1.856	212
		3	1.676	311
20	1.585	14	1.567	321
30	1.565	16	1.563	240
		25	1.557	042
10	1.441	1	1.424	331
40	1.368	3	1.360	400
		11	1.352	242
		5	1.346	004
		2	1.339	410
20	1.223			
10	1.110			
20	1.033			

Unit cell dimensions (Å)

	a	b	c
CL-1h	5.472	7.720	5.452
Standard	5.4405	7.6436	5.3812

* ASTM card 22-153

Ref: NBS Mono. 25, Sec. 9 (1971).

CRYSTAL SURFACE TEXTURES

One of the most unusual aspects of the Cascade Slide is the presence of irregular markings on the faces of the augite megacrystals and, to a lesser extent, on some of the constituents of the augite marble. Figure 26 shows one type of marking on the $(\bar{1}10)$ face of an augite megacrystal (SC-37). These are apparently etch markings, caused in the late stages of crystallization by the concentrated fluid phase. It is attractive to hypothesize a fluorine-containing fluid which would act like HF in the etch process. These etchings are all randomly oriented and distributed. There is no apparent crystallographic control over their development.

The second type of surface marking is shown in Figure 27. These fingerprint-like crenulations or wrinkles are much finer than the etch marks and much more densely spaced. Again, they display no symmetry or orientation that can be considered as structurally controlled. The crenulations are observed to occur on a variety of faces, but primarily on terminations (001), (111), and (321). Figure 28 shows the development of these markings over the entire (001) face of megacrystal SC-40. The prevalence of crenulations on terminal faces implies that they formed on free-growing surfaces. In the marble similar markings are seen on the faces of augite crystals and associated calcite, in a cast/mold relationship where there does not appear to be any preferred face for development. Apatite, and to some degree, vesuvianite also display the same randomly oriented crenulations.

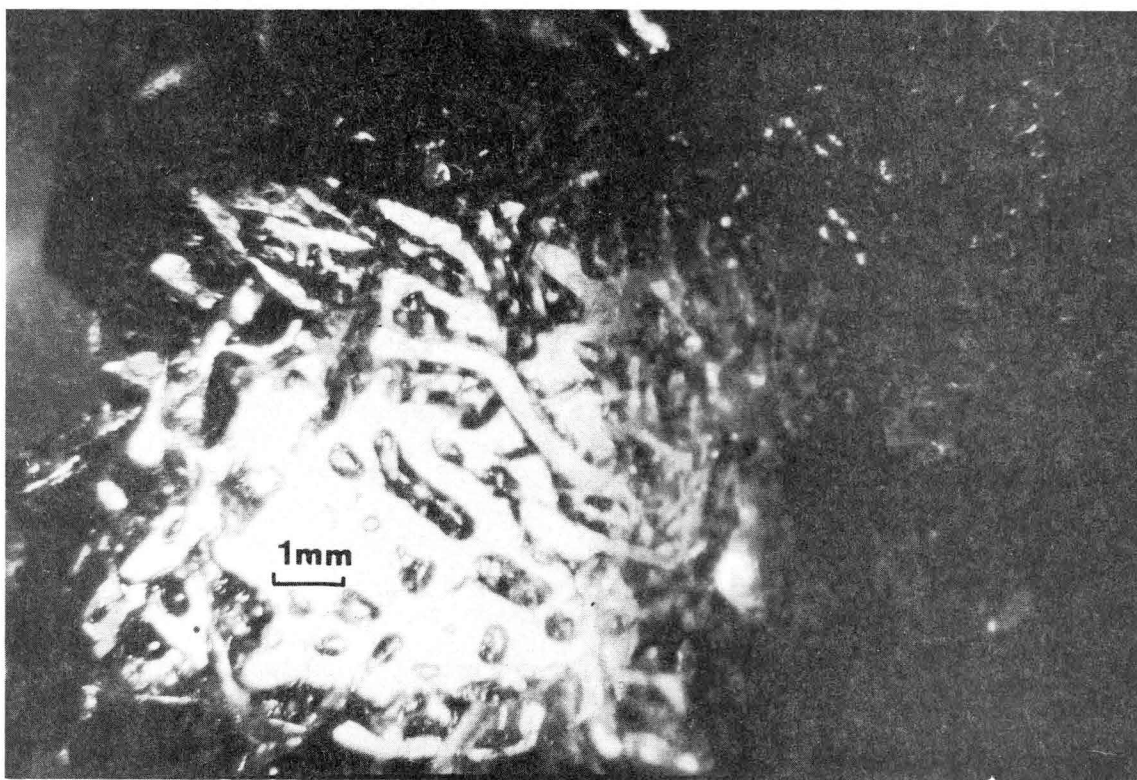


Figure 26.- Etch markings on the $(\bar{1}\bar{1}0)$ face of an augite megacrystal. Note the random orientation of the features.

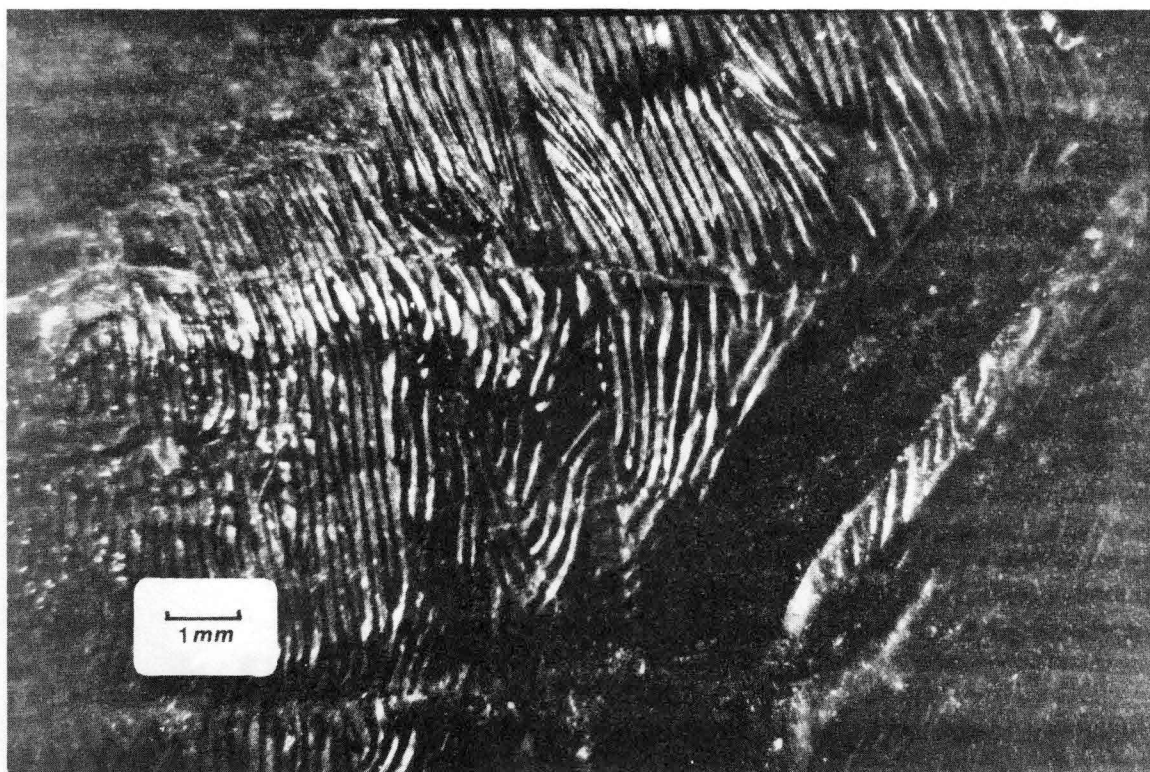


Figure 27.- Typical fingerprint-like crenulations on the terminal faces of an augite megacrystal.

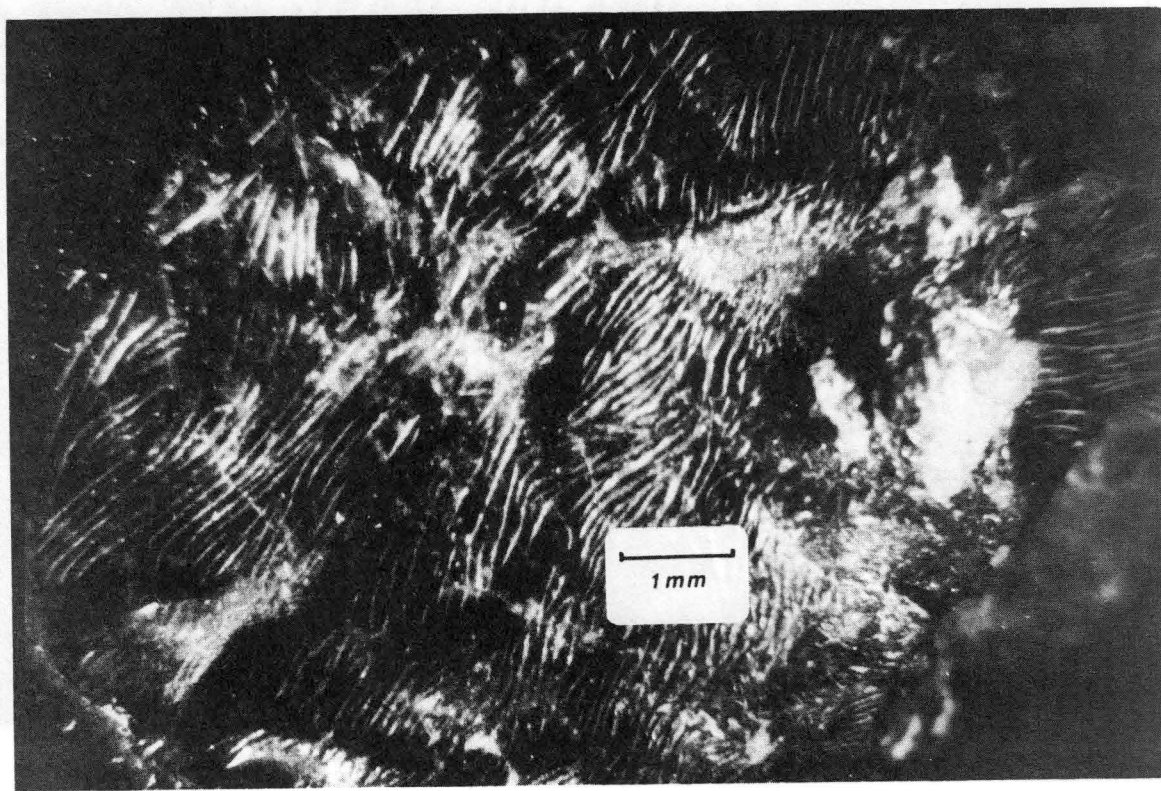


Figure 28.- Crenulations covering the entire (001) face of an augite megacrystal.

The idea of considering these surface features as etch marks is unattractive. Compared with the actual etchings seen on the augite in Figure 26, these crenulations are too even, too finely formed to have had a similar origin. Also, the fact that they occur on a variety of mineral types, and in several locations argues against their being solely a chemical phenomenon.

A search of the available literature on the subject of crystal surface features brought to light several papers about step-grown irregularities caused by screw dislocations and differential growth, both related to the actual crystal structure (Sunagawa, 1963; Komatsu and Sunagawa, 1965; Sunagawa and Koshino, 1975; Kirkpatrick, 1975). All of these reported surface features have a distinctly visible symmetry related either to the crystal as a whole or to the particular face on which they occur. Nowhere have I been able to locate references about randomly occurring crystal surface markings.

The only other occurrence of marks of this type that I have observed was on recrystallized ice sheets formed over the face of boulders. The ice crystals were not in actual contact with the rock and did not carry any imprint of the rock face. The markings on the individual crystals of ice were identical to those observed on the augite. These wavy crenulations were apparently caused by contraction of the ice sheet under its own weight. This argues for some sort of contraction phenomenon occurring during a late stage in the metamorphism of the Slide. Many questions still exist about the effects of high pressure and fluids on minerals.

COMPARISONS AND CONCLUSIONS

The Cascade Slide has been described as a regionally metamorphosed, layered siliceous/argillaceous dolomite with associated volcanics. Based on the mineral assemblages present the degree of metamorphism must have reached the granulite facies. Some metasomatism occurred in the presence of an unknown fluid phase, but the extent of ion exchange appears to have been restricted. Differences in mineralogy between the various calc-silicate assemblages can be related to original sedimentary layering. Conditions at the time of metamorphism caused the formation of large megacrystals of augite and scapolite. The augite frequently shows unusual morphology, with (010) only weakly developed. Several periods of deformation are recorded for the Cascade Slide.

Petrologically, the assemblages now present indicate silica undersaturation, except in very restricted areas, and aluminum oversaturation. Ca-bearing minerals are extremely calcic, owing to the nature of the original rock. The presence of monticellite in a regionally metamorphosed calc-silicate suite necessitates the presence of a diluent for CO_2 at the time of formation. As only very minor hydrous phases are present, water may not have been the major diluent of the fluid phase. The actual diluent or diluents continue to pose a petrologic problem. Whatever the fluid phase, it was probably also responsible for the development of etched surfaces on numerous augite megacrystals. Other unusual crystal surface features are fingerprint-like crenulations caused by apparent contraction of the crystal face.

Few regionally metamorphosed calc-silicate bodies have ever been reported in the literature, but there are several famous contact metamorphosed limestone or dolomite skarns discussed. The similarities and differences of these skarns to the Cascade Slide are worth noting.

Probably the most famous skarn body is the one at Crestmore, California. Here, a block of relatively pure limestone has been caught up as a roof pendant in the Southern California Batholith (Carpenter, 1967). A major body of quartz monzonite porphyry, with associated minor quartz diorite and related pegmatites, has intruded the Sky Blue and Chino limestones, creating a contact zone 1.5-35 m wide. This contact zone has undergone extensive metasomatism, notably of Si and Mg (Burnham, 1959). The contact zones have generally followed the decarbonation sequence of Bowen (1940) but have been modified by the metasomatism. In the rocks at Crestmore some 120 different minerals have been described, several of unique occurrence. Minerals range in metamorphic grade from calcite through akermanite. Those minerals common to both Crestmore and the Cascade Slide are: andradite, apatite, grossular, monticellite, augite, vesuvianite, scapolite, sphene, spinel, and wollastonite (Woodford et al., 1941). The monticellite has been reported as appearing brown when containing iron, and grey when not.

Crestmore differs from the Slide in the degree of metasomatism, zoning, and in the presence of rare hydrous phases. At Crestmore it appears that large amounts of water were present in the intrusives and that CO_2 was either diluted, or could escape. Thus monticellite is found, as are the humite minerals, zeolites, and amphiboles. In the Slide CO_2 was trapped, but is presumed to have been diluted by a non-hydrous

fluid phase. Also, the assemblages in the Slide have generally reached equilibrium whereas those at Crestmore are in disequilibrium.

Another famous contact metamorphosed skarn is that of Scawt Hill in the Broadford area on the Isle of Skye (Tilley, 1951). Here there has been boron-fluoride metasomatism of a dolomite by an intrusive granite. Once again, zones are present representing a progressive decarbonation of the calcareous rock, although lower temperature assemblages occur than at Crestmore. Minerals common to both Scawt Hill and the Slide are: andradite, augite, grossular, forsterite, phlogopite, vesuvianite, spinel, wollastonite, magnetite, and harkerite. Tilley does not record the presence of scapolite, possibly because the metamorphic grade was too low to form scapolite. Silica metasomatism was less at Scawt Hill than at Crestmore, with wollastonite forming only near the intrusive contacts. Monticellite generally contains 3-5% iron and appears brown. Iron-free varieties are grey or colorless. The ore minerals associated with the skarn are assumed to have come from a hydrothermal intrusion into the dolomite.

Once again, numerous hydrous phases exist: talc, brucite, serpentine, hydrogrossular, tremolite, and the humites; indicating the presence of H_2O , F, and the release of CO_2 .

The Cascade Slide actually has little similarity to either of these two skarns beyond the minerals common to both. The original dolomite of the Slide was Si- and Al-rich, providing all the necessary elements for the present assemblages without the need of extensive metasomatism. Scapolite is the only mineral species showing any large scale metasomatic exchange, and even then it occurs only at the margin of the calc-silicates in contact with pyroxene-microperthite orthogneiss. As

far as H_2O is concerned, the Slide has obviously been dry. Only the volumetrically minor vesuvianite, scapolite, harkerite, and phlogopite contain significant amounts of water. This may be due to the dry nature of the original anorthosite magma, although one would think that the Grenville sediments, in particular the argillaceous layers, must have contained considerable water.

The features of the Cascade Slide pose more questions than they answer. How could there have been a major fluid phase without its leaving a trace? How could there not have been one? What caused the etch features and crenulations on the augite crystals? How are forsterite and monticellite able to coexist in what is otherwise an equilibrium assemblage? It is hoped that further study will answer some of these questions. A prime place to begin will be a more detailed analysis of the volatile constituents of the vesuvianite, apatite, and scapolite.

REFERENCES

- Azaroff, L.V. and Buerger, M.J., 1958, The powder diffraction method in X-Ray crystallography, McGraw-Hill, New York, 342 pp.
- Bowen, N.L., 1940, Progressive metamorphism of siliceous limestone and dolomite, *J. Geol.*, v. 48, pp. 225-274.
- Brown, J.S. and Engel, A.E.J., 1956, Revision of Grenville stratigraphy and structure in the Balmat-Edwards district, Northwest Adirondacks, New York, *G.S.A. Bull.* 67, pp. 1599-1622.
- Buddington, A.F., 1939, Adirondack igneous rocks and their metamorphism, *Memoir 7, Geol. Soc. Amer.*
- _____, 1968, The Adirondack anorthosite series, *in* *Origins of Anorthosite and related rocks*, Univ. of New York Memoir 18, pp. 215-232.
- _____, and Lindsley, D.H., 1964, Iron-titanium minerals and synthetic equivalents, *J. Petrol.* 5, pp. 310-357.
- Burham, C.W., 1959, Contact metamorphism of magnesian limestones at Crestmore, California, *G.S.A. Bull.* 70, pp. 879-920.
- Carpenter, Alden B., 1967, Mineralogy and petrology of the system $\text{CaO-MgO-CO}_2\text{-H}_2\text{O}$ at Crestmore, California, *Amer. Min.*, v. 52, pp. 1341-1363.
- Cawthorn and Collerson, 1974, The recalculation of pyroxene end-member parameters and the estimation of ferrous and ferric iron content from electron microprobe analysis, *Amer. Min.*, v. 59, pp. 1203-1209.
- Chayes, F., 1945, Petrographic analysis by fragment counting, *Econ. Geol.*, v. 40, pp. 517-525.
- Dana, J.D., 1959, *Manual of Mineralogy*, 17th Ed., rev. by C.S. Hurlbut Jr., Wiley, New York, 609 pp.
- Deer, W.A., Howie, R.A., and Zussman, J., 1966, *Introduction to the rock forming minerals*, John Wiley and Sons, Inc., New York, 327 pp.
- Emmons, E., 1836, First Annual Report of the Second Geological District of the State of New York, Rept. of the Sec'y of State in relation to a Geol. Surv. of the State of New York, Albany, pp. 110-111.

- Gibbs, G.V. and Bloss, D.F., 1961, Indexed powder diffraction data for scapolite, *Amer. Min.*, v. 46, pp. 1493-1497.
- Gleason, S., 1960, Ultraviolet guide to minerals, D. Van Nostrand Co., Inc., Princeton, New Jersey, 244pp.
- Hall C.E., 1885, Laurentian magnetic iron ore deposits of northern New York, in the New York State Geologist's Annual Rept., 1884, p. 28.
- Hutton, C.O., 1956, Mangan-pyrosomalite, bustamite, and ferroan johannsenite from Broken Hill, New South Wales, Australia, *Amer. Min.*, 56, p. 589.
- Hyndman, D.W., 1972, Petrology of igneous and metamorphic rocks, McGraw-Hill, New York, 533pp.
- Isachsen, Yngvar W., 1968, Origin of anorthosite and related rocks-- a summarization; in Origin of anorthosite and related rocks, Univ. of New York Memoir 18, pp. 435-445.
- Jaffe, H.W., 1947, Reexamination of sphene (titanite), *Amer. Min.*, v. 32, p. 637.
- Jaffe, H.W., Robinson, P., Tracy, R.J., and Ross, M., 1974, Orthoferrosilite in Adirondack gneiss, Abs., Sect. of Volc., Geochem., and Petrol., Amer. Geoph. Union Ann. Mtg., Trans. Amer. Geoph. Union, v. 55, April.
- _____, 1975, Orientation of pigeonite exsolution lamellae in metamorphic augite: correlation with composition and calculated optimal phase boundaries, *Amer. Mineral.*, vol. 60, pp. 9-28.
- Kelly, W.M., 1974, Occurrence of scapolite in the vicinity of Chapel Pond and Keene Valley, Central Adirondacks, New York, Unpubl. M.S. Thesis, Univ. of Mass., 65 pp.
- Kemp, J.F., 1893, Preliminary report on the geology of Essex County, in Thirteenth Annual Rept. of the State Geologist for 1893, Albany, p. 469.
- Kirkpatrick, R.J., 1975, Crystal growth from the melt: a review, *Amer. Min.*, v. 60, p. 798.
- Komatsu, H. and Sunagawa, I., 1965, Surface structures of sphalerite crystals, *Amer. Min.*, v. 50, p. 1046.
- McDougall, D.J., 1952, Some factors influencing fluorescence in minerals, *Amer. Min.*, v. 37.
- McKie, D. and McKie, C., 1974, Crystalline Solids, Halsted Press, John Wiley and Sons, New York, 628 pp.

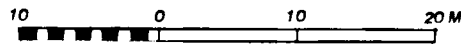
- Merwin, H.E., and Larsen, E.S., 1912, Mixtures of amorphous sulphur and selenium as immersion media for the determination of high refractive indices with the microscope, *Am. Jour. Sci.*, v. 34, pp. 42-47.
- Metz and Trommsdorf, 1968, On phase equilibria in metamorphosed siliceous dolomites, *Contr. Min. and Petr.* 18, pp. 305-309.
- Pringsheim, P. and Vogel, M., 1946, *Luminescence and solids*, Interscience Publ. Inc., New York.
- Roberts, W.L., Rapp, G.R. Jr., Weber, J., 1974, *Encyclopedia of Minerals*, Van Nostrand, New York, 693 pp.
- Silver, L.T., 1968, A geochronological investigation of the anorthosite complex, Adirondack Mtns., New York; in *Origin of anorthosite and related rocks*, Univ. of New York State Memoir 18, pp. 233-252.
- Stoiber, R.E. and Morse, S.A., 1972, *Microscopic identification of crystals*, Ronald Press, New York, 278 pp.
- Sunagawa, I. and Koshino, H., 1975, "Growth spirals on kaolin group minerals," *Amer. Min.*, v. 60, p. 407.
- Sunagawa, I., 1963, *Studies of crystal surfaces*, *Amer. Min. Spec. Pap.* #1, p. 258.
- Terpstra, P., and Codd, L.W., 1961, *Crystallometry*, Academic Press, New York, 420 pp.
- Tilley, C.E., 1951, The zoned contact skarns of the Broadford area, Skye: a study of boron-fluorine metasomatism in dolomites, *Min. Mag.*, v. 29, pp. 640-643.
- Tröger, W.E., 1971, *Optische Bestimmung der gesteinsbildenden Minerale*, Teil I, E. Schweizerbart'sche Verlagsbuchhandlung, Stuttgart, 147 pp.
- de Waard, Dirk, 1968, The anorthosite problem: The problem of the anorthosite suite of rocks, in *Origin of anorthosite and related rocks*, Univ. of New York Memoir 18, pp. 71-92.
- Woodford, A.O., Crippen, R.A., and Garner, K.B., 1941, Section across Commercial Quarry, Crestmore, California, *Amer. Min.*, v. 26, pp. 351-381.

GEOLOGIC MAP

CASCADE SLIDE

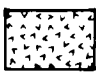

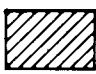
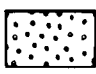


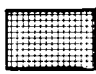
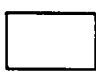


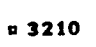
CASCADE MOUNTAIN
KEENE, NEW YORK

Scale: 1:330



Anorthosite

KEY

-  ANORTHOSITE AND GABBROIC ANORTHOSITE
-  PYROXENE - MICROPERTHITE GNEISS
-  AUGITE-GARNET GNEISS
-  AUGITE GRANULITE
-  WOLLASTONITE - GARNET GRANULITE
-  SCAPOLITE GNEISS AND GRANULITE
-  MONTICELLITE MARBLE
-  AUGITE MARBLE
-  DIABASE AND LAMPROPHYRE DIKES
-  FOLD AXIS
-  ■ 3210 ELEVATION ABOVE SEA LEVEL (FEET)

CALC-SILICATE ROCKS

Anorthosite

Map compiled from a tape and compass survey, elevations by altimeter.

